GENETIC ANALYSIS AND QTL DISCOVERY IN TETRAPLOID GARDEN ROSES: A STUDY OF DISEASE AND HORTICULTURAL TRAITS

A Dissertation

by

JEEKIN LAU

Submitted to the Office of Graduate and Professional Studies of
Texas A&M University
in partial fulfillment of the requirements for the degree of

DOCTOR OF PHILOSOPHY

Chair of Committee,	David H. Byrne
Co-Chair of Committee,	Patricia E. Klein
Committee Members,	Brent H. Pemberton
	Kevin Ong
	William L. Rooney
Head of Department,	Patricia E. Klein

May 2021

Major Subject: Horticulture

ABSTRACT

Currently, there are only three high density single-nucleotide polymorphism (SNP) based linkage maps available in tetraploid garden and cut flower roses (*Rosa* spp.). Two populations, *Rosa* L. 'ORAfantanov' (Stormy Weather™) x *Rosa* L. 'Radbrite' (Brite Eyes™) (SWxBE) and *Rosa* L. 'Radbrite' (Brite Eyes™) x *Rosa* L. 'BAIgirl' (Easy Elegance® My Girl) (BExMG), were genotyped using the WagRhSNP 68K Axiom SNP array and evaluated for the incidence of rose rosette disease (caused by rose rosette virus), black spot of rose (*Diplocarpon rosae* F.A. Wolf), and cercospora leaf spot (*Cercospora rosicola* Pass.) and assessed for defoliation, flowering intensity, plant size, and apical dominance. The clonally propagated populations and were evaluated in Somerville, TX, Overton, TX, and Crossville, TN. Linkage maps were created and quantitative trait loci (QTL) interval mapping and genome-wide association analysis (GWAS) were used to identify QTL. QTL for resistance were discovered for rose rosette disease on LGs 3 and 5, black spot on LGs 3, 5, and 7, cercospora leaf spot on LGs 1, 4, and 5, and for defoliation on LGs 3, 5, and 7. We discovered a cluster of QTL for black spot, cercospora, and defoliation near a black spot resistance locus, *Rdr4*, on LG 5. QTL for flower intensity were found on LGs 1, 3, 4, and 5, and for plant size (length, width, height, primary stem lengths) on LGs 1, 3, 5, and 6, for plant shape on LGs 3 and 7, and stem color on LG 6. We discovered plant architecture related QTL are near the everblooming gene, *RoKSN*, on LG 3, floral activation gene, *RoFT*, on LG4, GA signaling gene, *RoSLEEPY*, on LG 6, and a gene involved in deactivation of GA, *RoGA2ox*, on LG 5. In addition to QTL

discovery, we were able to isolate 18 progeny in the BExMG family that carried 2 resistance alleles against black spot and one resistance allele for cercospora leaf spot for use in future breeding.

ACKNOWLEDGEMENTS

I would like to thank my major advisor Dr. David Byrne for the opportunity he provided for me to learn the art and craft of plant breeding. I am thankful for the many learning opportunities he provided as we traveled all over the world, attending conferences and visiting labs which helped me strengthen my understanding in this subject area. I would also like to thank my co-chair Dr. Patricia Klein for all the bioinformatics help she provided. I would like to also thank Dr. Brent Pemberton for his help in planting and maintaining my experiment in Overton, TX. I would also like to thank Dr. William Rooney and Dr. Kevin Ong for spending their valuable time both teaching me and serving on my committee. I would like to also thank Dr. Oscar Riera-Lizarazu for serving as an honorary committee member and guiding me in my analysis of the data.

A special thanks to Natalie Anderson and Pamela Hornby for the help maintaining my plants in the greenhouses and fields. I am also extremely grateful to Natalie Patterson who helped me extract all my DNA samples during a crazy rush towards a funding deadline.

I would like to thank my lab mates and fellow graduate students: Zena Rawandoozi, Ellen Young, Seza Noyan, Stella Kang, and Nolan Bentley for both their friendships, for helping with data collection, and for helping me with problems I could not understand.

I would like to thank my father, Tin-Man Lau for inspiring me to pursue an academic career and also providing financial help during this time. I would like to thank

my mother, Tsai Miao Lau for the encouragement and push to finish my research. And I would like to thank my sister, Mojen Lau for all the times she would call to check in on me during this time.

I would also like to thank my wife Hannah Leigh Lau who patiently stayed up many nights just sitting quietly with me while I would code new scripts, try to understand the results from different software, and the many hours writing this dissertation.

Thanks to the Department of Horticultural Sciences and the USDA's National Institute of Food and Agriculture Specialty Crop Research Initiative project, "Combating Rose Rosette Disease: Short Term and Long Term Approaches" for funding my research.

CONTRIBUTORS AND FUNDING SOURCES

Contributors

This work was supervised by a dissertation committee consisting of chair and co-chair, Dr. David H. Byrne and Dr. Patricia E. Klein of the Department of Horticultural Sciences, and committee members, Dr. Brent H. Pemberton of the Department of Horticultural Sciences, Dr. William L. Rooney of the Department of Soils and Crop Sciences, and Dr. Kevin Ong of the Department of Plant Pathology and Microbiology.

The data analysis interpretation for mixed models used to estimate heritability in chapters II and III were a joint effort of Dr. David H. Byrne and Dr. Oscar Riera-Lizarazu of the Department of Horticultural Sciences and myself.

The genotypic data presented in chapters II and III was provided by multiple sources. Natalie Patterson in Dr. Patricia Klein's Lab of the Department of Horticultural Sciences extracted the rose DNA. Samples were shipped to ThermoFisher Scientific for genotyping on the WagRhSNP 68k SNP array.

The phenotypic data collection of plants in Overton, TX, in chapters II and III was collected by Dr. Brent Pemberton of the Department of Horticultural Sciences.

The phenotypic data for rose rosette disease from plants in Crossville, TN, in Chapter II was from Dr. Mark Windham of the University of Tennessee in the Department of Entomology and Plant Pathology.

The phenotypic data for architecture traits in chapter 3 was in part contributed by members of the Rose Breeding and Genetics Lab in the Department of Horticulture.

All other work conducted for the dissertation was completed by the student independently.

Funding Sources

This work was made possible by USDA's National Institute of Food and Agriculture Specialty Crop Research Initiative project, "Combating Rose Rosette Disease: Short Term and Long Term Approaches" Grant No.2014-51181-22644.

NOMENCLATURE

BE	*Rosa* L. 'Radbrite' (Brite Eyes™)
GWAS	Genome-wide association study
GBS	Genotyping by sequencing
LG	Linkage group
MG	*Rosa* L. 'BAIgirl' (Easy Elegance® My Girl)
SW	*Rosa* L. 'ORAfantanov' (Stormy Weather™)
RT-qPCR	Reverse Transcription Quantitative Polymerase Chain Reaction
QTL	Quantitative Trait Locus/Loci
REML	Restricted maximum likelihood
RRD	Rose Rosette Disease
RDR4	Resistance to *Diplocarpon rosae* 4
RoGA2ox	Gibberellin 2-oxidase rose homolog
RoFT	Flowering Locus T rose homolog
RoKSN	Terminal Flower 1 rose homolog
RoSLEEPY	Sleepy 1 rose homolog
RRV	Rose Rosette Virus
SNP	Single nucleotide polymorphism

TABLE OF CONTENTS

Page

LIST OF FIGURES

Page

LIST OF TABLES

Page

CHAPTER I

INTRODUCTION AND LITERATURE REVIEW

Economic Importance of Roses

Roses are an important horticultural crop worldwide. In 2003, an estimated 8500 ha of protected rose culture produced 15-18 billion stems worldwide (Blom and Tsujita, 2003). Potted miniatures production was estimated to be 60-80 million pots annually (Pemberton et al., 2003), and landscape roses estimated at 200 million bushes annually valued at $720 million USD (Short and Roberts, 1991). Worldwide, garden roses along with cut flowers were valued at 24 billion Euros in 2008 ($42.3 billion USD equivalent adjusted for both historical exchange rate and inflation) (Heinrichs, 2008).

In the USA, garden roses had about $203 million in sales in 2014 and $168 million in sales in 2019 (USDA NASS, 2015; 2020) and. In 2012, Steven B. Hutton, the President and CEO of Conard-Pyle (now owned by Ball Horticultural Company), estimated that the US produced around 30 million rose bushes per year. Mr. Hutton says that while rose production is only 70% as compared to about 40 years ago, the outlook of rose production in the US is one of hope as breeders continue to develop own root roses that are resistant to biotic and abiotic stresses (Hutton, 2012). Another major change in the production of landscape roses in the US is the shift from grafted plants to self-rooted plants and from field production to container production (Pemberton and Karlik, 2015). From the combined production of cut roses, potted miniature, and garden roses, the rose industry is of high economic importance worldwide.

The Rosaceae Family

Rosaceae includes herbs, shrubs, and trees. This family is one of the most economically important plant families as its worldwide farm gate value is worth $60 billion and consumer value is $180 billion annually (Hummer and Janick, 2009). Plants in this family sometimes have thorny stems (roses have prickles), and are characterized by rhizomes, alternate leaves, and showy flowers that are usually hermaphroditic (Judd et al., 1999). Rosaceae includes fruit, berry, and ornamental crops and is divided into subfamilies Prunoideae (peach, nectarine, plum, apricot, cherry, and almond), Maloideae (apple, pear, quince and loquat), Rosoideae (rose, strawberry, blackberry, and raspberry), and Spiraeoideae (some ornamental trees and bushes of lesser economic importance) (Arús and Gardiner, 2007). Taxonomists have reorganized the subfamilies into three: Rosoideae, Dryadoideae, and Spiraeoideae (*Malus* and *Prunus* have moved into this subfamily) (Potter et al., 2007).

Rose Breeding and Genetics

The majority of garden roses today are either diploid (2n=2x=14), triploid, or tetraploid, while species roses range from diploid to octoploid (Zlesak, 2007; Krussmann, 1981) with one report of a decaploid species (Jian et al., 2010). Almost all of the cultivated roses come from interspecific crosses from the following species: *Rosa canina* L., *R. chinensis* Jacq., *R. foetida* Herrm., *R. gallica* L., *R. gigantea* Collet ex Crép., *R. moschata* Herrm., *R. multiflora* Thunb., *R. phoenicea* Boiss., *R. rugosa* Thunb., and *R. wichuraiana* Crép. (Gudin, 2000). The rose was domesticated in Europe, where

traits for winter hardiness, pest resistance, floral complexity, and doubling were selected, while in China the traits of recurrent flowering and color brightness were selected (Martin et al., 2001). Garden roses have been recorded in history as far back as the Han Dynasty dating back to 141 to 87 BC where roses were planted in the palace gardens (Guoliang, 2003). Today, roses are used in a variety of ways ranging from the classic cut flowers and garden rose to fragrances and culinary uses (Hummer and Judd, 2009).

Rose breeding prior to the 20th century primarily consisted of developing new cultivars from seedlings derived from open pollination (Zlesak, 2007). As the use of designed crosses began, the horticultural traits from the two areas of domestication were further incorporated into new superior cultivars. Attempts at mutation breeding has produced viable plants but is not commonly used as a tool for introducing genetic variation (Zlesak, 2007; Yamaguchi et al., 2003). Current breeding of commercial roses is predominantly elite by elite crosses. However, frequently the ploidy of parents is not known and there are a number of triploids released that are the result of tetraploid by diploid crosses. These resulting triploids can often be good garden varieties and the pollen can sometimes be viable and used for crosses. Current breeding goals include creating visually appealing roses that are resistant to biotic and abiotic stresses, as such plants need less attention and pesticide applications while being easy to root for the production of own root container grown plants (Pemberton and Karlik, 2015; Debener and Byrne, 2014).

In the designing of crosses, parents are selected for desirable traits, namely disease resistance along with flower color, flower type, and plant architecture. In the

spring, pollen is collected by harvesting anthers and drying them for two days at room temperature then stored in a freezer (-20°C) until use. Pollen is applied to the stigmas via makeup brushes after emasculating flowers that are at the correct stage (not yet open but about to open). Crosses are then marked to distinguish hips that were results of designed crosses from outcrosses and selfs. Seeds from resulting hips are collected in the fall and undergo a cold treatment prior to placement in greenhouses for seedling selection.

Within the first three months, seedlings can be screened for powdery mildew resistance and remontancy. Once bloomers along with unattractive flowers and those extremely susceptible to powdery mildew are typically discarded (Zlesak, 2007). Commercial programs will discard up to 75-95% of their seedlings during these first few months. However, Zlesak points out that while selecting based on flowering characteristics brings a rapid gain of selection for flower related traits, the massive discarding of seedlings may leave little variation for selecting non-floral traits such as disease resistance. Seedlings that make it past the greenhouse stage are planted in one location for phenotypic evaluation for other traits such as growth type, disease resistance, and general health of the plant. In the second year, plants that make it past the initial field test are clonally propagated (either by budding, grafting, or rooted cuttings) to test in multiple locations to evaluate the plant's adaptation to those areas or to expose the progeny to higher disease pressures. Selections can be sent to collaborators throughout the world for further commercial evaluation for adaptation and ornamental qualities in other environments.

Major Rose Diseases

Even though a heavy emphasis is placed on the appearance of the flower, disease resistance is very important as the chemical control of diseases and insects associated with producing and maintaining roses in a landscape is of environmental, health, and monetary concern (Zlesak, 2007). Creating resistant cultivars would make the plants less costly to produce for the grower and ultimately require less care from the end user. Depending on the breeding program, most breeders in the United States will breed for resistance among the cultivated material while others try to incorporate resistance from species. The former takes less time to develop commercially acceptable cultivars as the cultivated material has more favorable alleles conditioning exceptional horticultural traits from hundreds of years of accumulating those alleles through designed crosses and selection. Going to the wild species however may capture resistance alleles that are not currently found among commercial rose germplasm. However, using rose species and species hybrid roses brings along unfavorable alleles through linkage drag that must be bred out while maintaining the favorable alleles of interest.

The major production and processing areas of roses in the United States are California, Arizona, and Texas. Major centers for container production are in the Midwest, South Central, and Eastern seaboard of the United States including Florida (Pemberton and Karlik, 2015). The roses produced in these major nurseries are shipped across the country to be used in the landscape. The Southeastern United States is characterized by hot humid summers causing the prevalence of black spot (*Diplocarpon rosae* F.A. Wolf) and cercospora (*Cercospora rosicola* Pass.), however, the production

areas in California and Arizona rarely deal with these diseases since their climate is much drier and cooler (DeVor et al., 2013). Powdery mildew (*Podosphaera pannosa* var. *rosae* Wallr.) is a problem throughout the United States especially during cool (18-25°C) humid nights accompanied with dry days during the spring and fall (Horst and Cloyd, 2007). Greenhouses provide high relative humidity and cooler temperatures which favors powdery mildew. In Texas powdery mildew is only a problem in the greenhouse during the spring. Rust is only a problem on the Pacific coast of the United States (DeVor et al., 2013).

The most important fungal disease that affects field grown roses as well as roses in landscapes is black spot. It is a fungal pathogen which causes black spots with feathery margins on the upper portion of the leaf (Horst and Cloyd, 2007). Black spot is favored by humid summer climates and as the infection progresses, leaves yellow which can be followed by defoliation. Often bad infections leave rose bushes completely defoliated.

Powdery mildew is also a major fungal disease affecting roses. While Horst and Cloyd (2007) believe powdery mildew to be the most serious disease of cut roses, from a breeder's view, highly susceptible seedlings can be identified and discarded in the greenhouse within a few months of germination. Symptoms most commonly include the heavy white mycelium growth on the upper portion of leaves, stems, and flower buds (Horst and Cloyd, 2007). Powdery mildew does not require free water on the leaf surfaces to form as does black spot (Karlik et al., 2020). In addition, overhead irrigation actually inhibits the spore release of the fungi as it requires a dry period. In the breeding

program at Texas A&M University, powdery mildew is primarily seen inside the greenhouse during the spring. Once the seedlings are planted outside, little to no disease pressure makes it difficult to phenotype for disease resistance.

Another major fungal disease affecting roses is cercospora leaf spot. It forms lesions characterized by circular spots with a small white or tan necrotic area in the center with concentric (target-like) look. Normally, the edges of the lesion are smooth when compared to black spot (Mangandi and Peres, 2012). In the past, cercospora was not considered a major rose problem, however as major strides were made in selecting roses resistant to black spot, cercospora has emerged as an important disease. Cercospora has most likely been present and affecting roses but the effects were masked by the presence of black spot which causes defoliation. Only in extreme cases of cercospora infection is defoliation observed. Hagan et al. (2005), observed that many of the roses with the highest resistance to black spot showed infection by cercospora. Similar observations were made in the Texas A&M Rose Breeding and Genetics program. The most probable explanation is that the defoliation caused by blackspot does not allow for cercospora to develop properly on highly blackspot susceptible genotypes.

Current breeding efforts are aimed towards the few major diseases mentioned above in the garden rose industry. Diseases that are of less economic importance are rust (*Phragmidium* spp. Pers.), downy mildew (*Peronospora sparsa* Berk.), and anthracnose (*Sphaceloma rosarum* Pass.). Crown gall from *Agrobacterium tumefaciens* can also be a major problem, however, this is a problem producers deal with much more than the homeowner. Bacterial leaf spot caused by *Xanthomonas* spp. has also been reported in

Florida and Texas (Huang et al., 2013). Sequence data from Huang et al. (2013) shows that it is within the *Xanthomonas axonopodis* subgroup however the principal coordinate analysis grouped the rose isolates together in a distinct group from others in this subgroup. Thus far *Xanthomonas* has not been a major problem in the Texas A&M cultivar trial block.

Typically, it takes two to three years to properly phenotype seedlings for resistance to diseases as new plantings take time for natural disease inoculum pressure to build up (Debener and Byrne, 2014; Lühmann et al., 2010). However, the use of genetic markers could speed up the breeding process by reducing the number of seedlings going to the field, which reduces the costs (labor and land) associated with field-based phenotyping (Byrne et al., 2018). However, if high numbers of seedlings in the field can be sustained by the program, using marker assisted selection could mean many more seedlings first screened via markers in the greenhouse and increasing the number of seedlings with favorable alleles being phenotyped in the field, increasing the rate of breeding progress within the program.

In addition to disease resistance work in the breeding of roses, work developing garden roses resistant to abiotic stresses is essential to creating low maintenance roses. Abiotic stresses considered are heat, cold, drought, salt, and soil pH extremes. Breeders test their selections in many different environments to test both GxE and the stability of their selections in stressed environments. A key environmental stress that the Texas A&M rose breeding program evaluates is heat tolerance. Potential parents and progeny are evaluated in Somerville and Overton, TX. Both these locations are hot and humid

creating optimal environments to test the performance of garden roses to the abiotic stress of Texas summer heat along with biotic factors including black spot and cercospora.

Rose Rosette Disease

One emerging biotic stress is rose rosette disease (RRD) caused by the Emaravirus, *Rose Rosette Virus* (RRV) (Pemberton et al., 2018). Emaravirus (European mountain ash ringspot associated virus) is a new genus of viruses containing negative sense RNA (Miekle-Ehret and Mühlbach, 2012). Viruses included in this family are ringspot disease of European Mountain Ash (EMARaV) (Kegler, 1960), fig mosaic virus (FMV) (Condit and Horne, 1933), rose rosette virus (RRV) (Conners, 1941), raspberry leaf blotch virus (FLBV) (Gordon and Taylor, 1976; Jones et al., 1984), pigeonpea sterility mosaic virus (PPSMV) (Jones et al., 2004; Mitra 1931), and high plains virus (recently renamed maize red stripe virus) (Jensen and Lane, 1994; Slykhuis, 1956). RRV was first described to have 4 negative RNA strands (Laney et al., 2011), however, more recently, 3 more strands were discovered (Di Bello et al., 2015; Babu et al., 2016). These RNA strands are encapsulated by double membranes. Protocols have been established for the detection of the presence of RRV using RT-PCR (Dobhal et al., 2016).

The virus is vectored by an eriophyid mite (*Phyllocoptes fructiphilus* Keifer) (Armine et al., 1988; Allington et al., 1968). The virus is transmitted via the mite and grafts but not by mechanical means (pruners) (Armine et al., 1988; Doudrick et al., 1987). Although drop inoculations when suspended in proper buffers were reported

(Doudrick et al. 1987), subsequent trials have not been very successful. A major reason why RRD has spread at such an accelerated rate is the widespread distribution of *R. multiflora*, introduced in the United States as a garden plant, breeding parent, and a conservation plant which was planted by the government for soil erosion and wildlife conservation efforts (Armine, 1996). *R. multiflora* is susceptible to the mite and RRV. The virus was even suggested to be a biocontrol method to eradicate *R. multiflora* (Armine et al., 1996; Doudrick et al., 1986; Epstein and Hill, 1995; Epstein et al., 1997; Epstein and Hill, 1999; Hindal et al., 1988;). However due to the prolific seed production of the plant, *R. multiflora* can produce thousands of seeds before the virus can kill it. Thus, the population survives the virus in spite of its high susceptibility. At first it was observed that RRD would not spread to the cultivated ornamental roses if they were more than 100 meters away (Epstein et al., 1997), however, Armine described the microscopic eriophyid mites as able to be carried hundreds of feet up in the air via wind and thus able to travel long distances (Armine, personal communication). Mites travelling via the wind can land on ornamental roses in the landscape and since ornamental roses are typically planted in large closely spaced groups, mites and the virus can easily spread from plant to plant.

Symptoms of rose rosette disease were first described in the early 1940's in Manitoba, Wyoming, and California (Conners, 1941). The descriptions of the disease were "witches' broom" type growth, misshapen leaflets and flowers (Pemberton et al., 2018). The disease was then found in the United States on possibly *Rosa pisocarpa* and *Rosa woodsii* (Amrine, 1996). Modern descriptions of disease symptoms include large

masses of reddish prolific twisted growth extending from an otherwise healthy-looking bush. These prolific growths (rosettes) are identified by containing strapped leaves (long and thin) accompanied with shorter internodes and increased thorniness on cultivars with prickles (Windham et al., 2014). This abnormal growth pattern can be easily confused with glyphosate (Roundup®) damage. However, glyphosate damage differs in that it causes a yellow to light green excessive twisted growth instead of red. The early symptoms of RRD before the obvious witches' broom include: 1) strapped leaves, 2) flattened stems, and 3) increased thorniness. If two of these symptoms are present, there is a high probability that the plant has the virus (Windham, personal communication).

Dr. Mark Windham at the University of Tennessee has developed a scale for rating the severity and the number of rosettes per plant in an effort to try to capture the quantitative nature of the disease assuming disease resistance is quantitative. To rate the severity, 0 = no rosette, 1 = small single shoot with aforementioned symptoms, 2 = 2-3 shoots in the rosette, 3 = 4 or more shoots in the rosette. Rosettes per plant are rated as following 0 = no rosettes, 1 = 1 rosette per plant, 2 = 2 rosettes per plant, 3 = 3 or more rosettes per plant (Windham, personal communication).

The current best management practices are to remove the infected plant so it does not serve as a reservoir of inoculum for the virus or for the mite. This includes bagging the plant to prevent mite movement and removing it from the site. Complete removal of the crown is important to prevent the regrowth of infected plant tissue from the crown. This approach of aggressively rouging infected plants under high disease pressure in the Beall Family Rose Garden at University of Tennessee has been successful at limiting

losses to 2-4% per year of the plants. Other approaches to managing the disease being studied are the use of miticides to control the mite vector, the use of nonhost plants to restrict the movement of the mite vector and an antiviral compound (Windham et al., 2014). The best management practices described are the current solutions to RRD until cultivars resistant to RRV are created and can be incorporated into best management practices.

To develop new cultivars that are resistant to RRD, both cultivated material and species are being screened for resistance to find potential parents to use for crosses. Trials in Delaware and Tennessee screened 141 and 264 commercial cultivars and *R. spp.* collected, respectively, with 2-5 reps at each location. The material was exposed to natural surrounding inoculum as well as augmentation with mite infested RRD symptomatic branches 2-3 times a year in Delaware and Tennessee (Byrne et al., 2017). Not all cultivars and *Rosa* species were at both locations.

Rose Architecture

Plant architecture is important in garden roses as in all horticultural plants. There is much diversity in garden rose germplasm as there are architecture types that include climbers, bush types, and ground covers. Depending on the landscape use of the rose, the end user may want to incorporate these many architecture types. As there is much diversity in these growth types, this creates a wide genetic germplasm base in which to select for desirable growth types. The ideal plant architecture for most garden roses is a plant with many primary and secondary shoots which creates a plant with dense foliage

and high flower productivity. However, measuring plant architecture is limited in accuracy and time consuming.

Plant architecture consists of many components of plant growth which contribute to the overall shape of the plant. Branching angles of shoots and of roots can significantly alter the final structure of a plant and thus alter not only the appearance but also the yield of a plant. Plant architecture has been an important part of plant breeding as exemplified by the "Green Revolution" focus on plants with dwarfing plant architectures to increase the grain yield by reducing lodging (Wang and Li, 2008). Similarly, plant architecture can affect the flower productivity of roses.

Plant architecture is driven by many pathways that alter plant hormones of auxin, gibberellins, and brassinosteroids within the shoot, root, and axillary meristems (Wang and Li, 2008). Different ratios of these plant hormones can alter the expression of these architectural traits. *RoKSN* (Genebank ID: HQ174211.1) is an insertion of a Copia transposon in the TERMINAL FLOWER 1, *TFL1* gene (Iwata et al., 2012). Both *RoKSN* and *TFL1* control the continuous blooming trait. It is suggested that these two genes may either have pleiotropic effects on other things like plant architecture and flowering time, or these traits are controlled by other genetic factors closely linked with *RoKSN* (Kawamura et al., 2015; Goretti et al., 2020; Shannon and Meeks-Wagner, 1991; and Ratcliffe et al., 1998).

Another gene of importance is the antagonist to *RoKSN*, *RoFT* (Remay et al., 2009). In Arabidopsis, *TFL1* and *FT* are antagonistic where *TFL1* represses flowering and *FT* initiates flowering (Moraes, et al., 2019). Other genes that are involved in plant

architecture are the genes relating to gibberellin pathways, *RoGA2ox* (Remay et al., 2009) and *RoSLEEPY* (Foucher, et al., 2008). These gibberellins play roles in plant architecture as they are a one of the main classes of plant hormones associated with plant cell elongation and flower signaling.

Rose Genetic Work

Recurrent vs non-recurrent (ever blooming vs once blooming) is a very well understood trait and possibly one of the most frequently selected trait. This is controlled by one gene (*RoKSN*) in which the non-recurrent gene is dominant over recurrent (De Vries and Dubois, 1978). Selection for this trait is easy as ever bloomers will bloom when the seedling is young whereas once bloomers need to be at least a year old to bloom. Because the recurrent bloomer is desired in garden roses, crosses that result in once blooming progeny are discarded or need to be selfed or back crossed to regain the ever blooming trait.

Four genes (*Rdr1*, *Rdr2*, *Rdr3*, *Rdr4*) controlling vertical resistance to black spot have been described (Von Malek and Debener, 1998; Hattendorf et al., 2004; Whitaker et al., 2010; Zurn et al., 2018; Zurn et al., 2020). In addition to vertical resistance to black spot, partial or horizontal resistance has been observed in roses (Xue and Davidson, 1998; Whitaker et al., 2007; Shupert, 2005; Dong et al., 2017; Yan et al., 2019). By pyramiding different sources of partial resistance, a breeder can potentially create a more robust resistance than single partial resistance genes. A meta analysis has been conducted on black spot resistance which found meta-QTL on LGs 3 and 5 (Lopez

Arias et al., 2020). Various genes (*Rpp*1, *Pm*1, *Pm*2, *Glu*7) for resistance to powdery mildew have also been reported (Linde and Debener, 2003; Dugo et al., 2005; Xu et al., 2007).

Horticultural traits such as flower size (Liang et al., 2017), flower color, flower production, shrub size, and architecture (Wu et al., 2019; Kawamura et al., 2011, 2015; Li-Marchetti et al., 2017) are also key traits a breeder considers when making selections. However, because of the complexity of these traits and their interaction with the environment (GxE effect), the genes of interest are more difficult to identify. For instance, flower color is controlled by many different pigments all produced in different pathways and the summer heat alters pigment production making the rose lighter in color than it would appear in the spring or fall (Dela et al., 2003).

Although many studies have been conducted in *Arabidopsis thaliana* to understand the genetic complexities of plant architecture, few have been done with roses. What has been done on plant architecture of rose is mainly just characterization of plant architecture with some studies looking at how cultural practices affect plant architecture (Kool, 1997; Kool and Lenssen, 1997; Kool et al., 1997; Mascarini et al., 2006; Crespel et al., 2013). There have been a few studies on plant and flower architecture on rose (Kawamura et al., 2011, 2015; Li-Marchetti et al., 2017). Kawamura et al. (2011, 2015), looked at the plant architecture from a primary shoot perspective. Kawamura et al. (2011) found heritabilities (H^2) ranging from 0.82 to 0.93 when looking at numbers of nodes on different parts of the primary shoot. Kawamura et al. (2015) found similar broad sense heritabilities ranging from 0.75 - 0.89 when looking at plant

architectural traits such as plant height, primary shoot angles, internode length, and stem diameters. Wu et al. (2019) found low to moderate narrow sense heritabilities (0.12-0.50) and low to high broad sense heritabilities (0.04-0.92) when looking at plant architecture related traits.

Diploid Versus Tetraploid Genetics

While diploid genetics follows normal Mendelian inheritance through bivalent pairing during meiosis, tetraploids are much more complex in the segregation of genes since they have four sets of chromosomes (Voorrips et al., 2011). Tetraploidy resulting from the doubling of a diploid species is called autotetraploidy which presents difficult genetic analysis because during meiosis, a tetrad can form allowing crossover between any of the four homologs. The implications of having tetravalents form is that at any given site there are 4 corresponding positions. If there are only two alleles which is the case for most SNP markers, there are 5 possible dosage classes (AAAA, ABBB, AABB, AAAB, BBBB). Tetraploidy resulting from the combination of unreduced gametes between two individuals of different species or distant relatives of the same species produces allotetraploids. Allotetraploid chromosomes pair bivalently due to the differences between the homeologs therefore the preferential pairing of the homeologs allows us to study the segregation of alleles as a diploid. Furthermore, segmental allotetraploids may have some chromosomes that preferentially pair during meiosis and some that form tetravalents, making analysis even more complicated. To make matters

even more complicated the addition of null alleles further complicates segregation ratios (Hackett et al., 1998).

Because of the complexities of tetraploid genetics, one must consider which genotyping platform would be the best for analysis of tetraploids. The choices among current genotyping technologies are Genotyping by Sequencing (GBS) or a SNP array; the 68k WagRhSNP Axiom Array is used for roses (Koning-Boucoiran et al., 2015). GBS on the Illumina platform reads DNA by attaching single stranded DNA fragments that have been cut using restriction enzymes on a surface then adding fluorescent labeled bases and observing the different colors when added (Illumina, 2015). GBS obtains short reads (50-300 bp) and either aligns them to a reference genome for SNP calling or if a reference genome is not available, Stacks (Catchen et al., 2013), can be used to call SNP by "stacking" the short reads and looking for SNP variants. SNP micro arrays, also called SNP chips work by using 25-mer probes that target the different variants of the SNPs. When the homologous DNA binds to the probe on the chip, a florescent signal is produced and tells which version of the SNP was on the DNA fragment (LaFramboise, 2009). SNP arrays are created from SNPs identified from transcriptomes from a representative range of genotypes of the organism in question (Koning-Boucoiran et al., 2015). For example the WagRhSNP 68k array for rose was made using transcriptomes from a range of cut and garden roses from both leaf and flower tissue. A diploid *Rosa multiflora* hybrid was also used after being wounded, heat stressed, or inoculated with blackspot, powdery mildew, or downy mildew. Biases towards the transcriptome and

genotypes used for SNP discovery for the development of SNP micro-arrays can skew the resulting genotype data (Bourke et al., 2018).

Currently GBS methods are much cheaper than SNP arrays. While the GBS method may be cheaper up front, the time and expertise associated with SNP calling and data cleanup from the GBS reads may outweigh the costs of using the SNP chip. However, as described in Bajgain et al. (2016), they compared GBS and a SNP chip for QTL mapping in wheat and they found 8 and 9 QTL, respectively, and only one was a shared QTL. They also found that because the SNP chip had a bias on the germplasm, one of the wheat genomes was underrepresented. When they described the workflow of the two systems, GBS required much higher computational power and resources when compared to the SNP chip. Given that the 68k WagRhSNP. was constructed using both cut and garden roses (‘Morden Fireglow’, ‘Adelaide Hoodless’, ‘Prairie Joy’, ‘Morden Blush’, ‘Diamond Border’, ‘Nipper’, ‘J.P. Connell’, ‘Princess of Wales’, ‘Heritage’, ‘Graham Thomas’, ‘Morden Centennial’, and ‘Red New Dawn’), the SNP chip should not be too biased when genotyping the tetraploid families at Texas A&M as our tetraploid crosses are within cultivated material. In addition, SNP arrays can better differentiate dosage of alleles for polyploid analysis.

Linkage Mapping and QTL Analysis

Genomics work within Rosaceae that has led to the development of markers for use in breeding include peach (*Prunus persica* (L.) Batsch.), apple (*Malus* x *domestica* Borkh.), strawberry (*Fragaria vesca* L.), and sweet and tart cherries (*Prunus avium* L.)

since the genome assemblies for these species have been created and released for use (Arus and Gardiner, 2007; Jung et al., 2014; Peace et al., 2012; Genome Database for Rosaceae, 2017). However, the work in these four crops has laid the foundation for other Rosaceae crops. Rose genotyping work has utilized the strawberry genome as a 'proxy' reference genome (Gar et al., 2011; Vukosavljev et al., 2016; Yan et al., 2018) since the rose genome was not available until doubled-haploids of *Rosa chinensis* 'Old Blush' plants were sequenced (Raymond et al., 2018; Saint-Oyant et al., 2018).

Early linkage maps for rose were based on RAPD and AFLP markers and the density of the two parental maps was only 278 markers spread over 14 linkage groups with an average distance between markers of 2.4 and 2.6 cM (Debener and Mattiesch, 1999). In addition to constructing this map, Debener and Mattiesch (1999) were able to find markers corresponding with loci controlling petal number and flower color. Other maps constructed with RAPDs, microsatellites, and morphological markers, attempted to locate QTL for flower size, days to flowering, leaf size, and powdery mildew (Dugo et al., 2005). However due to the relatively low marker density in relation to the technology we presently have using SNPs, the results are putative. Crespel et al. (2002) released a map using AFLP markers and their study focused on finding QTL for recurrent blooming, double corolla, and stem-prickle quantity. This map was later improved by adding 44 EST-SSRs and 20 genomic SSR markers, and focused on flower petal number and blooming date (Hibrand-Saint Oyant et al., 2008). Yan et al. (2005) used Debener and Mattiasch's (1999) population to create an integrated map utilizing 520 markers (AFLP, SSR, PK, RGA, RFLP, SCAR, and morphological markers). The integrated map

consisted of a total length of 545 cM. The parental maps had marker density ranging from 0.4 to 0.7 markers per cM. The two parental maps were able to be merged into an integrated map because of common markers in both parents whereas with Debener and Mattiesch's (1999) earlier map in did not have common markers and/or common positioning of the markers on groups 6, 3, 5, and 7. This is likely due to the fact that Yan et al. (2005) had almost twice the markers than Debener and Mattiesch (520 vs 278). These few examples show the importance of collaboration of different research groups in order to collaboratively answer the different questions being addressed. Probably the pinnacle of mapping in rose prior to the introduction of Next Generation Sequencing and SNPs as the marker of choice, was the creation of an integrated consensus map from four diploid populations resulting in a map with 597 markers spanning 530 cM (Spiller et al., 2011). This map utilized AFLP, SSR, NBS-LRR, Protein Kinase, and RGA markers. With the creation of this map, the naming of the rose linkage groups was standardized and loci associated with floral development, flower number, number of prickles, blackspot resistance, and powdery mildew resistance were mapped. This map was similar in length and marker number when compared to Yan et al. (2005) but Spiller et al. (2011) state that their marker order is more reliable due to more populations and individuals used for analysis. With the introduction of Genotyping by Sequencing (GBS), many more SNP markers are used for mapping. However, due to the sheer quantity of markers found using GBS, many filtering steps and binning is necessary to cut down on the number of markers used in mapping to help with computation time. An integrated consensus map was created by Yan et al. (2018), combining three diploid

populations resulting in a map with 3527 total markers (20 SSR markers as anchors, and 3507 SNPs). These populations were phenotyped for blackspot resistance, architectural traits, and flowering traits.

Markers used in tetraploid rose mapping populations have historically been limited to dominantly scored markers scored as present or absent as the marker technologies of AFLP, RFLP, and SSR, have limitations in seeing SNPs, small indels, and determining dosage of alleles (Rajapakse et al., 2001; Zhang et al., 2006; Gar et al., 2011; Koning-Boucoiran et al. 2012; Yu et al., 2015; Bourke et al., 2018). In addition to the restrictive marker types, small polyploid mapping families further constrict the ability to distinguish the dosage of the alleles due to large segregation ratios (Sorrells, 1992). However, as the technology has evolved to use SNPs, dosage of the SNPs can be determined via deep GBS sequencing (50X depth) or using the signal intensity of SNP arrays (Bajgain et al., 2016; Voorrips et al., 2011). A tetraploid cut rose mapping population was genotyped using the 68k WagRhSNP Axiom Array (Koning-Boucoiran et al., 2015) and the authors found that 3 chromosomes showed disomic preferential pairing whereas all the rest paired tetrasomically (Bourke et al., 2017). They state that the preferential pairing is dependent on the mapping population and the genetic background of the roses being used.

The Rose Genome Sequence Initiative has sequenced the diploid rose *Rosa chinensis* ‘Old Blush’ (Foucher et al., 2015; Bendahmane et al., 2015). The rose however is a highly heterozygous crop making it difficult to create a high quality assembly. To circumvent this issue, a double haploid was created for use in sequencing

(Saint-Oyant et al., 2018; Raymond et al., 2018). Before the rose sequence was released for public use, the strawberry sequence (v2.0.a1) was used for the alignment of the rose GBS data due to synteny between strawberry and rose to construct a diploid rose consensus map with five inter-related populations at Texas A&M University (Yan et al., 2018; Bourke et al., 2017). Work is being done to identify QTL regions responsible for black spot resistance, cercospora resistance, architectural traits, and flower traits, using the consensus map created.

The long term goal of this project is to determine if there are alleles for resistance to black spot, cercospora, defoliation, and RRV, and alleles for flower intensity and plant architecture within our rose germplasm. If there are such alleles, the goal is to find the specific haplotypes conferring disease resistance. If a Mendelian trait locus (MTL) or quantitative trait loci (QTL) and haplotypes are found for resistance, validation studies need to be performed with closely related or unrelated populations to confirm that the marker(s) are useful in predicting resistance. This information could then be used to create less expensive KASP assays which would allow the breeder to screen progeny in the greenhouse for potential resistant seedlings before placing the seedlings out in 3+ year field trials (Debener and Byrne, 2014). This ultimately will save time and money while simultaneously accelerating breeding efforts to release roses with disease resistance and favorable horticultural traits.

Conclusions

The objective of this dissertation research is to create two inter-related tetraploid rose families, consisting of 150-200 individuals each to study the inheritance of rose rosette virus, black spot of rose, cercospora, defoliation, flowering intensity, plant size and apical dominance. To study the inheritance of these traits, we have to genotype and phenotype these individuals, create a linkage map, and perform a QTL analysis on these traits.

Literature Cited

Allington, W.B., R. Staples, and G. Viehmeyer. 1968. Transmission of rose rosette virus by the Eriophyid mite *Phyllocoptes fructiphilus*. Journal of Economic Entomology 61:1137-1140.

Armine, J.W. 1996. *Phyllocoptes fructiphilus* and biological control of multiflora rose. World Crop Pests 6:741-749.

Armine, J.W., D.F. Hindal, T.A. Stasny, R.L. Williams, and C.C. Coffman. 1988. Transmission of the rose rosette disease agent to *Rosa multiflora* by *Phyllocoptes fructiphilus* (Acari: Eriophyidae). Entomological News 99:239-252.

Arús, P. and S. Gardiner. 2007. Genomics for improvement of Rosaceae temperate tree fruit. Genomics-Assisted Crop Improvement. Springer Netherlands. pp. 357-397.

Babu, B., B.K. Washburn, K. Poduch, G.W. Knox, and M.L. Paret. 2016. Identification and characterization of two novel genomic RNA segments RNA5 and RNA6 in rose rosette virus infecting roses. Acta virologica 60:156–165.

Bajgain, P., M.N. Rouse, and J.A. Anderson. 2016. Comparing genotyping-by-sequencing and single nucleotide polymorphism chip genotyping for quantitative trait loci mapping in wheat. Crop Science 56:1-17.

Bendahmane, M., J. Just, P. Vergne, O.Raymond, A. Dubois, J. Szcesi, S-H. Yang, X. Fu, J. Gouzy, S. Carrere, L. Legrand, P. Wincker, A. Lemainque, J-M. Aury, A. Couloux, F. Foucher, L. Hamama, L. Hilbrand-Saint_Oyant, S. Sakr, N. Choisne, H. Quesneville, M. Le Bris, B. Goveto, S. Baudino, S. Moja, J.C. Caissard, K. Van Iaere, J. De Riek, T. Debener. J.M.S. Smulders, J. Salse, D. Zamir, D. Sargent, A. Bruneau, H. Yan, K. Tang, D. Byrne, S. Hokanson, A. Torres, and I. Amaya. 2015. The rose genome sequencing initiative, prospects and perspectives. Plant and Animal Genome XXIV Conference Abstract.

Blom, T.J. and M. J. Tsujita. 2003. Cut rose production, p. 594-600 in: A.V. Roberts,T. Debener, S. Gudin (eds.). Encyclopedia of Rose Science, Elsevier AcademicPress, Amsterdam, Netherlands.

Bourke, P.M., P. Arens, R.E. Voorrips, G.D. Esselink, C.F.S. Koning-Boucoiran, W.P.C. van't Westende, T. Santos Leonardo, P. Wissink, C. Zheng, G. van Geest, R.G.F. Visser, F.A. Krens, M.J.M. Smulders, and C. Maliepaard. 2017. Partial preferential chromosome pairing is genotype dependent in tetraploid rose. The Plant Journal 90:330–343.

Bourke, P.M., G. van Geest, R.E. Voorrips, J. Jansen, T. Kranenburg, et al. 2018. polymapR—linkage analysis and genetic map construction from F1 populations of outcrossing polyploids. Bioinformatics 34: 3496–3502. doi: 10.1093/bioinformatics/bty371.

Bourke, P.M., R.E. Voorrips, R.G.F. Visser, and C. Maliepaard. 2018. Tools for Genetic Studies in Experimental Populations of Polyploids. Frontier in Plant Science 9: 513. doi: 10.3389/fpls.2018.00513.

Byrne, D., N. Anderson, T. Evans, S. Collins, B. England, K. Solo, A. Windham, F. Hale, M. Windham. 2017. Evaluation of rose cultivars for resistance to rose rosette disease. International Society of Horticultural Science. VII International Symposium on Rose Research and Cultivation. Abstract.

Byrne, D.H., P. Klein, M. Yan, E. Young, J. Lau, et al. 2018. Challenges of breeding rose rosette–resistant roses. HortScience 53:604-608.

Catchen, J., P.A. Hohenlohe, S. Bassham, A. Amores, and W.A. Cresko. 2013. Stacks: an analysis tool set for population genomics. Molecular ecology 22: 3124–3140.

Condit, I.J. 1933. A mosaic of the fig in California. Phytopathology 23:887–896.

Conners, I.L. 1941. Twentieth annual report of the Canadian plant disease survey, 1940.

Crespel, L., M. Chirollet, C. E. Durel, D. Zhang, J. Meynet, S. Gudin. 2002. Mapping of qualitative and quantitative phenotypic traits in *Rosa* using AFLP markers. Theoretical and Applied Genetics 105:1207-1214.

Crespel, L., M. Sigogne, N. Donès, D. Relion, and P. Morel. 2013. Identification of relevant morphological, topological and geometrical variables to characterize the architecture of rose bushes in relation to plant shape. Euphytica 191:129–140.

De Vries, D.P. and L. A. M. Dubois. 1978. On the transmission of the yellow flower colour from *Rosa foetida* to recurrent flowering hybrid tea-roses. Euphytica. 27:205-210.

Debener, T. and D.H. Byrne. 2014. Disease resistance breeding in rose: Current status and potential of biotechnological tools. Plant Science 228:107-117.

Debener, T. and L. Mattiesch. 1999. Construction of a genetic linkage map for roses using RAPD and AFLP markers. Theoretical and Applied Genetics 99:891-899.

Dela, G., E. Or, R. Ovadia, A. Nissim-Levi, D. Weiss, and M. Oren-Shamir. 2003. Changes in anthocyanin concentration and composition in 'Jaguar' rose flowers due to transient high-temperature conditions. Plant Science 164:333–340.

DeVor, B., A. Chase, L. Adcock, L. Gragnani, D. Kuack. 2013. Greenheart's guide to container rose production. Messick Company LLC. Campbell, CA.

Di Bello, P.L., T. Ho, I.E. Tzanetakis. 2015. The evolution of Emaraviruses is becoming more complex: seven segments identified in the causal agent of Rose rosette disease. Virus Research 210:241-244.

Dobhal, S., J. D. Olson, M. Arif, J. A. Garcia Suarez, and F.M. Ochoa-Corona. 2016. A simplified strategy for sensitive detection of *Rose rosette virus* compatible with three RT-PCR chemistries. Journal of Virological Methods. 232:47-56.

Dong, Q., X. Wang, D.H. Byrne, and K. Ong. 2017. Characterization of partial resistance to black spot disease of *Rosa* sp. HortScience 52:49–53.

Doudrick, R.L., W.R. Enns, M.F. Brown, and D.F. Millikan. 1986. Characteristics and role of the mite *Phyllocoptes fructiphilus* (Acari: Eriophyidae) in the etiology of Rose Rosette. Entomological News 97:163-168.

Doudrick, R.L., M.F. Brown, J.A. White, and D.F. Millikan. 1987. Graft and mechanical transmission of the Rose Rosette Agent. Transactions of the Missouri Academy of Science 21:81-86.

Dugo, M.L., Z. Satovic, T. Millian, G. I. Cubero, D. Rubiales, A. Cabrera, A.M. Torres. 2005. Genetic mapping of QTL controlling horticultural traits in diploid roses. Theoretical and Applied Genetics 111:511-520.

Epstein, A.H. and J.H. Hill. 1995. The biology of Rose Rosette Disease: A mite-associated disease of uncertain aetiology. Journal of Phytopathology 143:353-360.

Epstein, A.H. and J.H. Hill. 1999. Status of rose rosette disease as a biological control for multiflora rose. Plant Disease 83:92-101.

Epstein, A.H., J.H. Hill, and F.W. Nutter. 1997. Augmentation of rose rosette disease for biocontrol of multiflora rose (*Rosa multiflora*). Weed Science 45:172-178.

Foucher, F., L. Hibrand-Saint Oyant, L. Hamama, S. Sakr, H. Nybom, et al. 2013. Towards the rose genome sequence and its use in research and breeding. VI International Symposium on Rose Research and Cultivation 1064:167–175

Foucher, F.F., M.C. Chevalier, C.C. Corre, V.S.-F. Soufflet-Freslon, F.L. Legeai, et al. 2008. New resources for studying the rose flowering process. Genome 51:827-837. doi: 10.1139/G08-067.

Gar, O., D.J. Sargent, C.-J. Tsai, T. Pleban, G. Shalev, D.H. Byrne, and D. Zamir. 2011. An autotetraploid linkage map of rose (*Rosa* hybrida) validated using the strawberry (*Fragaria vesca*) genome sequence. PLOS ONE 6: e20463.

Genome Database for Rosaceae. 2017. Prunus avium; cerasus. 6 November 2017. <https://www.rosaceae.org/organism/Prunus/avium%3B-cerasus>.

Goretti, D., M. Silvestre, S. Collani, T. Langenecker, C. Méndez, et al. 2020. TERMINAL FLOWER1 functions as a mobile transcriptional cofactor in the shoot apical meristem. Plant Physiology 182: 2081-2095. doi: 10.1104/pp.19.00867.

Gordon, S.C., and C.E. Taylor. 1976. Some aspects of the biology of the raspberry leaf and bud mite (*Phyllocoptes (Eriophyes) Gracilis* Nal.) Eriophyidae in Scotland. Journal of Horticultural Science 51:501-508. doi: 10.1080/00221589.1976.11514719.

Gudin, S. 2000. Rose: genetics and breeding. Plant breeding reviews 17:159-190.

Guoliang, W. 2003. History of roses in cultivation. Encyclopedia of Rose Science. Elsevier, Oxford. 388-395.

Hackett, C.A., J.E. Bradshaw, R.C. Meyer, J.W. McNICOL, D. Milbourne, and R. Waugh. 1998. Linkage analysis in tetraploid species: a simulation study. Genetics Research 71:143–153.

Hagan, A., M. E Rivas-Davila, J. Akridge, and J. W Olive. 2005. Resistance of shrub and groundcover roses to black spot and Cercospora leaf spot, and impact of fungicide inputs on the severity of both diseases. Journal of Environmental Horticulture 23:77–85.

Hattendorf, A., M. Linde, L. Mattiesch, T. Debener, and H. Kaufmann. 2004. Genetic analysis of rose resistance genes and their localisation in the rose genome. Acta Horticulturae 651:123-130.

Heinrichs, F. 2008. International statistics flowers and plants vol. 56. AIPH. Union Fleurs. Brussels, Belgium.

Hindal, D.F., J.W. Armine, R.L. Williams, T.A. Stasny. 1988. Rose rosette disease on multiflora rose (*Rosa multiflora*) in Indiana and Kentucky. Weed Technology. 2:442-444.

Hibrand-Saint Oyant, L. Crespel, S. Rajapakse, L. Zhang, and F. Foucher. 2008. Genetic linkage maps of rose constructed with new microsatellite markers an locating QTL controlling flowering traits. Tree Genetics & Genomes 4:11-23.

Horst, R.K. and R.A. Cloyd. 2007. Compendium of rose diseases and pests. 2nd ed. The American Phytopathological Society, St. Paul, M.N.

Huang, C.H., G.E. Vallad, H. Adkison, C. Summers, E. Margenthaler, C. Schneider, J. Hong, J.B. Jones, K. Ong, and D. J. Norman. 2013. A Novel *Xanthomonas* sp. Causes bacterial spot of rose (*Rosa* spp.). Plant Disease 97:1301-1307.

Hummer, K.E. and J. Janick. 2009. Rosaceae: taxonomy, economic importance, genomics, p.1-17. In: K.M. Folta and S.E. Gardiner (eds.). Genetics and Genomics of Rosaceae. Springer, New York, NY.

Hutton, S. 2012. The future of the rose industry. American Rose Society Annual. 2012:36-37.

Illumina, I. 2015. An introduction to next-generation sequencing technology. <https://www.illumina.com/content/dam/illumina-marketing/documents/products/illumina_sequencing_introduction.pdf>.

Iwata, H., A. Gaston, A. Remay, T. Thouroude, J. Jeauffre, et al. 2012. The TFL1 homologue KSN is a regulator of continuous flowering in rose and strawberry. The Plant Journal 69:116–125. doi: https://doi.org/10.1111/j.1365-313X.2011.04776.x.

Jensen, S.G., and L.C. Lane. 1994. A new virus disease of corn and wheat in the High Plains. Phytopathology 84:1158.

Jian, H., H. Zhang, K. Tang, S. Li, Q. Wang, T. Zhang, X. Qiu, and H. Yan. 2010. Decaploidy in *Rosa praelucens* Byhouwer (Rosaceae) Endemic to Zhongdian Plateau, Yunnan, China. Caryologia 63:162–167.

Jones, A.T., S.C. Gordon, and D.L. Jennings. 1984. A leaf-blotch disorder of tayberry associated with the leaf and bud mite (*Phyllocoptes gracilis*) and some effects of three aphid-borne viruses. Journal of Horticultural Science 59:523–528. doi: 10.1080/00221589.1984.11515227.

Jones, A.T., P.L. Kumar, K.B. Saxena, N.K. Kulkarni, V. Muniyappa, et al. 2004. Sterility mosaic disease—the "green plague" of pigeonpea: advances in understanding the etiology, transmission and control of a major virus disease. Plant Disease 88:436–445.

Judd, W.S., C.S. Campbell, E.A. Kellogg, P.F. Stevens, and M.J. Donoghue. 1999. Plant systematics: a phylogenetic approach. Ecologia mediterranea 25:290-302.

Jung, S., S.P. Ficklin, T. Lee, C.-H. Cheng, A. Blenda, P. Zheng, J. Yu, A. Bombarely, I. Cho, S. Ru, K. Evans, C. Peace, A.G. Abbott, L.A. Mueller, M.A. Olmstead, and D. Main. 2014. The Genome Database for Rosaceae (GDR): year 10 update. Nucleic Acids Research 42:D1237–D1244.

Karlik, J.F., D.A. Golino, M.L. Flint. 2020. Roses: Diseases and Abiotic Disorders Management Guidelines--UC IPM. March 2021 <http://ipm.ucanr.edu/PMG/PESTNOTES/pn7463.html>.

Kawamura, K., L. Hibrand-Saint Oyant, L. Crespel, T. Thouroude, D. Lalanne, et al. 2011. Quantitative trait loci for flowering time and inflorescence architecture in rose. Theoretical and Applied Genetics 122:661–675. doi: 10.1007/s00122-010-1476-5.

Kawamura, K., L. Hibrand-Saint Oyant, T. Thouroude, J. Jeauffre, and F. Foucher. 2015. Inheritance of garden rose architecture and its association with flowering behaviour. Tree Genetics & Genomes 11:22. doi: 10.1007/s11295-015-0844-3.

Kegler, H. 1960. Das Ringfleckenmosaik der Eberesche (Sorbus aucuparia L.). Journal of Phytopathology 37:214–216. doi: 10.1111/j.1439-0434.1960.tb04035.x.

Kool, M.T.N. 1997. Importance of plant architecture and plant density for rose crop performance. Journal of Horticultural Science 72:195–203.

Kool, M.T.N., and E.F.A. Lenssen. 1997. Basal-shoot formation in young rose plants: effects of bending practices and plant density. Journal of Horticultural Science 72:635–644.

Kool, M.T.N., R. De Graaf, and C.H.M. Rou-Haest. 1997. Rose flower production as related to plant architecture and carbohydrate content: effect of harvesting method and plant type. Journal of Horticultural Science 72:623–633.

Koning-Boucoiran, C.F.S., G.D. Esselink, M. Vukosavljev, W.P.C. van 't Westende, V.W. Gitonga, et al. 2015. Using RNA-Seq to assemble a rose transcriptome with more than 13,000 full-length expressed genes and to develop the WagRhSNP 68k Axiom SNP array for rose (*Rosa* L.). Frontiers in Plant Science 6:249. doi: 10.3389/fpls.2015.00249.

Krussmann G. 1981. The complete book of roses. Timber Press. Portland OR.

LaFramboise, T. 2009. Single nucleotide polymorphism arrays: a decade of biological, computational and technological advances. Nucleic Acids Research 37:4181-4193. doi: 10.1093/nar/gkp552.

Laney, A.G., K.E. Keller, R.R. Martin, and I.E. Tzanetakis. 2011. A discovery 70 years in the making: characterization of the Rose rosette virus. The Journal of General Virology 92:1727-1732.

Liang, S., X. Wu, and D. Byrne. 2017. Flower-size heritability and floral heat-shock tolerance in diploid roses. HortScience 52:682–685. doi: 10.21273/HORTSCI11640-16.

Li-Marchetti, C., C. Le Bras, A. Chastellier, D. Relion, P. Morel, et al. 2017. 3D phenotyping and QTL analysis of a complex character: rose bush architecture. Tree Genetics & Genomes 13:112. doi: 10.1007/s11295-017-1194-0.

Linde. M. and T. Debener. 2003. Isolation and identification of eight races of powdery mildew of roses (*Podosphaera pannosa*) (Wallr.: Fr.) de Bary and the genetic analysis of the resistance gene *Rpp1*. Theoretical and Applied Genetics 107:265-262.

Lopez Arias, D.C., A. Chastellier, T. Thouroude, J. Bradeen, L. Van Eck, et al. 2020. Characterization of black spot resistance in diploid roses with QTL detection, meta-analysis and candidate-gene identification. Theoretical and Applied Genetics 133:3299-3321. doi: 10.1007/s00122-020-03670-5.

Lühmann, A.-K., M. Linde, and T. Debener. 2010. Genetic diversity of Diplocarpon rosae: implications on practical breeding. Acta Horticulturae 870:157-162.

Mangandi, J. and N.A. Peres. 2012. Cercospora leaf spot of rose. UF/IFAS Extension. 9 March 2017. <https://edis.ifas.ufl.edu/pdffiles/PP/PP26700.pdf>.

Martin, M., F. Piola, D. Chessel, M. Jay, and P. Heizmann. 2001. The domestication process of the modern rose: genetic structure and allelic composition of the rose complex. Theoretical and Applied Genetics 102:398-404.

Mascarini, L., G.A. Lorenzo, and F. Vilella. 2006. Leaf area index, water index, and red: far red ratio calculated by spectral reflectance and its relation to plant architecture and cut rose production. Journal of the American Society for Horticultural Science 131:313–319.

Mielke-Ehret, N. and H.P. Mühlbach. 2012. Emaravirus: a novel genus of multipartite negative strand RNA plant viruses. Viruses 4:1515-1536.

Mitra, M. 1931. Report of the imperial mycologist. https://www.cabdirect.org/cabdirect/abstract/19311100879.

Moraes, T.S., M.C. Dornelas, and A.P. Martinelli. 2019. FT/TFL1: Calibrating plant architecture. Frontiers in Plant Science 10. doi: 10.3389/fpls.2019.00097.

Peace, C., N. Bassil, D. Main, S. Ficklin, U.R. Rosyara, T. Stegmeir, A. Sebolt, B. Gilmore, C. Lawley, T.C. Mockler, D.W. Bryant, L. Wilhelm, and A. Iezzoni. 2012. Development and evaluation of a genome-wide 6K SNP array for diploid sweet cherry and tetraploid sour cherry. PLOS ONE 7:e48305.

Pemberton, H.B. and J.F. Karlik. 2015. A recent history of changing trends in USA garden rose plant sales, types, and production methods. In VI International Symposium on Rose Research and Cultivation 1064:223-234.

Pemberton, H.B., J.W. Kelly, and J. Ferare 2003. Pot rose production, p.587-593 in: A.V. Roberts,T. Debener, S. Gudin (eds.). Encyclopedia of Rose Science, Elsevier AcademicPress, Amsterdam, Netherlands.

Pemberton, H.B., K. Ong, M. Windham, J. Olson, and D.H. Byrne. 2018. What is rose rosette disease? HortScience 53:592–595.

Potter, D., T. Erikson, R.C. Evans, S. Oh, J.E. Smedmark, D.R. Morgan, M. Kerr, K.R. Roberson, M. Arsenault, T.A. Dickinson, and C.S. Campbell. 2007. Phylogeny and classification of Rosaceae. Plant Systematics and Evolution 226:5-43.

Raymond, O., J. Gouzy, J. Just, H. Badouin, M. Verdenaud, et al. 2018. The Rosa genome provides new insights into the domestication of modern roses. Nature Genetics 50:772. doi: 10.1038/s41588-018-0110-3.

Rajapakse, S., D.H. Byrne, L. Zhang, N. Anderson, K. Arumuganathan, and R.E. Ballard. 2001. Two genetic linkage maps of tetraploid roses. Theoretical and Applied Genetics 103:575–583.

Ratcliffe, O.J., I. Amaya, C.A. Vincent, S. Rothstein, R. Carpenter, et al. 1998. A common mechanism controls the life cycle and architecture of plants. Development 125:1609–1615.

Remay, A., D. Lalanne, T. Thouroude, F. Le Couviour, L. Hibrand-Saint Oyant, et al. 2009. A survey of flowering genes reveals the role of gibberellins in floral control in rose. Theoretical and Applied Genetics 119:767–781. doi: 10.1007/s00122-009-1087-1.

Saint-Oyant, L.H., T. Ruttink, L. Hamama, I. Kirov, D. Lakhwani, et al. 2018. A high-quality genome sequence of *Rosa chinensis* to elucidate ornamental traits. Nature Plants 4:473. doi: 10.1038/s41477-018-0166-1.

Shannon, S., and D.R. Meeks-Wagner. 1991. A mutation in the arabidopsis TFL1 gene affects inflorescence meristem development. The Plant Cell 3:877-892. doi: 10.1105/tpc.3.9.877.

Short, K.C. and A.V. Roberts. 1991. Rosa spp. (roses): in vitro culture, micropropagation, and the production of secondary products, p. 377–397. In: Y.P.S. Bajaj (ed.). Biotechnology in Agriculture and Forestry: Medicinal and Aromatic Plants III, vol. 15, Springer-Verlag, Amsterdam, Netherlands.

Shupert, D. A. 2005. Inheritance of flower, stem, leaf, and disease traits in three diploid interspecific rose populations. Master's thesis, Texas A&M University. Available electronically from http://hdl.handle.net/1969.1/4450.

Slykhuis, J.T. 1956. Wheat spot mosaic, caused by a mite-transmitted virus associated with wheat streak mosaic. Phytopathology 46:682-687.

Sorrells, M.E. 1992. Development and application of RFLPs in polyploids. Crop Science 32:1086-1091.

Spiller, M., M. Linde, L.H.-S. Oyant, C.-J. Tsai, D.H. Byrne, M.J.M. Smulders, F. Foucher, and T. Debener. 2011. Towards a unified genetic map for diploid roses. Theoretical and Applied Genetics 122:489–500.

Catchen, J. M., Amores, A., Hohenlohe, P., Cresko, W., & Postlethwait, J. H. 2011. Stacks: building and genotyping loci de novo from short-read sequences. G3: Genes| genomes| genetics, 1:171-182.

United States Department of Agriculture. 2015. 2012 Census of agriculture: census of horticultural specialties. Washington: United States Department of Agriculture.

United States Department of Agriculture. 2020. 2017 Census of agriculture: census of horticultural specialties. Washington: United States Department of Agriculture.

Von Malek, B. and T. Debener. 1998. Genetic analysis of resistance to blackspot (*Diplocarpon rosae*) in tetraploid roses. Theoretical and Applied Genetics 96:228-231.

Voorrips, R.E., G. Gort, and B. Vosman. 2011. Genotype calling in tetraploid species from bi-allelic marker data using mixture models. BMC Bioinformatics 12:172. doi: 10.1186/1471-2105-12-172.

Vukosavljev, M., P. Arens, R.E. Voorrips, W.P. van ‘t Westende, G. Esselink, P.M. Bourke, P. Cox, W.E. van de Weg, R.G. Visser, C. Maliepaard, and M.J. Smulders. 2016. High-density SNP-based genetic maps for the parents of an outcrossed and a selfed tetraploid garden rose cross, inferred from admixed progeny using the 68k rose SNP array. Horticulture Research 3: 16052.

Wang, Y., and J. Li. 2008. Molecular basis of plant architecture. Annual Review of Plant Biology 59:253-279. doi: 10.1146/annurev.arplant.59.032607.092902.

Whitaker, V.A., J.M. Bradeen, T. Debener, A. Biber, S.C. Hokanson. 2010. Rdr3, a novel locus conferring black spot disease resistance in tetraploid rose: genetic analysis, LRR profiling, and SCAR marker development. Theoretical and Applied Genetics 120:573-585.

Whitaker, V.M., K. Zuzek, and S.C. Hokanson. 2007. Resistance of 12 rose genotypes to 14 isolates of Diplocarpon rosae Wolf (rose blackspot) collected from eastern North America. Plant Breeding 126:83–88. doi: 10.1111/j.1439-0523.2007.01339.x.

Windham, M., A. Windham, F. Hale, and J. Armine Jr. 2014. Observations on rose rosette disease. University of Tennesee. 14 February 2017. <http://www.newenglandgrows.org/pdfs/ho_WindhamRoseRosette.pdf>.

Wu, X., S. Liang, and D.H. Byrne. 2019. Heritability of plant architecture in diploid roses (Rosa spp.). HortScience 54:236–239. doi: 10.21273/HORTSCI13511-18.

Xu, Q., X. Wen, and X. Deng. 2007. Cloning of two classes of PR genes and the development of SNAP markers for powdery mildew resistance loci in chestnut rose (*Rosa roxburghii* Tatt). Molecular Breeding 19:179-191.

Xue, A.G. and C. G. Davidson. 1998 Components of partial resistance to black spot disease (*Diplocarpon rosae* Wolf) in Garden Roses. HortScience. 33:96-99.

Yan, M., D.H. Byrne, P.E. Klein, J. Yang, Q. Dong, et al. 2018. Genotyping-by-sequencing application on diploid rose and a resulting high-density SNP-based consensus map. Horticulture Research 5:17. doi: 10.1038/s41438-018-0021-6.

Yan, M., D.H. Byrne, P.E. Klein, W.E. van de Weg, J. Yang, et al. 2019. Black spot partial resistance in diploid roses: QTL discovery and linkage map creation. Acta Horticulturae 1232:135–142. doi: 10.17660/ActaHortic.2019.1232.21.

Yan, Z., C. Denneboom, A. Hattendorf, O. Dolstra, T. Debener, P. Stam, and P.B. Visser. 2005. Construction of an integrated map of rose with AFLP, SSR, PK, RGA, RFLP, SCAR and morphological markers. Theoretical and Applied Genetics 110:766-777.

Yamaguchi, H., S. Nagatomi, T. Morishita, K. Degi, A. Tanaka, N. Shikazono, and Y. Hase. 2003. Mutation induced with ion beam irradiation in rose. Nuclear Instruments and Methods in Physics Research Section B: Beam Interactions with Materials and Atoms 206:561–564. doi: 10.1016/S0168-583X(03)00825-5.

Yu, C., L. Luo, H. Pan, X. Guo, H. Wan, and Q. Zhang. 2015. Filling gaps with construction of a genetic linkage map in tetraploid roses. Frontiers in Plant Science. doi: 10.3389/fpls.2014.00796

Zhang, L.H., D.H. Byrne, R.E. Ballard, and S. Rajapakse. 2006. Microsatellite marker development in rose and its application in tetraploid mapping. Journal of the American Society for Horticultural Science 131:380–387.

Zlesak, D. C. 2007. Rose, p. 695-738 In: Anderson N. O. (ed.). Flower breeding and genetics: issues, challenges and opportunities for the 21st century. Springer Science and Business Media. Netherlands.

Zurn, J.D., D.C. Zlesak, M. Holen, J.M. Bradeen, S.C. Hokanson, et al. 2020. Mapping the black spot resistance locus *Rdr3* in the shrub rose 'George Vancouver' allows for the development of improved diagnostic markers for DNA-informed breeding. Theoretical and Applied Genetics 133:2011-2020. doi: 10.1007/s00122-020-03574-4.

Zurn, J.D., D.C. Zlesak, M. Holen, J.M. Bradeen, S.C. Hokanson, et al. 2018. Mapping a novel black spot resistance locus in the climbing rose Brite Eyes™ ('RADbrite'). Frontiers in Plant Science 9:1730. doi: 10.3389/fpls.2018.01730.

CHAPTER II

MAPPING DISEASE RESISTANCE IN TWO TETRAPLOID GARDEN ROSE POPULATIONS AND FINDING MARKERS FOR MARKER ASSISTED SELECTION FOR ACCELERATED BREEDING

Abstract

Two populations, *Rosa* L. 'ORAfantanov' (Stormy Weather™) x *Rosa* L. 'Radbrite' (Brite Eyes™) (SWxBE) and *Rosa* L. 'Radbrite' (Brite Eyes™) x *Rosa* L. 'BAIgirl' (Easy Elegance® My Girl) (BExMG), were used to study resistance to rose rosette disease, black spot, cercospora leaf spot, and defoliation. The SWxBE and BExMG populations were used to construct linkage maps with R package 'polymapR' mapping 4,047 and 4,220 unique positions on 7 linkage groups (LGs), respectively. TetraploidSNPMap, R package 'QTLpoly', and R package 'GWASpoly' were used to identify QTL for rose rosette disease on LGs 3 and 5, black spot on LGs 3, 5, and 7; cercospora leaf spot on LGs 1, 4, and 5; and defoliation on LGs 3, 5, and 7. Markers associated with less disease incidence were used to identify and select 18 progenies in the BExMG family that carried 2 resistance alleles against black spot and one resistance allele to cercospora leaf spot for future breeding.

Introduction

Garden roses (*Rosa* spp.) are important ornamental plants worldwide. In the USA, garden roses had about $203 million in sales 2014 and $168 million in sales in

2019 (USDA NASS, 2015 & USDA NASS, 2020). Garden roses along with cut flowers were valued at 24 billion Euros worldwide in 2008 ($42.3 billion USD equivalent adjusted for both historical exchange rate and inflation) (Heinrichs, 2008). In addition to the horticultural characteristics of the plant, increased disease resistance is highly desirable to consumers (Byrne et al., 2017; Walizcek et al., 2018; Chavez et al., 2019). Therefore, breeding efforts are geared towards creating cultivars with superior disease resistance and horticultural traits when compared to what is currently commercially available (Debener and Byrne, 2014).

The most important fungal disease that affects garden roses is black spot (*Diplocarpon rosae* F.A. Wolf). This fungus causes black spots with feathery margins on the upper portion of the leaf (Horst and Cloyd, 2007). Black spot infection is favored by humid summer climates. As the infection progresses, the foliage becomes chlorotic and severe infections cause defoliation.

Another major fungal disease affecting roses is cercospora leaf spot (*Cercospora rosicola* Pass.). From here on, cercospora leaf spot will be called cercospora. It is a fungal pathogen with circular lesions characterized a small white or tan necrotic area in the center with brown concentric rings. Normally, the edges of the lesion are smooth when compared to black spot (Mangandi and Peres, 2012). In the past, cercospora was not considered a major rose problem, however as major strides were made in selecting roses resistant to black spot, cercospora has emerged as an important disease. Cercospora has most likely been present and affecting roses but the effects were masked

by the presence of black spot that causes defoliation (Hagan et al., 2005). Only in extreme cases of cercospora infection is defoliation observed.

A very important emerging disease that is significantly affecting the garden rose industry in the United States is Rose Rosette Disease (RRD), a disease caused by the Rose Rosette Virus (RRV) (Laney et al., 2011; Di Bello et al., 2015) and vectored by a microscopic eriophyid mite *Phyllocoptes fructiphilus* (Allington et al., 1968). Common RRD symptoms include large masses of reddish prolific twisted growth extending from an otherwise healthy-looking bush. The term "witches' broom" is often used to describe these growths. The rosettes are identified by having strapped leaves (long and thin) accompanied with shorter internodes and increased thorniness on cultivars with prickles/thorns (Windham et al., 2014). In addition to RRD causing visually displeasing growth, infection of RRV will normally kill susceptible plants within 2 to 3 years after infection.

Disease lesions and defoliation from severe black spot and cercospora infections influence the horticultural aesthetic of the plant. Thus breeding efforts in the Texas A&M University Rose Breeding program are focused on developing lines which have resistance to black spot, cercospora and rose rosette disease (Byrne et al., 2018).

Many garden roses are tetraploid which are genetically more complex than their diploid counter parts. Due to the genetic complexities and relative importance, there has been little genetic research done on tetraploid garden roses. Only three high density SNP tetraploid rose linkage maps have been published to date (Zurn et al., 2018; Zurn et al., 2020; Bourke et al., 2017). Therefore, in the present research, two bi-parental tetraploid

populations were created to study defoliation and disease resistance of black spot, cercospora, and RRD. Linkage maps were constructed, and QTL scans identified regions of interest for the traits studied.

Currently there are three linkage mapping software packages available for mapping autopolyploids. The oldest, TetraploidMap, was updated to allow for more markers and renamed TetraploidSNPMap (Hackett et al., 2017). TetraploidSNPMap can conduct linkage mapping for genotypes assigned allele dosage and conduct interval mapping QTL scans. However, the program has an upper limit of 8000 markers. Two newer software packages available for linkage mapping are polymapR (Bourke et al., 2018) and MAPpoly (Mollinari and Garcia, 2019). All three software packages can order markers using MDSmap (Preedy and Hackett, 2016). MDSmap implements multi dimension scaling for marker ordering. MAPpoly also has the ability to estimate the marker order given an *a priori* order which can be defined by the physical position of the markers.

After linkage mapping, phased maps can be imported into TetraploidSNPMap (Hackett et al., 2017) and QTLpoly (Pereira et al., 2020) for QTL interval mapping. A genome-wide association analysis (GWAS) using GWASpoly (Rosyara et al., 2016) was used to support these findings. Interval QTL mapping methods explore the probability that intervals between markers on a linkage map are affecting the trait we are studying. This takes into account both the marker order of the linkage map and the phasing of the markers for each individual used to create the linkage map (Miles and Wayne, 2008). GWAS methods are different in that they look for significant marker trait associations

and is testing each marker separately for significance to the trait. Due to the large number of markers compared to numbers of individuals used, Bonferroni corrections or a false discovery rate needs to be implemented to take into account false positives (Alqudah et al., 2020).

Materials and Methods

Population Development

Two F_1 populations, *Rosa* L. 'ORAfantanov' (Stormy Weather™) x *Rosa* L. 'Radbrite' (Brite Eyes™) (SWxBE) n=200 and *Rosa* L. 'Radbrite' (Brite Eyes™) x *Rosa* L. 'BAIgirl' (Easy Elegance® My Girl) (BExMG) n=157, were developed in spring 2016 by the Texas A&M University Rose Breeding and Genetics Lab and Weeks Roses. From here on out the trade names of these cultivars will be used instead of their proper scientific name which indicates their plant protection names. These trade names Stormy Weather™, Brite Eyes™, and Easy Elegance® My Girl, will be referred to as Stormy Weather, Brite Eyes, and My Girl. They will also be abbreviated as SW, BE, and MG, respectively. In 2017, the populations were grown from seeds in Somerville, TX, and propagated for multi-site evaluation (Table 2.1). The incidence of RRD was evaluated in Crossville, TN, and the incidence of black spot and cercospora resistance was assessed in Somerville and Overton, TX.

Table 2.1. Tetraploid garden rose (*Rosa* spp.) mapping populations planted in Crossville, TN, Somerville, TX, and Overton, TX in April 2018, for the assessment of RRD, black spot, and cercospora leaf spot incidence in 2019.

Female	Male	# of Individuals[d]
SW[a]	BE[b]	202 (200)
BE	MG[c]	161 (157)

[a] *Rosa* L. 'ORAfantanov' (Stormy Weather™)

[b] *Rosa* L. 'Radbrite' (Brite Eyes™)

[c] *Rosa* L. 'BAIgirl' (Easy Elegance® My Girl)

[d] Number of individuals genotyped and used for linkage mapping, number in parenthesis is number of individuals with both genotypic and phenotypic data used for QTL analysis

The two mapping populations (rooted cuttings) were planted in a randomized complete block design (RCBD) (2 reps) at 4 foot spacing in April of 2018 at the Texas A&M University Horticulture Teaching Research and Extension Center in Somerville, TX (30.52, -96.42), approximately ten miles from the campus of Texas A&M University, College Station, TX. Black landscape fabric was used for weed suppression and overhead irrigation was installed to encourage black spot development. The soil type at this location is Belk clay. Plants were fertilized and irrigated as needed. No fungicides were sprayed. Plants were pruned once in the spring of 2018 to a uniform size of around 1.5 cubic feet. At the Texas A&M AgriLife Research and Extension Center in Overton, TX (32.30, -94.98), 2 reps of the rooted cuttings were planted in April 2018 on 4 foot spacing in a RCBD. Rows were on 12 foot centers. Landscape fabric was used for weed suppression, and drip irrigation was placed underneath the landscape fabric. Irrigation and fertilizer was applied as needed. The soil type at this location was a Bowie Fine Sandy Loam. Plants were pruned in the winter to 50% reduction in canopy. No

fungicides were used and overhead irrigation was not necessary for disease development. At the University of Tennessee AgResearch Plateau Research and Education Center in Crossville, TN (36.01, -85.13), 2 reps of the rooted cuttings were planted in the Spring of 2018 using a RCBD on 4 foot spacing with drip irrigation and mulched with wood and bark chips for weed control. The soil type at this location is a Lily Loam. Natural RRD infections were augmented by planting inoculum rows with RRD infected plants on the outside rows and in the middle of the field. Natural infection was augmented by clipping rosettes collected from infected plants onto healthy plants 2-3 times a year. Infected wild roses (*Rosa multiflora*) growing in the woods surrounding the field also served as a source of inoculum.

Phenotyping

Plants were phenotyped monthly for black spot incidence, cercospora incidence, and level of defoliation from June to November 2019 in Somerville, TX, and in June, September, and August in Overton, TX. Data was recorded using Field Book (Rife and Poland, 2014). RRD visual ratings were taken in September 2019 in Crossville, TN. Plants were tested for the presence of the virus via real-time quantitative PCR (rt-qPCR) using methods described in Shires et al. (2018, 2020). RNA extraction was done using a modified direct antigen-capture method described by Shires et al. (2018, 2020) by crushing samples in ELISA bags and isolating the RRV viral particles via adhesion to the polypropylene walls of 1.5 ml microcentrifuge tubes. PCR detection of RRV was done using the RRV2 primer sets (Dobhal et al., 2016). The thermocycler was run for 40

cycles at 94°C for 30 seconds, 51°C for 30 seconds, and 72°C for 60 seconds. Final extension was set at 72°C for 10 minutes.

Black spot, cercospora, and defoliation were rated on a scale of 0-9 in which 0 represents no disease in canopy or a lack of defoliation. A rating of 1 would be representative of a plant that had 1-10% of the leaves with disease lesions or 1-10% of the leaves missing. A rating of 2 would represent 11-20%, et cetera.

Dr. Mark Windham at the University of Tennessee developed an assessment scale for RRD by rating the severity and the number of rosettes per plant. To rate the severity, 0 = no symptoms, 1 = small single shoot with rosetting, 2 = 2-3 shoots with rosetting, 3 = 4 or more shoots with rosetting. Rosettes per plant are rated as 0 = no rosettes, 1 = 1 rosette per plant, 2 = 2 rosettes per plant, 3 = 3 or more rosettes per plant (Windham et al., 2014). The rose rosette phenotyping was done by the Windham Lab at the University of Tennessee. In addition to visual phenotypic scores, RT-qPCR was used to quantify the viral load in the plants over the two years (Dobhal et al., 2016). Visual phenotypic ratings and the PCR results using the threshold cycle as the quantitative trait were used for QTL analysis. The C_t values for detection of RRV were between 5-37 cycles. Samples with C_t values less than or equal to 29 and greater than 5 were considered to be strong positives while samples between 30-37 were considered moderate to weakly positive for presence of RRV (Shires, 2020). The C_t values ranged from 18 to 33. These C*t* values were used for QTL scans and GWAS scans with the negative samples assigned the value of 37.

Phenotypic data was analyzed using JMP 15 (SAS Institute Inc. Cary, NC, USA) and SAS 9.4 (SAS Institute Inc. Cary, NC, USA). Normality and homogeneity of variance was checked for each trait. The raw phenotypic data of black spot, cercospora, defoliation, rose rosette ratings, and rose rosette RT-qPCR ratings did not fit a normal distribution. Transformations (square root, x^2, natural log, or log) did not make the data normal. Thus, comparisons should use non-parametric methods. However, the non-parametric comparisons grouped means similarly to Tukeys' Studentized Tests.

Heritability Estimates

Mixed models were used to estimate variance due to location, month, replication, family, and genotype using the Restricted Estimated Maximum Likelihood (REML) method in SAS 9.4 (SAS Institute Inc. Cary, NC, USA). Mixed models using REML methods are better at estimating model effects when there is random missing data which is common in field research (Holland, 2003). While REML methods require normality of data it seems that the method is still robust on skewed data (Banks et al., 1985). Heritabilities were calculated from the estimated variances. Models were constructed using both location's data separately and together by including both two-way (genetic x month) and three-way interactions (genetic x location x month). Models were considered with and without other disease phenotypes as covariates by setting them as fixed effects using proc mixed in SAS. Models that included the covariates showed significant effects of the covariates on the dependent variable, however, the Akaike information criterion (AIC) improvement was minimal while the residual increased. Other models tested

included considering each month by location interaction as a separate environment. The model selected for estimating variances to calculate heritability was based on which model had the lowest residuals, AIC, and Bayesian information criterion (BIC).

The area under the disease progress curve (AUDPC) (Simko and Piepho, 2011) was calculated using the following equation where y_i is the score of the disease, at the *i*th observation and t_i is time at the *i*th observation with *n* total observations. AUDPC was calculated for all traits.

$$AUDPC = \sum_{i=1}^{n-1} \frac{y_i + y_{i+1}}{2} \times (t_{i+1} - t_i)$$

Variance components were calculated using the models (Table 2.2) where y is the observed phenotypic score and all factors of the model were considered random. Additive variance (Va) was attributed to the variance between the families (σ_{family}) and the non-additive variance (Vd) was from the variance between the progeny within a family ($\sigma_{progeny[family]}$). In studies with multiple bi-parental families with several parents, the additive variance is calculated by estimating parental variances as the sum of the female and male parental variances (Liang et al., 2017). However, since our two mapping populations only have three parents, we can only estimate additive variance as the variance between the two half sib families. A good approximation for the combination of the male and female parental variances is the collapse of that term into a family term. Narrow and broad sense heritabilities were calculated from the variances obtained from the mixed models (Table 2.3).

Table 2.2. Models used to calculate heritability and environmental effects for two tetraploid garden rose mapping populations.

	Models
Somerville or Overton alone AUDPC	$y = \sigma^2_{family} + \sigma^2_{progeny[family]} + \sigma^2_{rep[month]} + \sigma^2_{month} + \sigma^2_{month\ x\ family} + \sigma^2_{month\ x\ progeny[family]} + \sigma^2_{error}$ $y = \sigma^2_{family} + \sigma^2_{progeny[family]} + \sigma^2_{environment} + \sigma^2_{rep[environment]} + \sigma^2_{environment\ x\ family} + \sigma^2_{environment\ x\ progeny[family]} + \sigma^2_{error}$
Full model with three-way interaction	$y = \sigma^2_{family} + \sigma^2_{progeny[family]} + \sigma^2_{location} + \sigma^2_{month\ [location]} + \sigma^2_{rep[location*\ month]} + \sigma^2_{location\ x\ family} + \sigma^2_{location\ x\ progeny[family]} + \sigma^2_{month\ x\ family} + \sigma^2_{month\ x\ progeny[family]} + \sigma^2_{location\ x\ month\ x\ family} + \sigma^2_{location\ x\ month\ x\ progeny[family]} + \sigma^2_{error}$
Models with each location by month combination as a separate environment	$y = \sigma^2_{family} + \sigma^2_{progeny[family]} + \sigma^2_{environment} + \sigma^2_{environment\ x\ family} + \sigma^2_{environment\ x\ progeny[family]} + \sigma^2_{error}$

Table 2.3. Variance components, abbreviations, and heritability calculations.

Va	Additive variance = σ^2_{family}
Vd	Non-additive variance = $\sigma^2_{progeny[family]}$
Vg	Genotypic variance = Va + Vd = $\sigma^2_{family} + \sigma^2_{progeny[family]}$
Vgxe	Genotype by Environment variance (including both locations) = $\sigma^2_{location\ x\ family} + \sigma^2_{location\ x\ progeny[family]} + \sigma^2_{month\ x\ family} + \sigma^2_{month\ x\ progeny[family]} + \sigma^2_{location\ x\ month*family} + \sigma^2_{location\ x\ month*progeny[family]}$ Genotype by Environment variance (locations calculated separately) = $\sigma^2_{month\ x\ family} + \sigma^2_{month\ x\ progeny[family]}$
Vp	Phenotypic variance = (Va+Vd+Vg×e/E)+(residual/rE)
r	Number of reps
e	Number of environments
h^2	Va/Vp
H^2	=(Va+Vd)/Vp

Heritability estimates were calculated using an entry means method where r is the number of evaluation environments and e is the number of reps:

$$H^2_{(progeny\ mean\ basis)} = \frac{\sigma^2_{progeny}}{\sigma^2_{progeny} + \frac{\sigma^2_{progeny\ x\ environment}}{r} + \frac{\sigma^2_{error}}{re}}$$

Narrow sense heritability, h^2, was calculated dividing the variance between the families by the total phenotypic variance $h^2 = (\sigma^2_{family}) / (\sigma^2_{family} + \sigma^2_{progeny[family]} + \sigma^2_{location\ x\ family} + \sigma^2_{location\ x\ progeny[family]} + \sigma^2_{month\ x\ family} + \sigma^2_{month\ x\ progeny[family]} + \sigma^2_{location\ x\ month\ x\ family} + \sigma^2_{location\ x\ month\ x\ progeny[family]} + \sigma^2_{error})$. The GxE interaction terms were divided by 9 as there were 9 individual environments in which data was recorded. The error term was divided by 18 as two replications were evaluated in each environment. The broad sense heritability (H^2) was calculated similarly with the only difference being the numerator being the sum of the variance between the families and the variance due to difference within the family $H^2 = (\sigma^2_{family} + \sigma^2_{progeny[family]}) / (\sigma^2_{family} + \sigma^2_{progeny[family]} + \sigma^2_{location\ x\ family} + \sigma^2_{location\ x\ progeny[family]} + \sigma^2_{month\ x\ family} + \sigma^2_{month\ x\ progeny[family]} + \sigma^2_{location\ x\ month\ x\ family} + \sigma^2_{location\ x\ month\ x\ progeny[family]} + \sigma^2_{error})$.

Genotyping and Allele Dosage Calling

Unexpanded young leaf tissue was collected, flash frozen in liquid nitrogen and stored at -80°C until DNA extraction. DNA was extracted using a the CTAB protocol described by Yan et al., (2018). Extracted DNA samples were incubated with RNase at 37°C and purified using the OneStep™ PCR Inhibitor Removal Kit (Zymo Research, Irvine, CA, USA). Extracted DNA samples were quantified using a DS-11

spectrophotometer (DeNovix Inc, Wilmington, DL, USA) using Accublue® high dsDNA Quantification standards (Biotium, Inc., Fremont, CA, USA). DNA samples with a concentration of greater than 50 ng/µL were sent to Thermo Fisher Scientific for genotyping on the Axiom WagRhSNP 68k array (Koning-Boucoiran et al., 2015). The SNPs on this array were designed using RNA-Seq from tetraploid cut and garden roses and a diploid *Rosa multiflora* hybrid. For each SNP on the WagRhSNP 68k array, there are two probes, one for the forward and another for the reverse strand of DNA. Parental genotypes were replicated as 4 separate extraction events as a quality control for making sure the parental genotypes were well genotyped.

The raw light intensity data files (.cel files) from Thermo Fisher were aggregated using Axiom Analysis Suite and R package 'SNPolisher' (v 2.0.3; Affymetrix, Inc.). Dosage allele calling was performed using the default parameters of the 'saveMarkerModels' function indicating the parents of the cross using the 'pop.parents' and 'population' arguments of the R package 'fitPoly' (v 3.0.0; Voorrips et al., 2011). The WagRhSNP 68k array was designed to have two probes (forward and reverse strand) per SNP and fitPoly scores all probes as separate "markers". A custom R script combined the data from both probes that represented each SNP. Probes with the same allele dosage assignment and those with only one probe that was called were kept, whereas probes that had differing genotype calls were discarded. About 18.9% of the markers were consistent between the two probes, 37% having only one probe being called, 12% having different calls, and 32% were not called (Table 2.4). Markers were then filtered for only those that had both parental calls resulting in 38,459 and 38,482

markers in the SWxBE and BExMG mapping populations respectively. Filtering for non-segregating markers, progeny incompatibility, markers with missing data cutoff = 0.01, missing genotype calls per individual cutoff = 0.075, and binning markers with identical segregation, resulted in 5,396 and 6,969 markers respectively used for linkage mapping in the SWxBE and BExMG mapping populations. The parental genotyping calls were less than 0.5% different between the 4 replicates (0.25% - 0.42% range) and a consensus parental call was created for the markers that were different between genotyping runs. Principle component analysis on the markers from the function 'PCA_progeny' in 'polymapR' identified off types (Figure 2.1) that were removed from the analysis.

Table 2.4. WagRhSNP 68K array marker call comparison between the two oligonucleotide fragments for each marker for two tetraploid garden rose families. Markers with congruent and single probe calls were kept while markers with probes that had different calls were discarded. Averages were calculated by summation of the number of markers classified in each group below for each individual in the mapping population.

Family	Congruent calls	Single probe calls	Different Probe calls	Not called
SWxBE	13000 (18.9%)	25285 (36.8%)	8500 (12.4%)	21939 (31.9%)
BExMG	12969 (18.9%)	25350 (36.9%)	8425 (12.2%)	21979 (32.0%)

SW - *Rosa* L. 'ORAfantanov' (Stormy Weather™)
BE - *Rosa* L. 'Radbrite' (Brite Eyes™)
MG - *Rosa* L. 'BAIgirl' (Easy Elegance® My Girl)

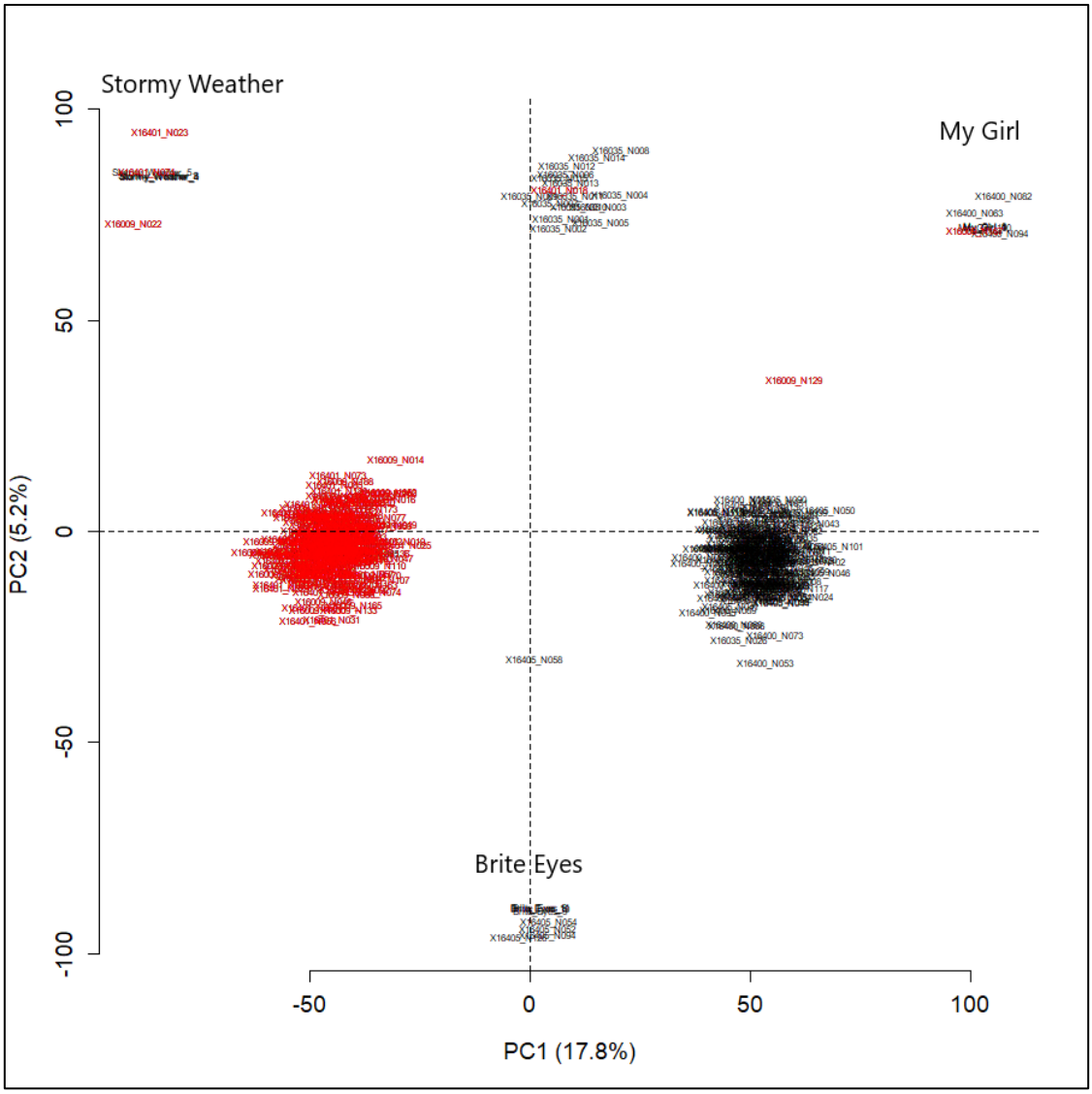

Figure 2.1. PCA of genotype calls in which off types, selfs, and a third population is observed in tetraploid garden rose. On the left and colored in red is the SWxBE and the group on the right colored in the black is BExMG population. The top left is Stormy Weather and any identified selfs, the top right is My Girl along with its selfs, and at the bottom is Brite Eyes along with its selfs. A third off type population can be seen in the center top in between Stormy Weather and My Girl. All genotypes not within the two main SWxBE and BExMG clusters were removed prior to linkage mapping.

Linkage Mapping

Linkage map construction was attempted using both MAPpoly and polymapR, however, due to the computational requirements of MAPpoly and difficulty grouping linkage groups, linkage mapping was performed using polymapR. Maps were created for both mapping populations. Parental maps were created then merged to create a consensus map for the population. Pairwise recombination was initially calculated between the simplex by nulliplex (SN markers) markers (roughly 2300 markers) to form 7 linkage groups with 4 homologs per linkage group using the "linkage" and "cluster_SN_markers" function. Marker groupings that did not cluster with any of the 28 homologs were removed (Figure 2.2). These simplex by nulliplex markers served as a scaffold of the linkage map. After establishing the linkage groups with their homologs, simplex by simplex, duplex by nulliplex, and all other marker types were fit to the map by calculating the linkage between the aforementioned markers and the simplex by nulliplex markers using "assign_linkage_group" and "homologue_lg_assignment" functions. MDSmap (Preedy and Hackett, 2016) was utilized to order the markers from within polymapR using the default Haldane mapping function. Markers on the end of the linkage groups that were greater than 5 cM from the next marker and had nnfit values greater than 10, were removed. The resulting maps were checked for preferential pairing and linkage groups with preferential pairing were rerun to account for the pairing behavior. Preferential pairing was only detected on LG 1 in the SWxBE and on LG 5 in the BExMG populations. The rerun maps resulted in maps that were 2-3 cM shorter and decreased largest gaps by 1-2 cM for those chromosomes. Markers that did not

physically map (Saint-Oyant et al., 2018) to the right LG were removed resulting in the removal of 1086 and 1355 markers from the SWxBE and BExMG maps respectively. After linkage mapping, the LGs were oriented in the same direction as the OBDH_1.0 rose genome assembly (Saint-Oyant et al., 2018).

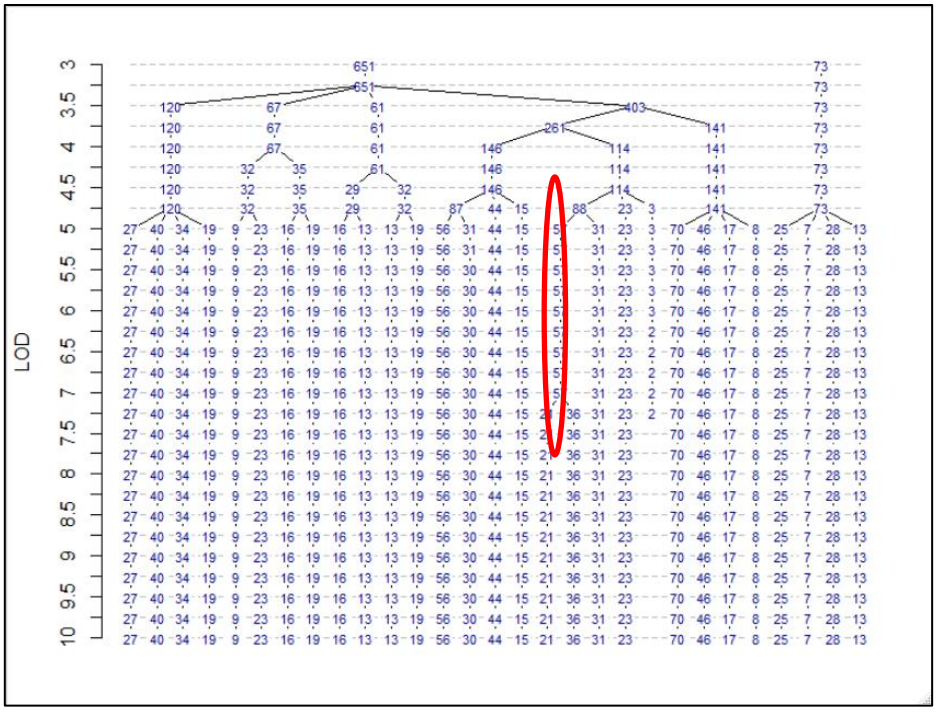

Figure 2.2. Simplex x nulliplex marker clusters for tetraploid garden rose Stormy Weather™. Plot generated from "cluster_SN_markers" function in polymapR where one cluster does not seem to group with any particular LG or homolog and is considered "noise" and discarded.

QTL Analysis

Phased maps generated by polymapR were imported into TetraploidSNPMap (Hackett et al., 2017) and QTLpoly (Pereira et al., 2019) for QTL interval mapping. Phenotypic values used in the QTL scans were best linear unbiased predictions (BLUPs)

calculated from mixed models using the PROC MIXED in SAS 9.4 (SAS Institute Inc. Cary, NC, USA). In order to use QTLpoly, the polymapR generated map was imported into MAPpoly and converted into conditional genotypic probabilities. QTL scans were run in QTLpoly using both the "remim" and "feim" functions. The "remim" function scans for QTL by first building a null model where the first round of score statistics are run for each trait, followed by rounds of forward search of QTL and backward elimination of QTL. The genome wide significance levels used for the forward search of QTL and backward eliminations are determined by using a score-based resampling method to establish a genome-wide significance by simulating QTL at every position in the linkage map (Zou et al., 2004). The simulation is run 1000 times prior to QTL mapping to obtain the p-values to be used for forward search and backward elimination of QTL in the remim method. After rounds of adding and eliminating QTL, the model of the location of the QTL is refined and confidence intervals are calculated for each QTL. The "feim" function implemented, first proposed by Hackett et al. (2001), does not account for multiple QTL and only scans for QTL at each interval specified. Thus, there is no stepwise addition and subtraction of QTL during the scan and the results are similar to TetraploidSNPMap. Allele effects estimated the effect of the QTL on the phenotypic mean in QTLpoly using the "qtl_effects" function. The interpretation of the allele effects results is clear with QTL segregating in a simplex x nulliplex manner (1x0) and as doses are added, it become more difficult to interpret the results due to population sizes of the mapping populations. We are able to interpret segregation patters of up to two doses (1x0, 0x1, 1x1, 2x0, and 0x2).

In addition to performing QTL analysis with TetraploidSNPMap and QTLpoly, genome-wide marker association (GWAS) analysis was performed with GWASpoly (Rosyara et al., 2016) using the markers' physical positions. Markers were not LD-pruned to detect QTL peaks in the populations. Initially, the two bi-parental populations were run together with the relatedness accounted for using a K-matrix derived from genotypic information. The bi-parental populations were then run separately to determine which QTL were present in each population.

Marker Assisted Progeny Selection

The most significant markers were used to select individuals that carried resistance alleles for both black spot and cercospora. The markers were then individually tested using ANOVA and Tukey's means separation to determine which allele state conferred resistance. Individuals carrying multiple resistance alleles are useful in breeding as resistance may come from different sources. Stacking many smaller effect resistance QTL may offer more stable resistance as multiple mechanisms must be overcome by the pathogen.

Results and Discussion

Populations Created and Seedling Rates

Initially, there were 405 SWxBE and 298 BExMG seedlings created however due to the number of replicates available and number of individuals genotyped, only 200 SWxBE and 157 BExMG individuals were used in linkage mapping and subsequent

QTL analysis (Tables 2.1 and 2.5). The creation of the mapping populations was a joint effort by Texas A&M University Rose Breeding and Weeks Roses. The BExMG family includes individuals pooled from a reciprocal cross in order to have enough individuals for better linkage map resolution.

Table 2.5 Tetraploid garden rose families developed by Texas A&M University and Weeks Roses for the study of black spot, cercospora leaf spot, and rose rosette disease. Number of hips, seed, seedlings, and percent germination shown.

Female parent	**Male parent**	**Number of hips**	**Number of seed**	**Number of seedlings**	**Percent germination**
Stormy Weather	Brite Eyes	91	1065	405	38.03%
Brite Eyes	My Girl	83	1030	298	28.93%

* The Brite Eyes x My Girl population includes individuals pooled from a reciprocal cross.

Phenotyping Results

There were differences between the months among most traits. The percentage of variance explained by month was between 2.6 and 7.1% when estimated by the model: $y=\sigma^2_{family} + \sigma^2_{progeny[family]} + \sigma^2_{location} + \sigma^2_{month\ [location]} + \sigma^2_{rep[location*\ month]} + \sigma^2_{location\ x\ family} + \sigma^2_{location\ x\ progeny[family]} + \sigma^2_{month\ x\ family} + \sigma^2_{month\ x\ progeny[family]} + \sigma^2_{location\ x\ month\ x\ family} + \sigma^2_{location\ x\ month\ x\ progeny[family]} + \sigma^2_{error.}$ As the data for black spot, cercospora, and defoliation was not normally distributed (Figures 2.3-2.4), nonparametric Spearman's correlations (Table 2.6, Figure 2.5) were conducted on BLUPs calculated from a mixed model. Although the correlations between defoliation and the disease incidence were weak to very weak, the two disease incidence ratings showed a moderate negative correlation.

The moderate negative correlation between black spot and cercospora is possibly due to the difficulty of assessing cercospora incidence on a plant largely defoliated by black spot or competition between the two fungal organisms. In recently defoliated plants, new leaves that form may not have the same inoculum pressure or may not have enough time for cercospora to colonize leading to a low cercospora disease score.

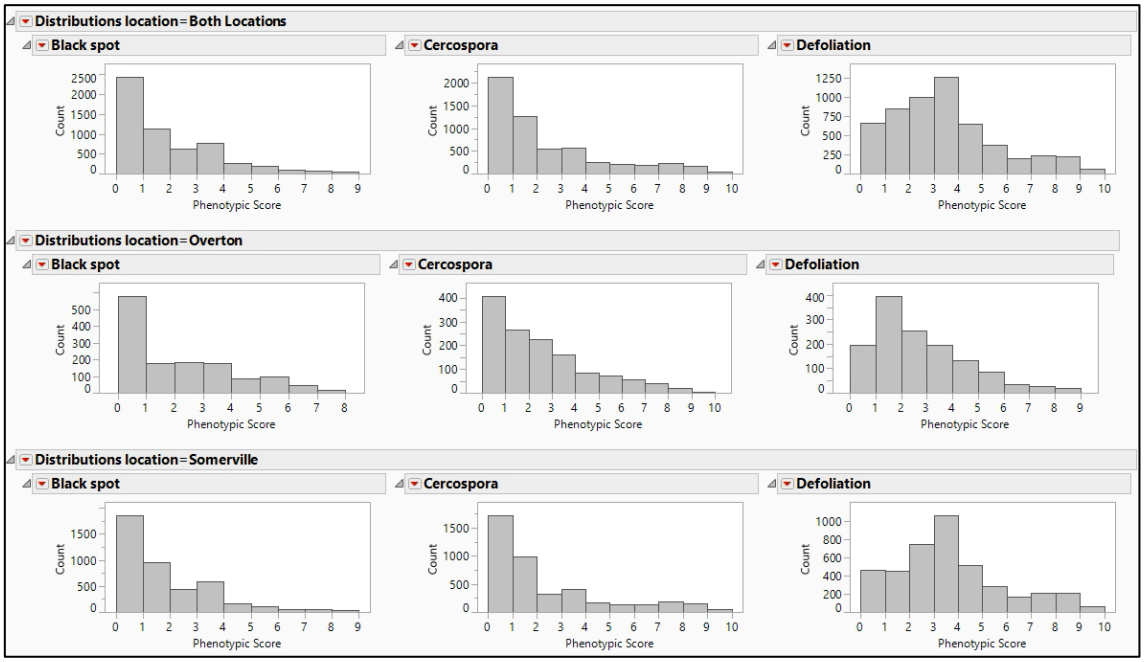

Figure 2.3. Histograms of black spot, cercospora leaf spot, and defoliation ratings evaluated on two tetraploid garden rose families Stormy Weather x Brite Eyes and Brite Eyes x My Girl in 2019 at Somerville, TX, and Overton, TX. Histograms are shown from these traits at both locations, Somerville, and Overton. Black spot, cercospora leaf spot, and defoliation were rated on a scale of 0-9 in which 0 represents no disease in canopy or a lack of defoliation. A rating of 1 would be representative of a plant that had 1-10% of the leaves with disease lesions or 1-10% of the leaves missing. A rating of 2 rating would indicate 11-20 % etc. Histograms are of raw data.

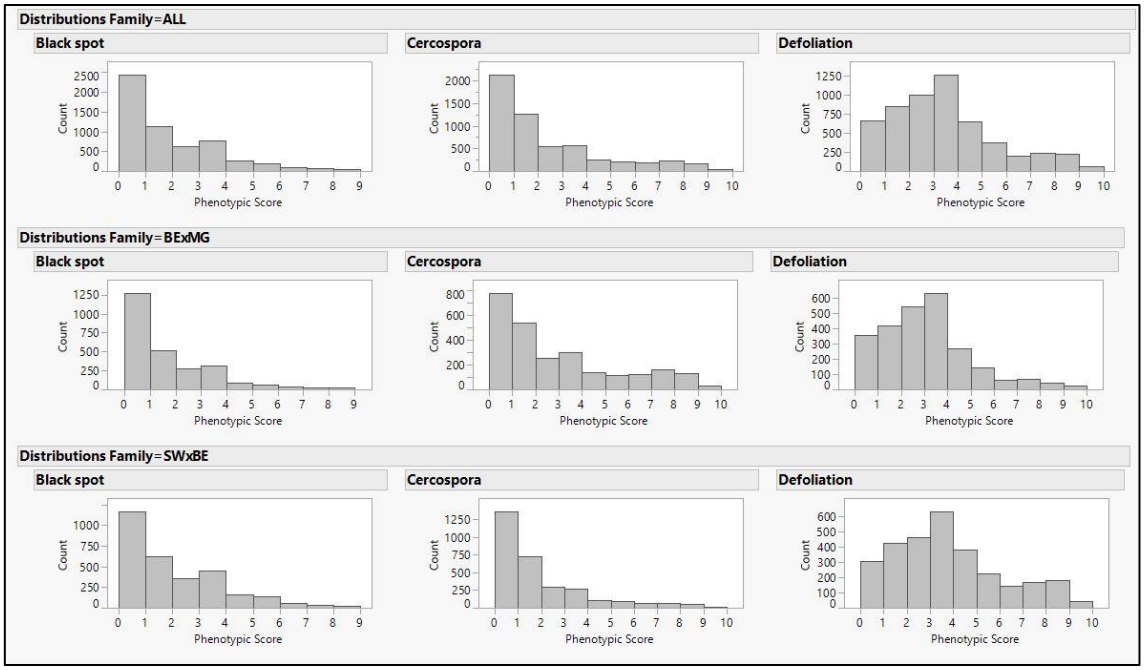

Figure 2.4. Histograms of black spot, cercospora leaf spot, and defoliation ratings evaluated on two garden rose families Stormy Weather x Brite Eyes and Brite Eyes x My Girl in 2019 at Somerville, TX, and Overton, TX. Histograms are showing the two populations together and separately. On the x axis is the disease severity score and the y axis is the number of observations of those scores. Histograms show data combined and by family. Black spot, cercospora leaf spot, and defoliation were rated on a scale of 0-9 in which 0 represents no disease in the canopy or a lack of defoliation. A rating of 1 would be representative of a plant that had 1-10% of the leaves with disease lesions or 1-10% of the leaves missing. A rating of 2 rating would indicate 11-20 % etc. Histograms are of raw data.

Table 2.6. Spearman correlations between phenotypic traits gathered from two tetraploid garden rose mapping populations.

Variable	by Variable	Spearman ρ	Prob>|ρ|
Cercospora	Black spot	-0.5614	<.0001
Defoliation	Black spot	0.317	<.0001
Defoliation	Cercospora	-0.1321	0.007

*correlations were conducted using best linear unbiased predictors calculated from a mixed model.

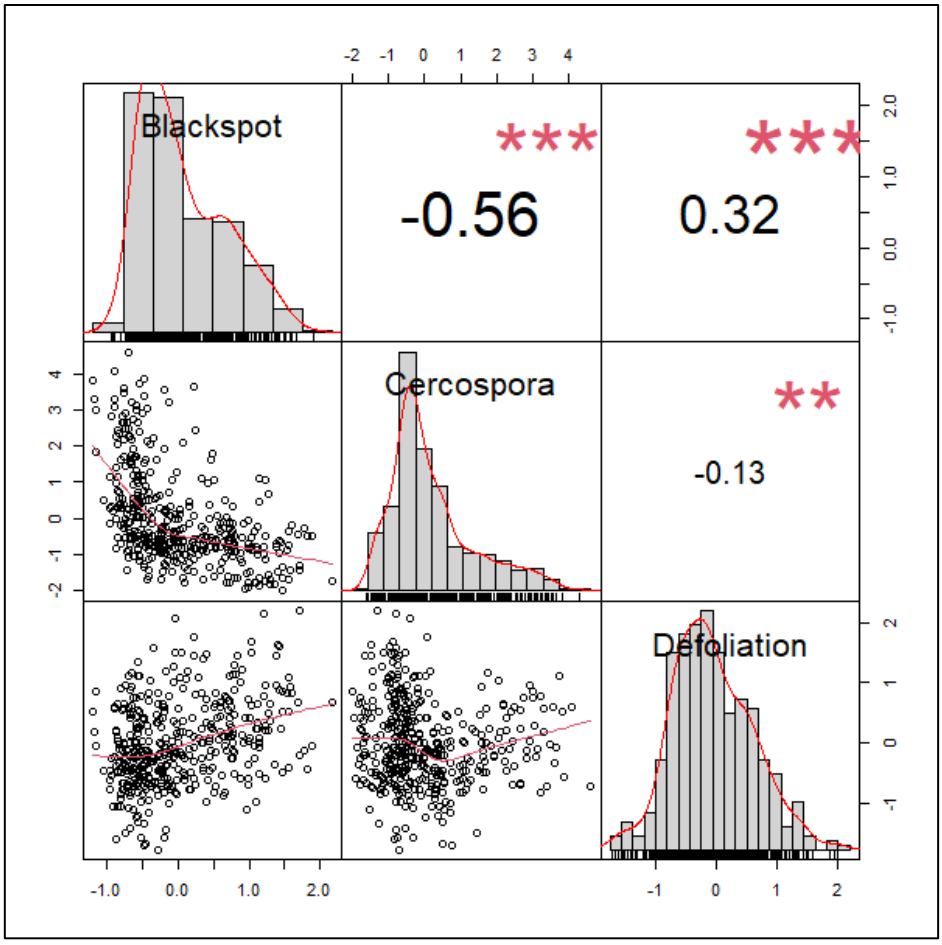

Figure 2.5. Scatterplot matrix of the correlations among black spot, cercospora, and defoliation on two tetraploid garden rose mapping populations. Correlations were conducted using best linear unbiased predictors (BLUPs) calculated from a mixed model. Numbers in the top right half of plots are the Spearman's correlation denoted with asterisks denoting significance. The bottom left half are the scatterplots of the BLUPs of all the genotypes and the red line is a fitted line.

Phenotypic Means Comparisons Between Month and Families.

In 2019 in Somerville, TX, black spot incidence increased from June to July, decreased in the months of August, September, and October, and peaked in November whereas cercospora incidence increased between June and July then decreased over the rest of the year. Defoliation was lower in the beginning of the year, however as the heat

and disease pressure increased during the year, so did defoliation (Figures 2.6-2.8). These trends are consistent over both populations. Differences between disease pressure and defoliation between the populations were significant in all months except for black spot ratings in September (Figures 2.9-2.11).

In Overton, TX, black spot incidence was lowest in September and highest in June and October. Defoliation decreased while cercospora incidence increased from June to October. These trends are consistent over both populations (Figures 2.12-2.14). The populations differed in disease incidence and defoliation except for defoliation in September and October (Figures 2.15-2.17).

The decrease in both black spot and cercospora during the summer and early fall months can be attributed to the lack of moisture as those were the driest months accompanied with the hottest temperatures (Figures 2.18-2.19). Both fungal diseases need moisture for development, and both can be hindered by extreme temperature. In addition to the lack of moisture and high temperature, the adverse summer weather conditions can also inhibit new growth on the plants on which the fungal pathogens can infect.

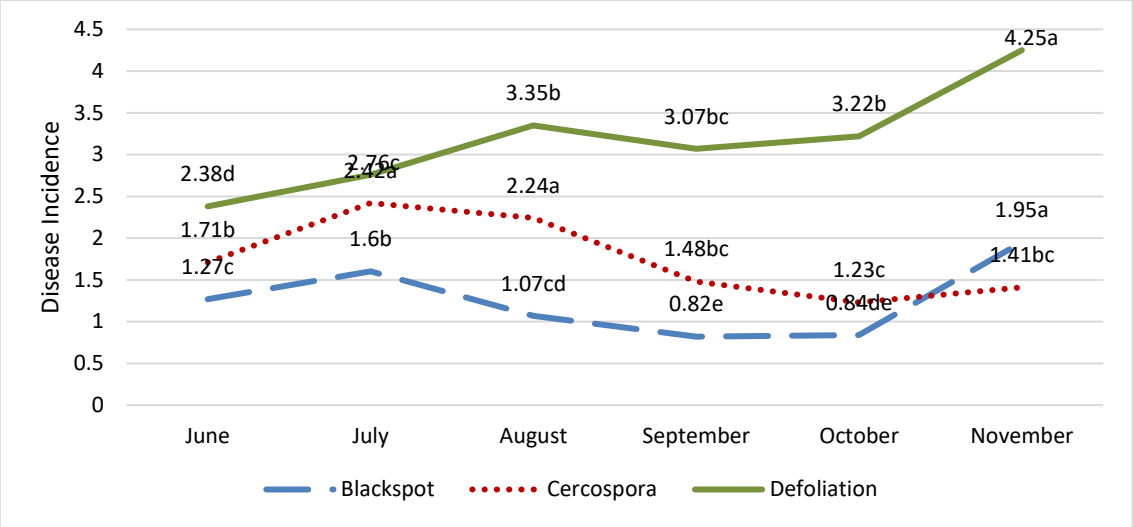

Figure 2.6. Monthly means of black spot, cercospora and defoliation of two tetraploid garden rose mapping populations in Somerville, TX in 2019. Means separation using Tukey's HSD. Means with differing letters are significantly different at P≤0.05. A rating of 1 would be representative of a plant that had 1-10% of the leaves with disease lesions or 1-10% of the leaves missing. A rating of 2 rating would indicate 11-20 % etc.

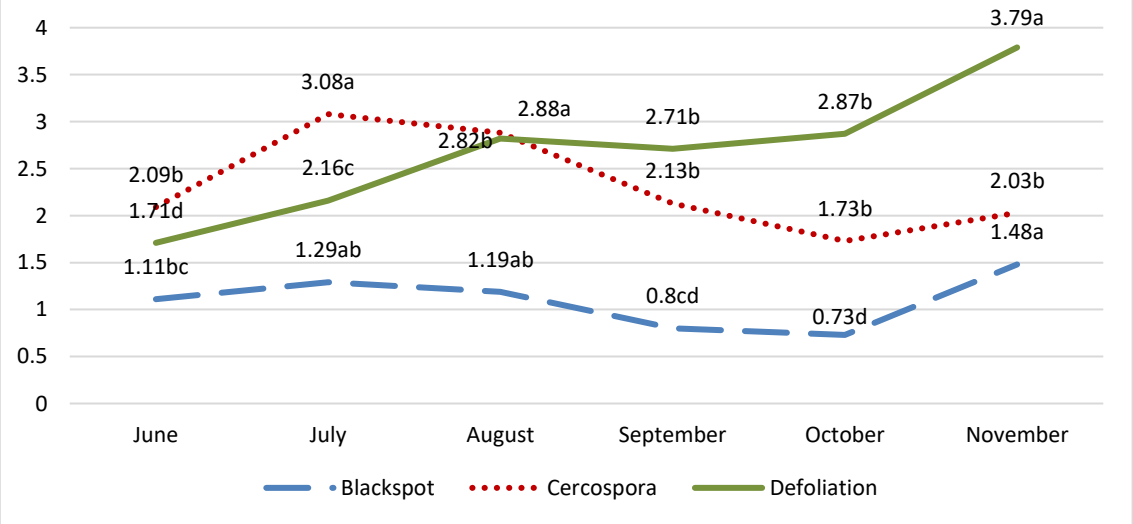

Figure 2.7. Monthly means of black spot, cercospora and defoliation of tetraploid garden rose mapping population Brite Eyes x My Girl in Somerville, TX in 2019. Means separation using Tukey's HSD. Means with differing letters are significantly different at P≤0.05. A rating of 1 would be representative of a plant that had 1-10% of the leaves with disease lesions or 1-10% of the leaves missing. A rating of 2 rating would indicate 11-20 % etc.

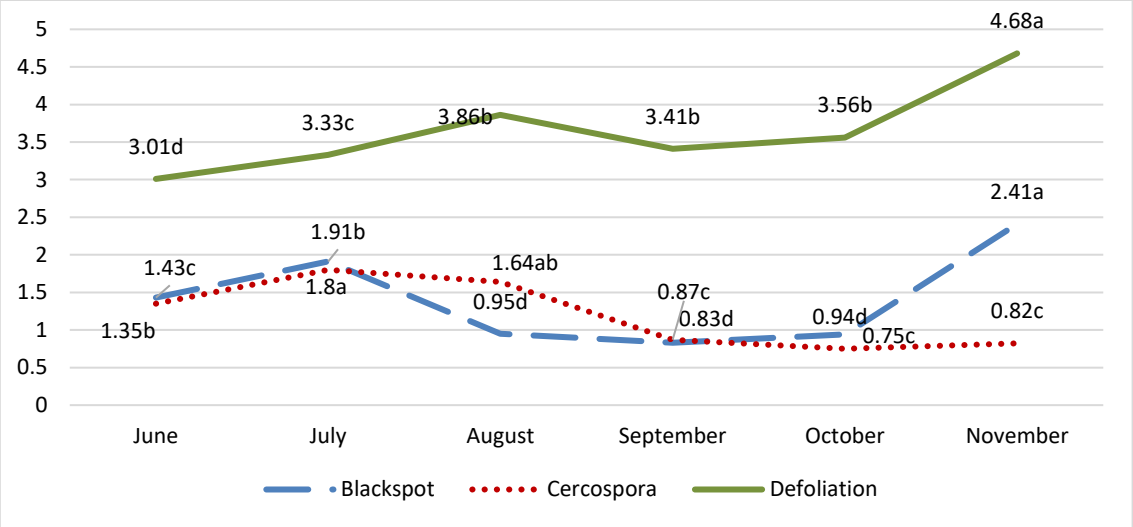

Figure 2.8. Monthly means of black spot, cercospora and defoliation of two tetraploid garden rose mapping Stormy Weather x Brite Eyes in Somerville, TX in 2019. Means separation using Tukey's HSD. Means with differing letters are significantly different at P≤0.05. A rating of 1 would be representative of a plant that had 1-10% of the leaves with disease lesions or 1-10% of the leaves missing. A rating of 2 rating would indicate 11-20 % etc.

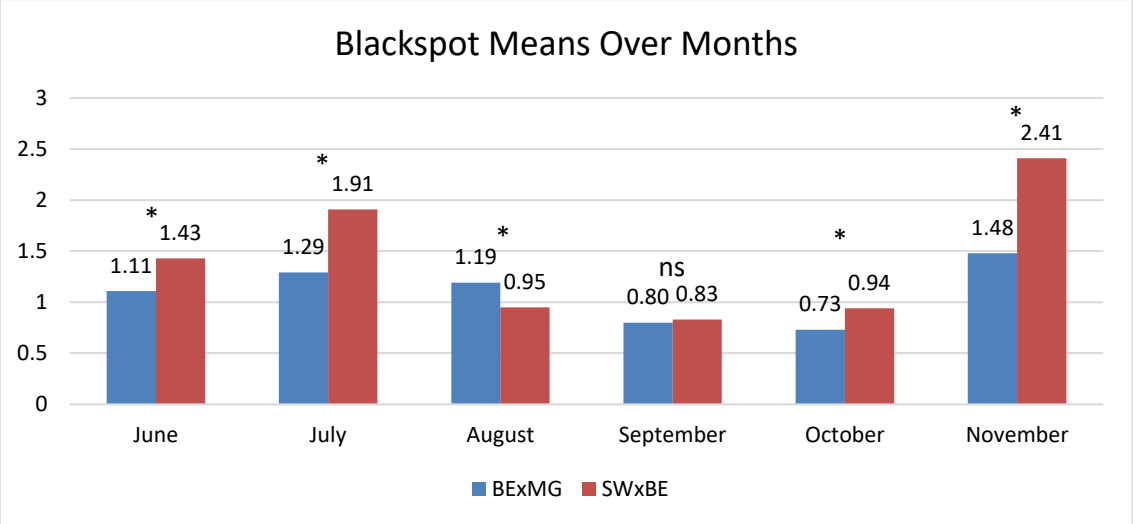

Figure 2.9. Comparison of monthly black spot incidence for the tetraploid garden rose mapping populations Brite Eyes x My Girl and Stormy Weather x Brite Eyes in Somerville, TX, in 2019. Differences between family means are significant at P≤0.05 except for months denoted with ns. A rating of 1 would be representative of a plant that had 1-10% of the leaves with disease lesions or 1-10% of the leaves missing. A rating of 2 rating would indicate 11-20 % etc.

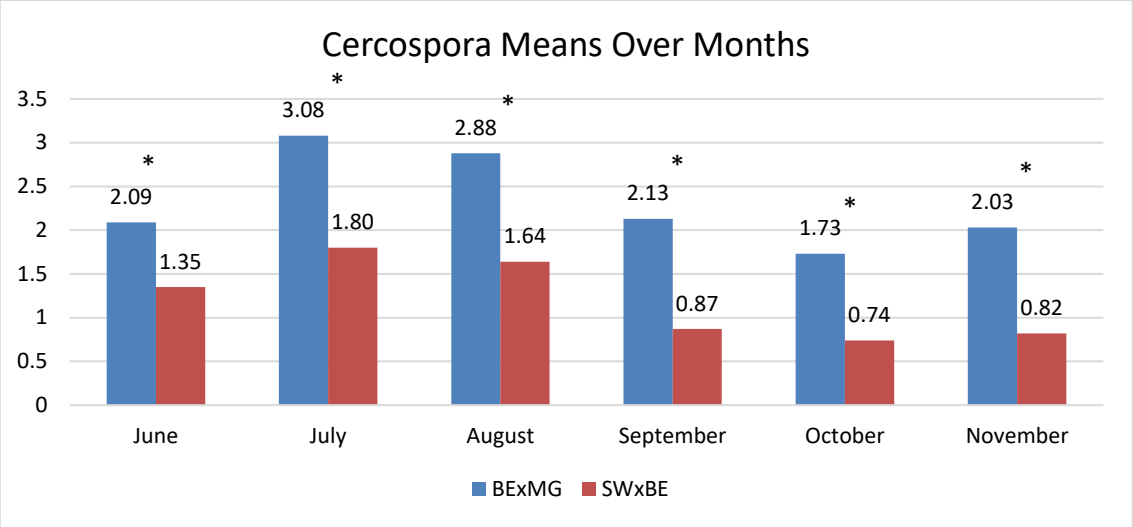

Figure 2.10. Comparison of monthly cercospora incidence for the tetraploid garden rose mapping populations Brite Eyes x My Girl and Stormy Weather x Brite Eyes in Somerville, TX, in 2019. Differences between family means are significant at P≤0.05 at all months. A rating of 1 would be representative of a plant that had 1-10% of the leaves with disease lesions or 1-10% of the leaves missing. A rating of 2 rating would indicate 11-20 % etc.

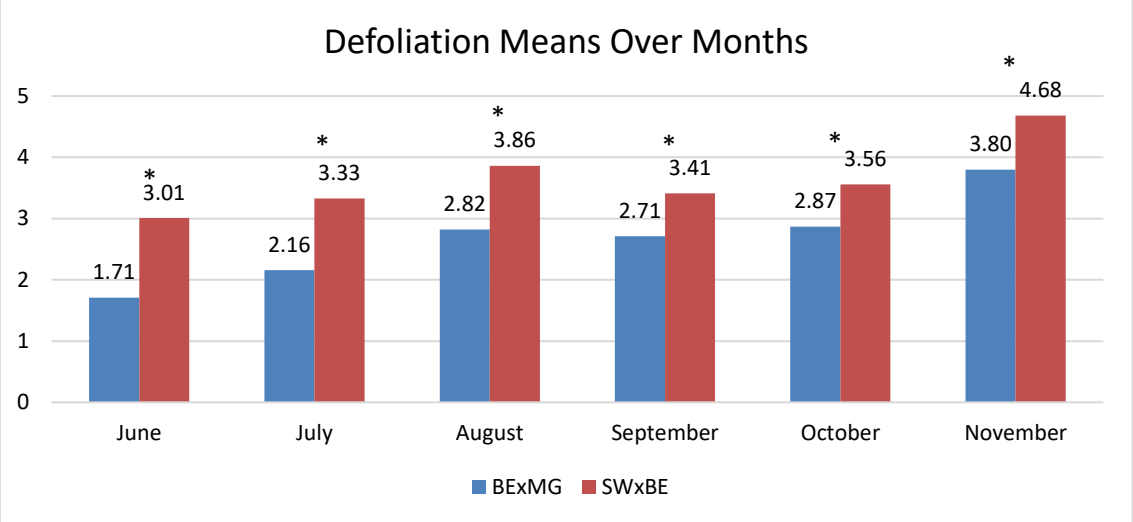

Figure 2.11. Comparison of monthly defoliation incidence for the tetraploid garden rose mapping populations Brite Eyes x My Girl and Stormy Weather x Brite Eyes in Somerville, TX, in 2019. Differences between family means are significant at P≤0.05 at all months. A rating of 1 would be representative of a plant that had 1-10% of the leaves with disease lesions or 1-10% of the leaves missing. A rating of 2 rating would indicate 11-20 % etc.

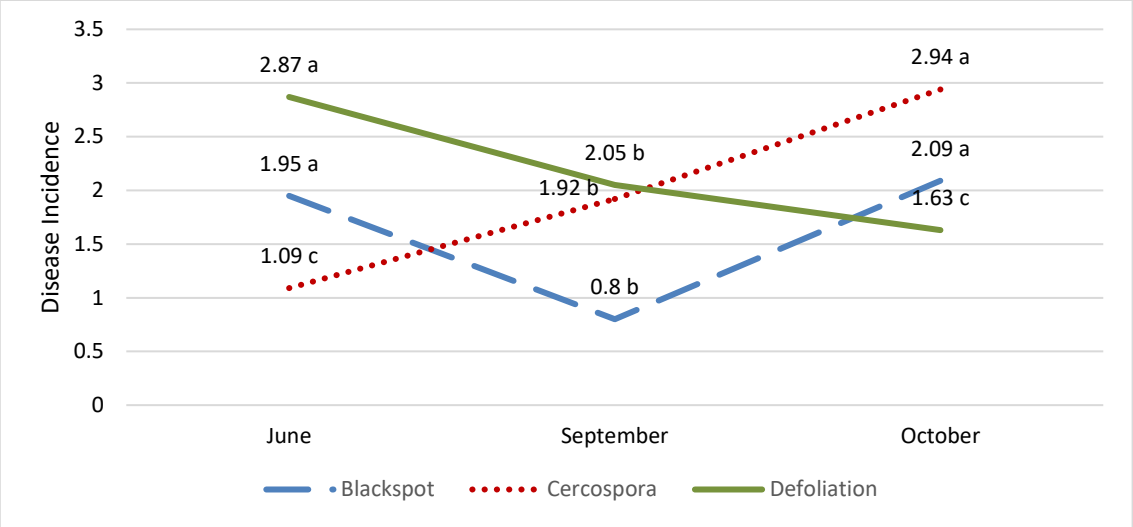

Figure 2.12. Monthly black spot, cercospora and defoliation evaluations of two tetraploid garden rose mapping populations in Overton, TX in 2019. Means separation using Tukey's HSD. Means with differing letters are significantly different at P≤0.05. A rating of 1 would be representative of a plant that had 1-10% of the leaves with disease lesions or 1-10% of the leaves missing. A rating of 2 rating would indicate 11-20 % etc.

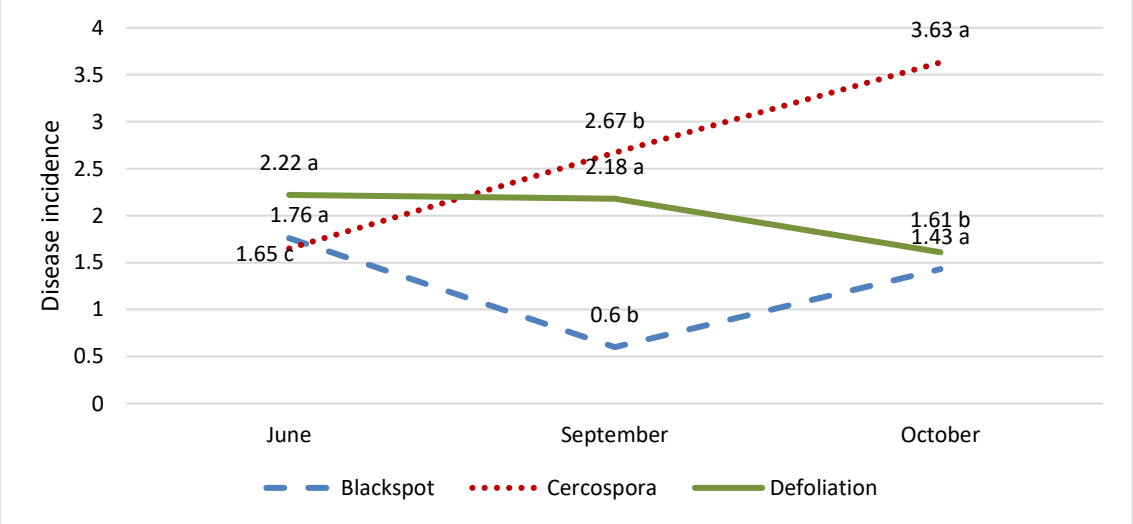

Figure 2.13. Monthly black spot, cercospora, and defoliation evaluations of tetraploid garden rose mapping population Brite Eyes x My Girl in Overton, TX in 2019. Means separation using Tukey's HSD. Means with differing letters are significantly different at P≤0.05. A rating of 1 would be representative of a plant that had 1-10% of the leaves with disease lesions or 1-10% of the leaves missing. A rating of 2 rating would indicate 11-20 % etc.

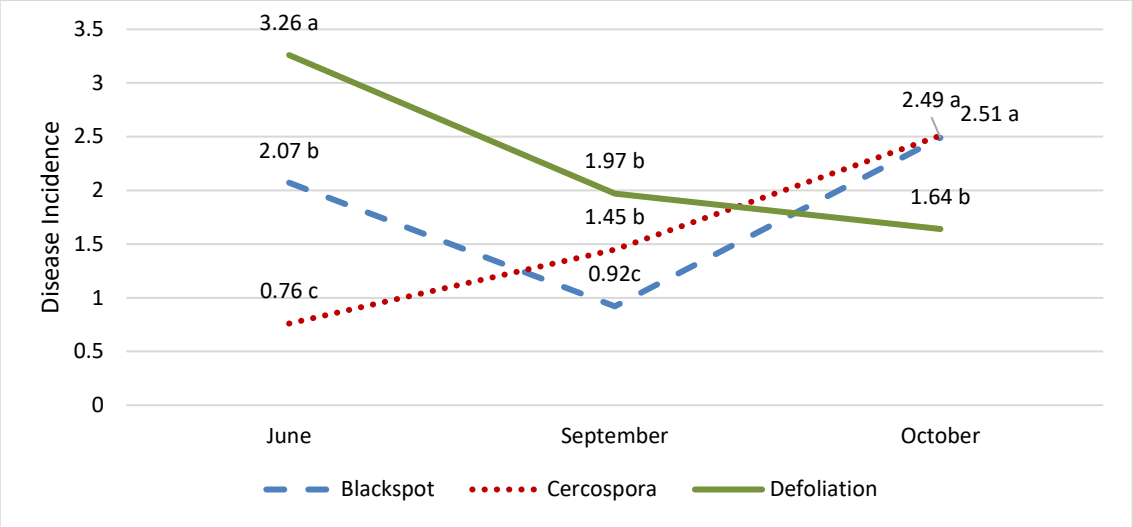

Figure 2.14. Monthly black spot, cercospora, and defoliation evaluations of tetraploid garden rose mapping population Stormy Weather x Brite Eyes in Overton, TX in 2019. Means separation using Tukey's HSD. Means with differing letters are significantly different at P≤0.05. A rating of 1 would be representative of a plant that had 1-10% of the leaves with disease lesions or 1-10% of the leaves missing. A rating of 2 rating would indicate 11-20 % etc.

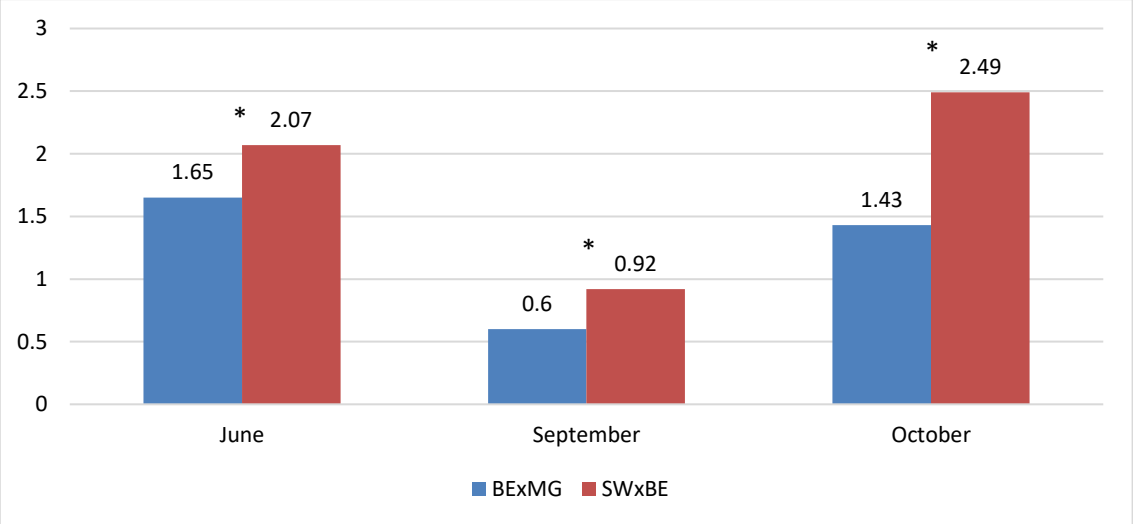

Figure 2.15. Comparison of monthly black spot ratings of two tetraploid garden rose mapping populations, Brite Eyes x My Girl and Stormy Weather x Brite Eyes, in Overton, TX in 2019. Means separation used Tukey's HSD. A rating of 1 would be representative of a plant that had 1-10% of the leaves with disease lesions or 1-10% of the leaves missing. A rating of 2 rating would indicate 11-20 % etc. An * denotes differences between the families at P≤0.05.

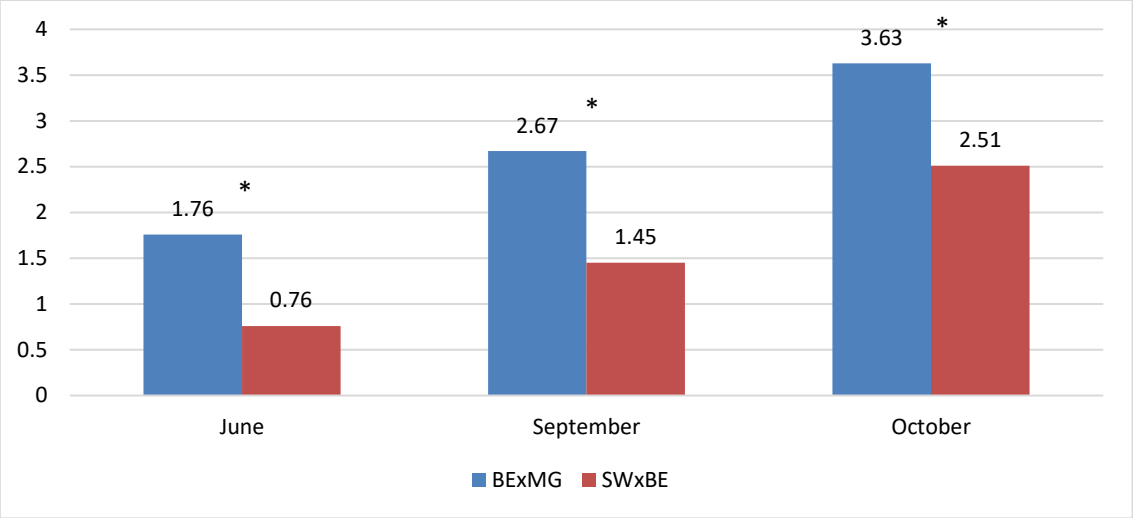

Figure 2.16. Comparison of cercospora leaf spot ratings of two tetraploid garden rose mapping populations, Brite Eyes x My Girl and Stormy Weather x Brite Eyes, in Overton, TX in 2019. Means separation used Tukey's HSD. A rating of 1 would be representative of a plant that had 1-10% of the leaves with disease lesions or 1-10% of the leaves missing. A rating of 2 rating would indicate 11-20 % etc. An * denotes differences between the families at P≤0.05.

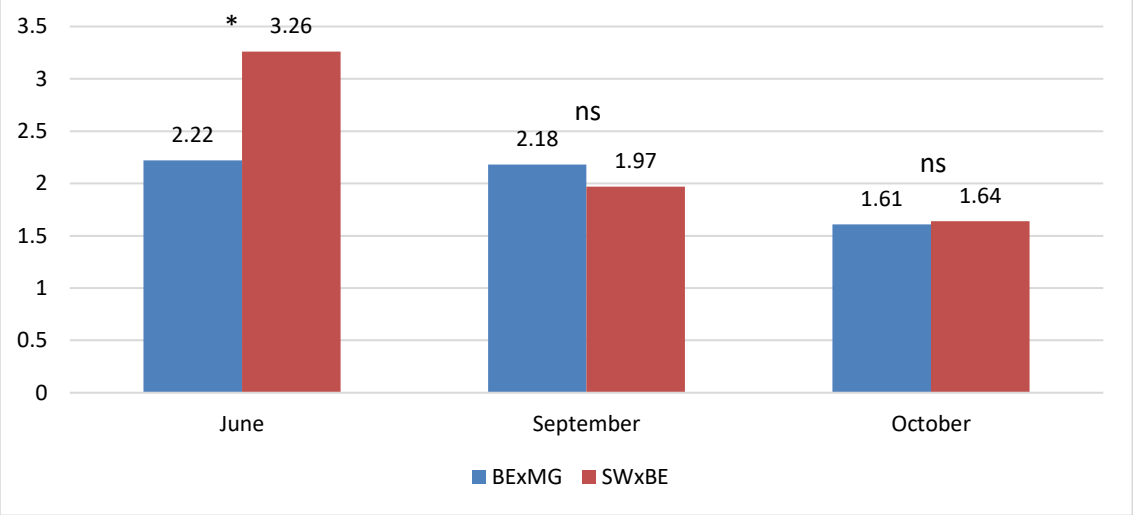

Figure 2.17. Comparison of monthly defoliation ratings of two tetraploid garden rose mapping populations, Brite Eyes x My Girl and Stormy Weather x Brite Eyes, in Overton, TX in 2019. Means separation used Tukey's HSD. A rating of 1 would be representative of a plant that had 1-10% of the leaves with disease lesions or 1-10% of the leaves missing. A rating of 2 rating would indicate 11-20 % etc. An * denotes differences between the families at P≤0.05 and ns denotes no difference between the two families.

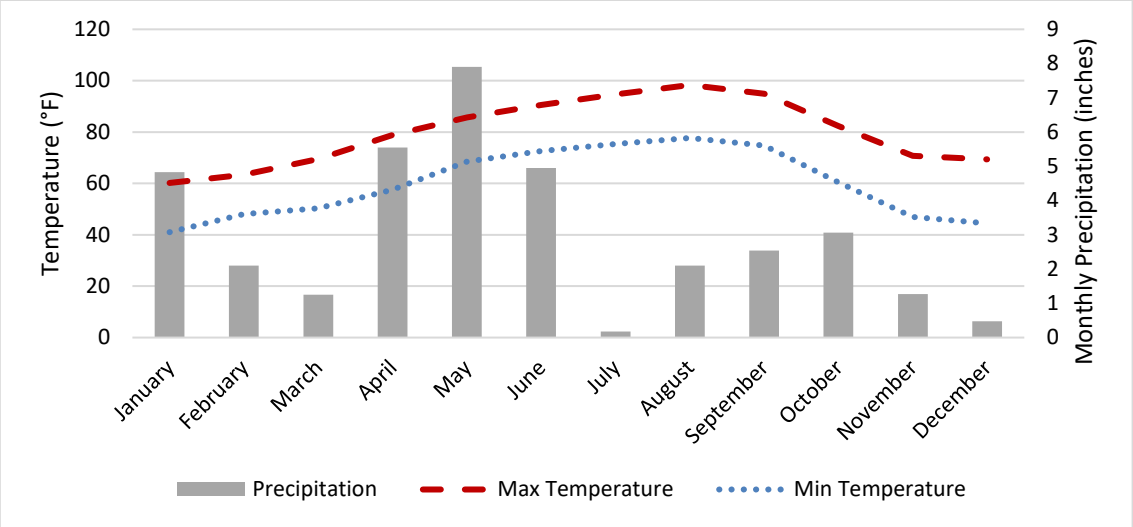

Figure 2.18. Average maximum and minimum monthly temperatures and corresponding accumulated monthly precipitation in 2019 for College Station, TX, (GHCND:USW00003904) approximately 5 miles from the Texas A&M University Horticulture Teaching Research and Extension Center in Somerville, TX. Temperature scale on left y-axis is in degrees Fahrenheit and precipitation's scale is on the right y-axis measured in inches.

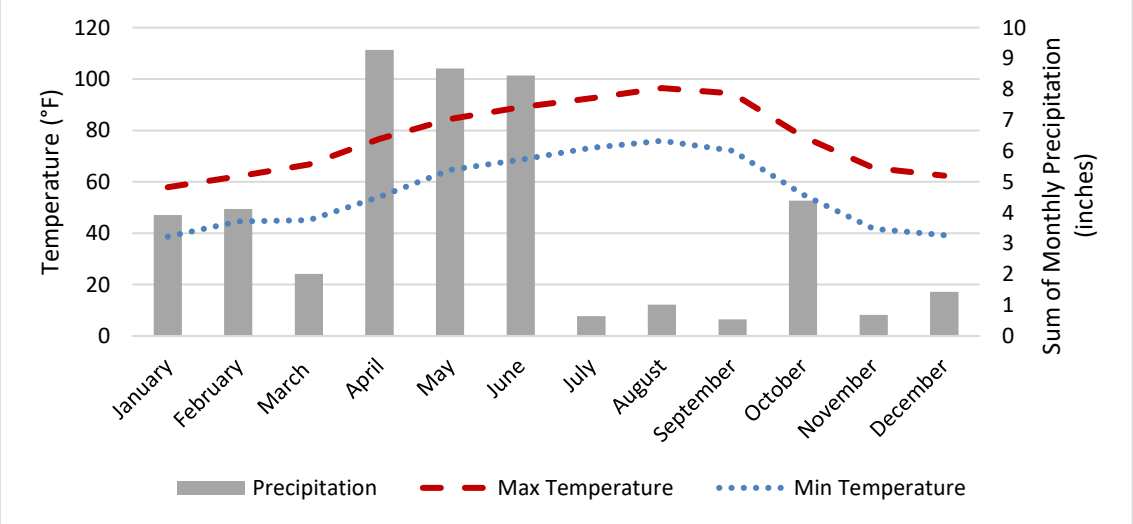

Figure 2.19. Average maximum and minimum monthly temperatures and corresponding accumulated monthly precipitation for in 2019 Tyler, TX, (GHCND:USC00419207) approximately 20 miles from the Overton experiment station. Temperature scale on left y-axis is in degrees Fahrenheit and precipitation's scale is on the right y-axis measured in inches.

Heritability Estimates

Black spot, cercospora, and defoliation, narrow sense heritability ranged from 2.3 to 9.3%, 16.4 to 21.5% and 0 to 19.8%, respectively. Black spot, cercospora, and defoliation broad sense heritability ranged from 49.3 to 85.5%, 85.7 to 95.4% and 35.2 to 86.5%, respectively (Tables 2.7-2.9). Over all traits, the narrow sense heritability was low indicating a low level of additive genetic effects. The broad sense heritabilities however are moderate to very high indicating large non-additive genetic effects for these traits. As seen later in the discussion of the QTL, many of these traits segregate in a simplex x nulliplex fashion (1x0 and 3x4).

The heritability estimates between the two locations differ as the disease pressure and the number of individuals at each test location were not the same (Table 2.10). As there were limited numbers of clonal propagates for each genotype, priority was given to planting two replicates in Somerville, TX, for ornamental and disease pressure screening and in Crossville, TN, for screening for RRD resistance. Because mixed models utilizing REML methods is robust when having unbalanced designs, heritability estimates calculated using models from both College Station, TX, and Overton TX, are a better estimate of heritability than looking at either location separately.

Along with heritability, the variance attributed to environmental effects on all traits was less than 20% of the variance. The GxE variance in most cases was greater than the variance observed on the environment alone. The implications from having a high GxE effect is that genotypic selections will differ depending on the environment in which the selection was made. However, for both black spot and cercospora, the GxE/G

ratio is less than 1 meaning that we should be able to make progress in selecting for individuals in most of the environments as the genetic variance is greater than the GxE variance. For defoliation, the GxE/G ratio is greater than 1 when considering both Somerville and Overton locations together. However, looking at Somerville alone, the GxE/G ratio is less than 1 meaning that at that location, we should be able to select for individuals with better resistance to defoliation throughout the year. The full model and the model which treated each month and location combination as a separate environment were the models we focused on as they were able utilize all the data from both locations. In the end, we chose the full model from the list of models listed in Tables 2.7-2.9. The individual variance components from the selected model are listed Table 2.11. BLUPs were obtained from the full model for use in QTL and GWAS scans; and the variances of the full model and percent of variance attributed to genetic, environmental, and error is listed in Table 2.11 and Figure 2.20. Standard errors to heritability estimates were calculated using the Dickerson approximation (Dickerson, 1969).

Table 2.7. Black spot heritabilities calculated from tetraploid garden rose mapping populations, Brite Eyes x My Girl and Stormy Weather x Brite Eyes, phenotyped in Somerville, TX, and Overton, TX, in 2019.

	Somerville	Overton	AUDPC both combined	Full model	Month and location combinations treated as separate environments
h^2	0.023	0.093	0.053	0.071	0.070
H^2	0.855	0.686	0.698	0.853	0.885
Parental	0.010	0.035	0.030	0.023	0.025
Progeny	0.349	0.226	0.400	0.250	0.296
Environment	0.059	0.107	0.017	0.078	0.070
GxE	0.154	0.098	0.205	0.206	0.346
G	0.359	0.261	0.429	0.272	0.322
GxE/G	0.430	0.374	0.479	0.758	1.076
residual	0.422	0.520	0.338	0.433	0.445
AIC	13606.7	5039.8	14680.5	18616.2	18644.6

Table 2.8. Cercospora leaf spot heritabilities calculated from tetraploid garden rose mapping populations, Brite Eyes x My Girl and Stormy Weather x Brite Eyes, phenotyped in Somerville, TX, and Overton, TX, in 2019.

	Somerville	Overton	AUDPC both combined	Full model	Month and location combinations treated as separate environments
h^2	0.164	0.211	0.215	0.195	0.189
H^2	0.942	0.857	0.861	0.931	0.954
Parental	0.104	0.105	0.169	0.104	0.108
Progeny	0.497	0.323	0.507	0.392	0.438
Environment	0.038	0.177	0.002	0.022	0.068
GxE	0.081	0.034	0.135	0.184	0.306
G	0.601	0.428	0.675	0.496	0.547
GxE/G	0.135	0.079	0.200	0.371	0.560
residual	0.278	0.359	0.164	0.295	0.293
AIC	15386.9	4965.3	15555.3	20204.6	20234.9

Table 2.9. Defoliation heritabilities calculated from tetraploid garden rose mapping populations Brite Eyes x My Girl and Stormy Weather x Brite Eyes phenotyped in Somerville, TX, and Overton, TX, in 2019.

	Somerville	Overton	AUDPC both combined	Full model	Month and location combinations treated as separate environments
h^2	0.198	0.000	0.070	0.147	0.175
H^2	0.859	0.322	0.623	0.800	0.865
Parental	0.087	0.000	0.026	0.038	0.058
Progeny	0.290	0.092	0.207	0.170	0.231
environment	0.062	0.066	0.347	0.093	0.104
GxE	0.209	0.194	0.145	0.287	0.616
G	0.377	0.082	0.233	0.208	0.289
GxE/G	0.555	2.360	0.619	1.380	2.133
residual	0.323	0.648	0.275	0.361	0.363
AIC	16104.9	5049.7	15455.7	21140.3	21199.4

Table 2.10. Number of genotypes from tetraploid garden rose mapping populations Brite Eyes x My Girl and Stormy Weather x Brite Eyes at each location in 2019 used for heritability calculations.

Location	Number of Genotypes	SWxBE	BExMG
Somerville, TX	363	188	172
Overton, TX	286	179	107
Together	412	234	178

*number of genotypes were not same in both locations due to number of clonal propagates available and due to seedling die off from weak clonal propagates.

Table 2.11. Sources of variation in two garden rose mapping populations Brite Eyes x My Girl and Stormy Weather x Brite Eyes phenotyped for black spot, cercospora and defoliation in Somerville, TX, and Overton, TX, in 2019.

Source of variation	**Black spot**	**Cercospora**	**Defoliation**
Family	0.06522	0.5571	0.1856
Progeny(Family)	0.7195***	2.1008***	0.825***
Location	0.0706	0.04806	0.305
Month	0.155	0.07232	0.1473
Rep(Location x Month)	0.03006*	0.01124	0.2448*
Location x Family	0	0	0.07682
Location x Genotype	0.1723***	0.3006***	0.3363***
Family x Month	0	0	0.0438
Genotype x Month	0.1291**	0.1264*	0.605***
Location x Family x Month	0.1199*	0.2943*	0.02027
Location x Genotype x Month	0.1732**	0.266**	0.3128***
Residual	1.2476***	1.5833***	1.7549***
Total	2.88248	5.36012	4.85759
Percent of total variance[abc]			
h^2	0.071 (0.122)	0.195 (0.504)	0.147 (0.312)
H^2	0.853 (0.151)	0.931 (0.305)	0.800 (0.292)
Parental	0.023	0.104	0.038
Progeny	0.250	0.392	0.170
Genotypic (G)	0.272	0.496	0.208
Environment (E)	0.078	0.022	0.093
GxE	0.206	0.184	0.287
Residual	0.433	0.295	0.361
GxE/G ratio	0.758	0.371	1.380

[a] Narrow sense heritability, $h^2 = \sigma^2_{family} / (\sigma^2_{family} + \sigma^2_{genotype[family]} + (\sigma^2_{location\ x\ family} + \sigma^2_{location\ x\ genotype[family]} + \sigma^2_{month\ x\ family} + \sigma^2_{month\ x\ genotype[family]} + \sigma^2_{location\ x\ month*family} + \sigma^2_{location\ x\ month*genotype\ [family]})/e + (\sigma^2_{error})/re)$

[b] Broad sense heritability, $H^2 = (\sigma^2_{family} + \sigma^2_{genotype[family]})/ (\sigma^2_{family} + \sigma^2_{genotype[family]} + (\sigma^2_{location\ x\ family} + \sigma^2_{location\ x\ genotype[family]} + \sigma^2_{month\ x\ family} + \sigma^2_{month\ x\ genotype[family]} + \sigma^2_{location\ x\ month*family} + \sigma^2_{location\ x\ month*genotype\ [family]})/e + (\sigma^2_{error})/re)$

r=reps

e=environments

[c] Standard Errors calculated for heritabilities in parenthesis and calculated using the Dickerson estimation

*, **, *** Variance components are significant at P≤0.05, 0.01, or 0.001, respectively using the Wald's Z test.

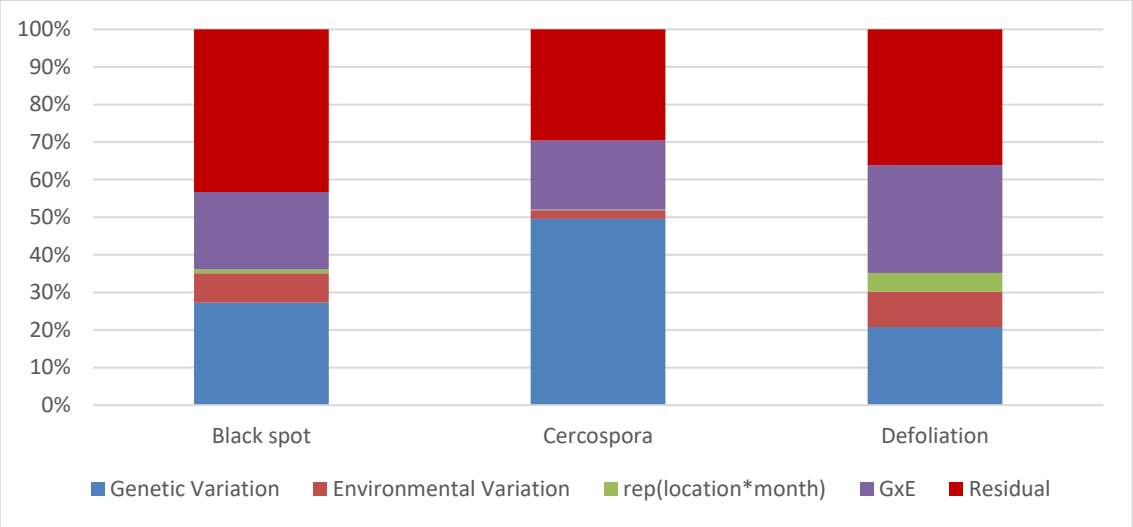

Figure 2.20. Percentage of phenotypic variance attributed to genetic, environmental, genotype by environment, and residual variance for two garden rose populations phenotyped for black spot, cercospora leaf spot, and defoliation, in Somerville, TX, and Overton, TX, in 2019. Mixed models were used to estimate variances.

Table 2.12. Black spot phenotypic variance and heritability calculations by environment for two garden rose mapping populations, Brite Eyes x My Girl and Stormy Weather x Brite Eyes, in Somerville, TX, and Overton, TX in 2019. Mixed models were used to estimate variances.

	SM6	SM7	SM8	SM9	SM10	SM11	OV6	OV9	OV10
Family	0.037	0.182	0.022	0.000	0.014	0.379	0.042	0.041	0.528
Progeny (family)	1.230	1.506	0.531	0.411	0.752	2.821	0.574	0.577	2.144
Rep	0.011	0.000	0.000	0.000	0.017	0.065	0.160	0.000	0.000
Residual	0.909	1.427	0.917	0.883	0.620	1.624	1.729	1.313	2.590
Total	2.187	3.114	1.469	1.293	1.403	4.889	2.506	1.930	5.262
Heritabilites and residual expressed as a percent of total variance									
h^2	0.022	0.076	0.021	0.000	0.013	0.094	0.028	0.032	0.133
H^2	0.736	0.703	0.547	0.482	0.712	0.798	0.416	0.485	0.674
Residual	0.416	0.458	0.624	0.682	0.442	0.332	0.690	0.680	0.492

[a] Environments are denoted as either SM or OV for Sommerville, TX, and Overton, TX, followed by the month in which the data was taken.
[b] Narrow sense heritability calculated by $h^2 = \sigma^2_{family} / (\sigma^2_{family} + \sigma^2_{genotype[family]} + \sigma^2_{error}/r)$
[c] Broad sense heritability calculated by $H^2 = (\sigma^2_{family} + \sigma^2_{progeny[family]}) / (\sigma^2_{family} + \sigma^2_{progeny[family]} + \sigma^2_{error} / r)$
r=reps

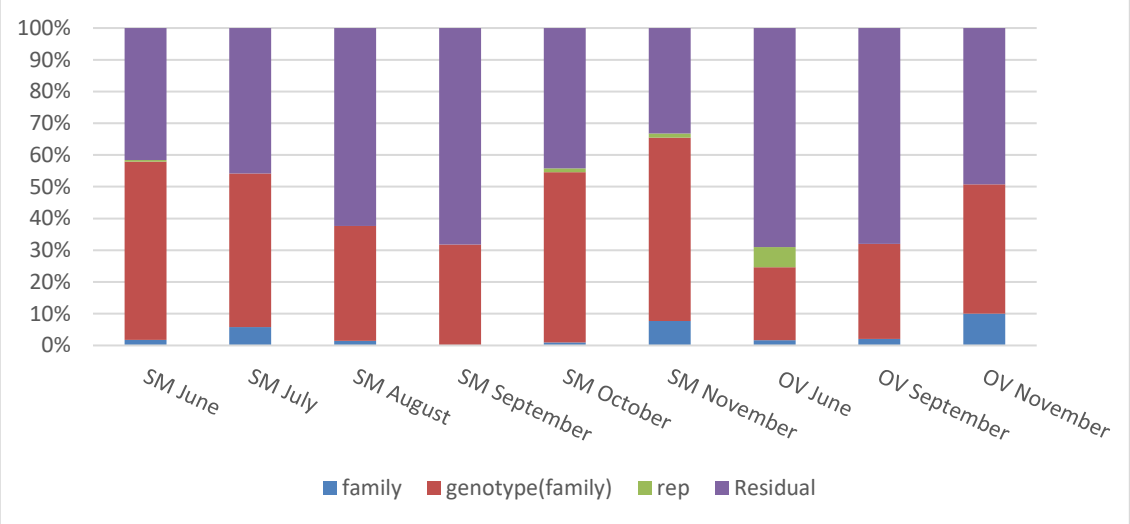

Figure 2.21. Distribution of genetic, replication, and residual variation for black spot by environment measured on two tetraploid garden rose mapping populations, Brite Eyes x My Girl and Stormy Weather x Brite Eyes, in Somerville, TX, (SM) and Overton, TX, (OV) in 2019. Mixed models were used to estimate variances.

Table 2.13. Cercospora phenotypic variance and heritability by environment for two garden rose mapping populations, Brite Eyes x My Girl and Stormy Weather x Brite Eyes, in Somerville, TX, and Overton, TX in 2019. Mixed models were used to estimate variances.

	SM6	SM7	SM8	SM9	SM10	SM11	OV6	OV9	OV10
Family	0.258	0.797	0.723	0.735	0.439	0.700	0.405	0.620	0.510
Genotype(Family)	3.024	5.100	4.739	2.530	2.033	1.980	1.236	1.895	2.035
Rep	0.000	0.006	0.009	0.026	0.044	0.000	0.000	0.034	0.000
Residual	1.428	1.914	1.922	1.512	1.163	1.557	1.399	1.737	1.866
Total	4.709	7.817	7.393	4.803	3.679	4.236	3.041	4.286	4.410
Heritabilites and residual expressed as a percent of total variance									
h^2	0.065	0.116	0.113	0.183	0.144	0.202	0.173	0.183	0.147
H^2	0.821	0.860	0.850	0.812	0.810	0.775	0.701	0.743	0.732
Residual	0.303	0.245	0.260	0.315	0.316	0.367	0.460	0.405	0.423

[a] Environments are denoted as either SM or OV for Sommerville, TX, and Overton, TX, followed by the month in which the data was taken.
[b] Narrow sense heritability calculated by $h^2 = \sigma^2_{family} / (\sigma^2_{family} + \sigma^2_{genotype[family]} + \sigma^2_{error}/r)$
[c] Broad sense heritability calculated by $H^2 = (\sigma^2_{family} + \sigma^2_{progeny[family]}) / (\sigma^2_{family} + \sigma^2_{progeny[family]} + \sigma^2_{error} / r)$
r=reps

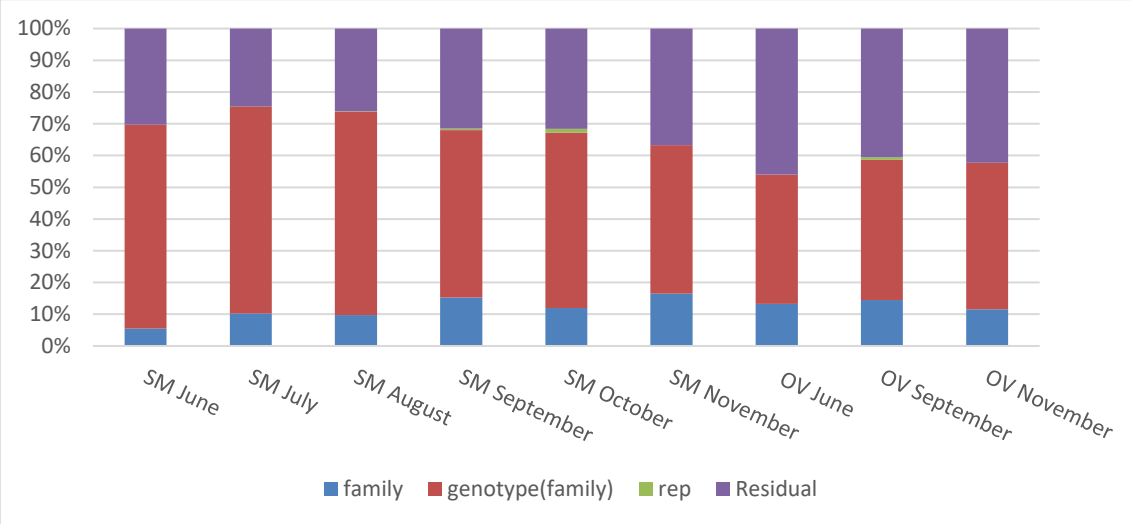

Figure 2.22. Distribution of percent variation contributed by genetic factors, rep, and residual calculated from cercospora measured on two garden rose mapping populations, Brite Eyes x My Girl and Stormy Weather x Brite Eyes, in Somerville, TX, (SM) and Overton, TX, (OV) in 2019. Mixed models were used to estimate variances.

Table 2.14. Defoliation phenotypic variance and heritability calculations for each set of phenotypic observations. Defoliation measured on two garden rose mapping populations, Brite Eyes x My Girl and Stormy Weather x Brite Eyes, in Somerville, TX, and Overton, TX, in 2019. Mixed models were used to estimate variances.

	SM6	SM7	SM8	SM9	SM10	SM11	OV6	OV9	OV10
Family	0.812	0.683	0.508	0.236	0.218	0.379	0.521	0.005	0.000
Genotype(family)	3.645	2.545	2.649	2.044	1.891	2.415	1.352	0.311	0.505
Rep	0.154	0.100	0.091	0.022	0.403	0.116	0.000	0.000	0.022
Residual	1.388	1.550	1.569	1.623	1.680	2.286	2.042	2.846	1.398
total	5.999	4.878	4.816	3.925	4.191	5.195	3.915	3.162	1.925
Heritabilites and residual expressed as a percent of total variance									
h^2	0.158	0.171	0.129	0.076	0.074	0.096	0.180	0.003	0.000
H^2	0.865	0.806	0.801	0.738	0.715	0.710	0.647	0.182	0.419
res	0.231	0.318	0.326	0.414	0.401	0.440	0.522	0.900	0.727

[a] Environments are denoted as either SM or OV for Sommerville, TX, and Overton, TX, followed by the month in which the data was taken.
[b] Narrow sense heritability calculated by $h^2 = \sigma^2_{family} / (\sigma^2_{family} + \sigma^2_{genotype[family]} + \sigma^2_{error} / r)$
[c] Broad sense heritability calculated by $H^2 = (\sigma^2_{family} + \sigma^2_{progeny[family]}) / (\sigma^2_{family} + \sigma^2_{progeny[family]} + \sigma^2_{error} / r)$
r=reps

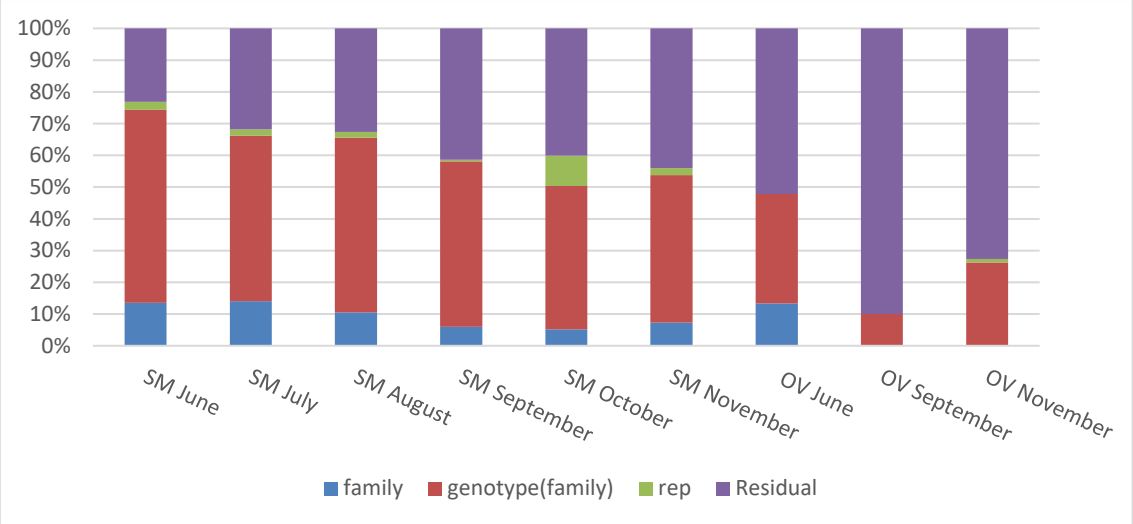

Figure 2.23. Distribution of genetic, replication, and residual variation for defoliation measured on two garden rose mapping populations, Brite Eyes x My Girl and Stormy Weather x Brite Eyes, in Somerville, TX, (SM) and Overton, TX, (OV) in 2019. Mixed models were used to estimate variances.

Mapping

The two parental maps created are comparable to the quality of previously published maps (Bourke et al., 2017; Zurn et al., 2018; 2020). The SWxBE map contained 8273 markers at 4047 unique positions spanning 536.23 cM with an average gap size of 0.14 cM and largest gap size of 4.58 cM located on LG5 (Table 2.15). The BExMG map contained a total of 9654 markers at 4220 unique positions over 526.31 cM with an average gap size of 0.13 cM and the largest gap of 4.01 cM on LG2 (Table 2.16). In comparison, the map by Bourke et al. (2017) contained 20,090 markers mapped over 654.84 cM with the largest gap being 4.3 cM. Zurn et al. (2018) constructed a map containing 10,835 markers spanning 421.92 cM with a largest gap of 3.6 cM. Subsequently, Zurn et al. (2020) constructed a map consisting of 6527 markers within 3273 unique bins, spanning 405.42 cM with the largest gap of 5 cM. Zurn et al. (2018; 2020) maps were both around 100 cM shorter than SWxBE, BExMG, and the K5 (Bourke et al., 2017) maps possibly due to differences in marker ordering functions as both we and Bourke used Haldane's while Zurn used Kosambi's mapping functions.

Table 2.15. Tetraploid rose mapping population Stormy Weather x Brite Eyes linkage map statistics.

Chr.	#markers	map_size	average gap_size	biggest gap_size	#unique positions
1	744	66.17	0.18	3.41	370
2	2345	86.16	0.08	1.21	1018
3	661	61.35	0.18	2.71	337
4	987	70.87	0.12	2.84	594
5	1147	96.99	0.15	4.58	653
6	1167	73.94	0.18	2.57	410
7	1222	80.75	0.12	1.89	665
all	8273	536.23	0.14	4.58	4047

Table 2.16. Tetraploid rose mapping population Brite Eyes x My Girl linkage map statistics.

Chr.	#markers	map_size	average gap_size	biggest gap_size	#unique positions
1	1066	71.06	0.14	2.29	515
2	2319	85.37	0.09	4.01	923
3	795	60.28	0.17	1.48	354
4	1312	78.14	0.14	2.44	576
5	1349	82.29	0.14	2.29	608
6	1659	75.15	0.11	1.96	655
7	1154	74.02	0.13	1.31	589
all	9654	526.31	0.13	4.01	4220

Table 2.17. Marker probe characteristics of markers of two tetraploid garden rose linkage mapping populations.

Family	Congruent calls	Single probe calls
Stormy Weather x Brite Eyes	4725 (57%)	3533 (43%)
Brite Eyes x My Girl	5362 (56%)	4275 (44%)

*numbers do not add up to total number of markers present in map as this is an average number of markers which were called by both probes vs just one probe

Both linkage maps (SWxBE and BExMG) have close to 10,000 markers and are comparable to the Morden Blush x Brite Eyes (Zurn et al., 2018) and Morden Blush x George Vancouver (Zurn et al., 2019) maps. However, Bourke et al. (2017) had twice as many markers in their map of P540 x P867 (K5 tetraploid cut rose population) (Figure 2.24). This is due to the differences in the populations that were used. The mapping population Bourke used was a population derived from the K5 cut rose mapping population in which the parents (P540 and P867) were used to develop the WagRhSNP 68k SNP array. Mapping with a population which has a direct relationship to genotypes used to develop the SNP array results in many more DNA fragments that adhere to the

SNP array when compared to populations that did not have parents used to create the SNP array (Figures 2.25-2.28).

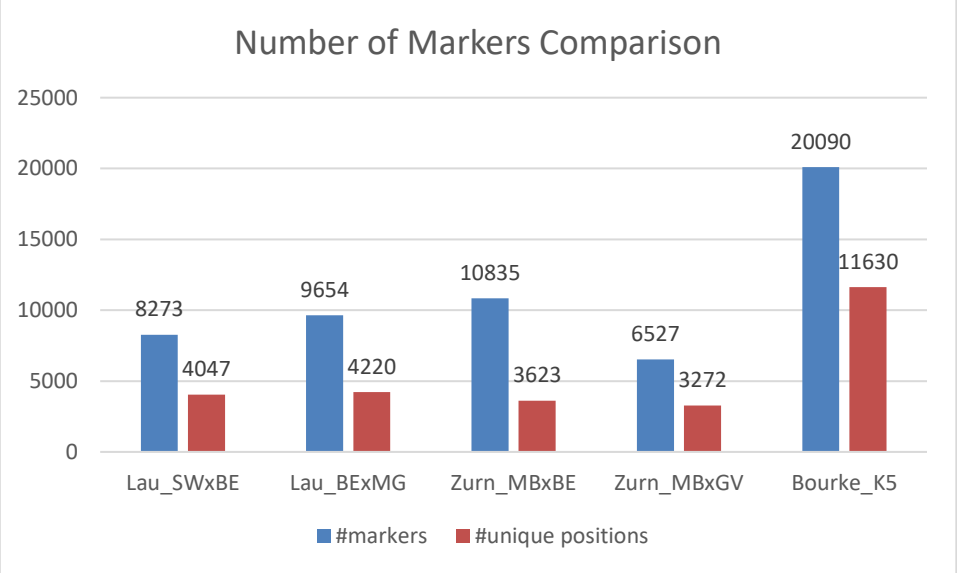

Figure 2.24. Marker number and unique positions in Stormy Weather x Brite Eyes and Brite Eyes x My Girl tetraploid rose linkage maps compared to other tetraploid rose maps (Zurn et al., 2018; Zurn et al., 2020; Bourke et al., 2017). Abbreviations: SWxBE (Stormy Weather x Brite Eyes), BExMG (Brite Eyes x My Girl), MBxBE (Morden Blush x Brite Eyes), MBxGV (Morden Blush x George Vancouver), K5 (K5 cut rose mapping population).

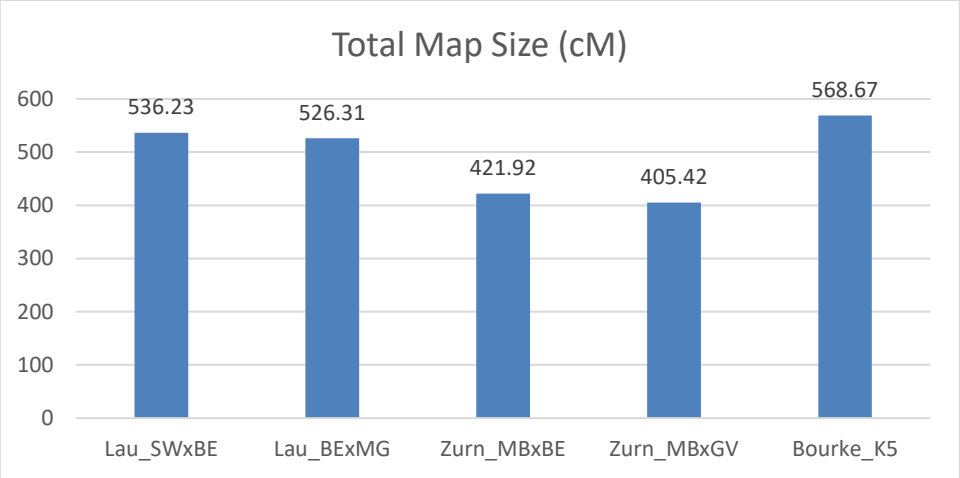

Figure 2.25. Total map length comparison of Stormy Weather x Brite Eyes and Brite Eyes x My Girl tetraploid rose linkage maps to other tetraploid rose maps (Zurn et al., 2018; Zurn et al., 2019; and Bourke et al., 2017). Abbreviations: SWxBE (Stormy Weather x Brite Eyes), BExMG (Brite Eyes x My Girl), MBxBE (Morden Blush x Brite Eyes), MBxGV (Morden Blush x George Vancouver), K5 (K5 cut rose mapping population).

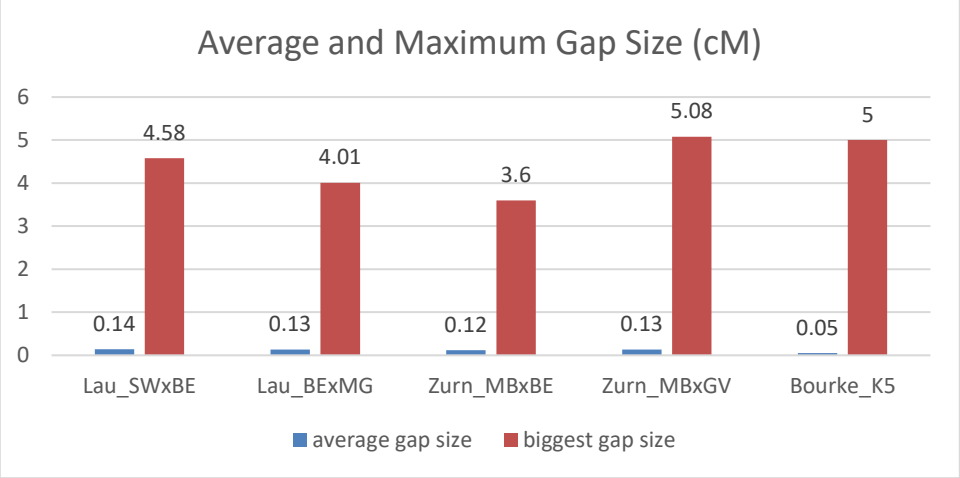

Figure 2.26. Average and maximum gap size comparison of Stormy Weather x Brite Eyes and Brite Eyes x My Girl tetraploid rose linkage maps to other tetraploid rose maps (Zurn et al., 2018; Zurn et al., 2020; Bourke et al., 2017). Abbreviations: SWxBE (Stormy Weather x Brite Eyes), BExMG (Brite Eyes x My Girl), MBxBE (Morden Blush x Brite Eyes), MBxGV (Morden Blush x George Vancouver), K5 (K5 cut rose mapping population).

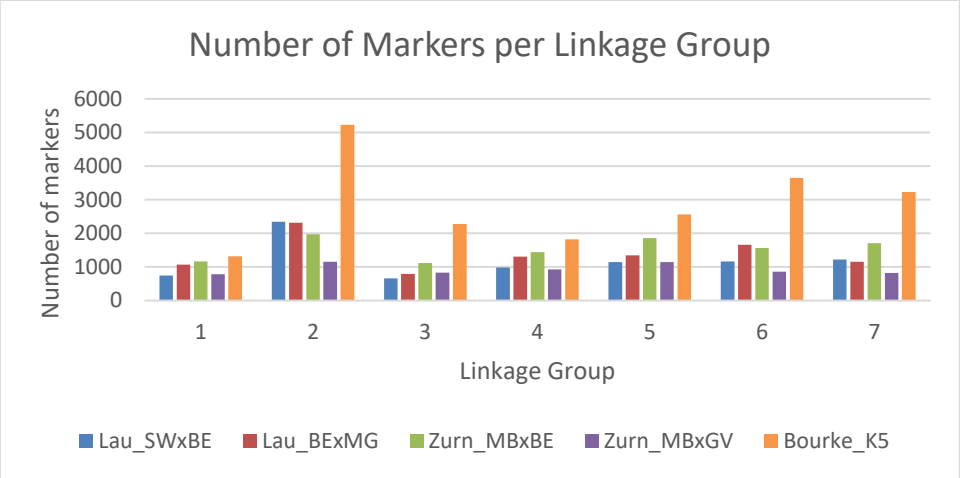

Figure 2.27. Number of markers mapped per LG comparison of Stormy Weather x Brite Eyes and Brite Eyes x My Girl tetraploid rose linkage maps to other tetraploid rose maps (Zurn et al., 2018; Zurn et al., 2020; Bourke et al., 2017). Abbreviations: SWxBE (Stormy Weather x Brite Eyes), BExMG (Brite Eyes x My Girl), MBxBE (Morden Blush x Brite Eyes), MBxGV (Morden Blush x George Vancouver), K5 (K5 cut rose mapping population).

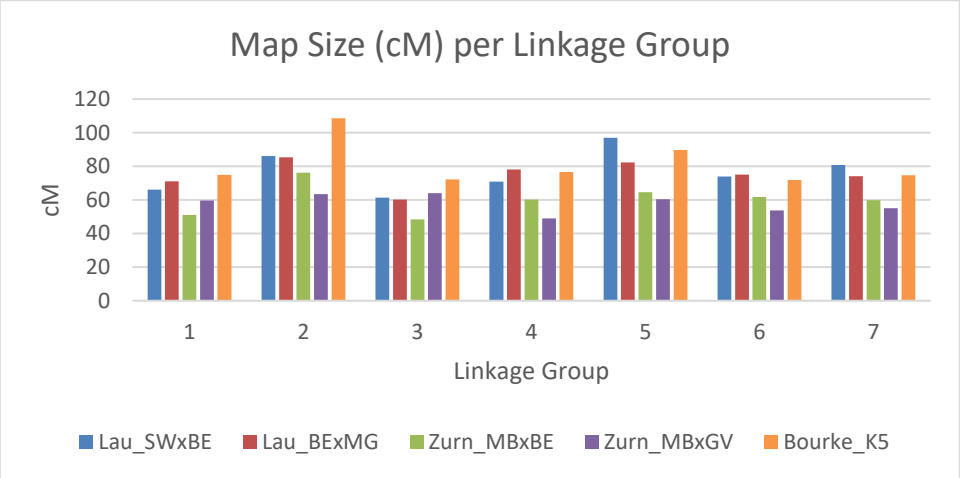

Figure 2.28. Map size per LG comparison of Stormy Weather x Brite Eyes and Brite Eyes x My Girl tetraploid rose linkage maps to other tetraploid rose maps (Zurn et al., 2018; Zurn et al., 2020; Bourke et al., 2017). Abbreviations: SWxBE (Stormy Weather x Brite Eyes), BExMG (Brite Eyes x My Girl), MBxBE (Morden Blush x Brite Eyes), MBxGV (Morden Blush x George Vancouver), K5 (K5 cut rose mapping population).

QTL Analysis

The different QTL mapping software packages use different algorithms to calculate the position of QTL and their support intervals (1.5 LOD) leading to differences between the positions and phenotypic variance assigned to each QTL. In most cases, the different software's QTL positions only varied a few cM (Tables 2.18-2.19). The only trait that had inconsistent QTL positions were the traits dealing with RRD. The 1.5 LOD 95% confidence intervals overlap when using different QTL mapping software packages thus giving us confidence that there are genetic factors on the chromosomes of interest. The convention used for the naming of QTL is the convention used for uploading results to the Genome Database for Rosaceae (GDR; www.rosaceae.org). Due to the naming convention for GDR, the naming of linkage group (LG) mentioned in the text and chromosome (ch) used in the QTL names are synonymous. The allele effects are described as the parent contributing the allele affecting the QTL and a ↑ or ↓ symbol describing whether the presence of the allele increases or decreases the phenotypic mean.

Table 2.18. QTL detected for the tetraploid mapping population Brite Eyes x My Girl for black spot, cercospora, and RRD.

QTL[a]	Trait	Contributing Allele[b]	Detection Method	LG	LOD	Position (cM)[c]	Position (Mb)[d]	Phenotypic Variance explained	GWASpoly position (bp)[e]
qRDR.BExMG-ch3	Black spot	MG (0x1) ↓	TetraploidSNPMap	3	12.83	43 (39 - 47)	28.30-40.85	27.1	28.22-40.98
			QTLPoly_feim	3	12.65	49.00 (43.16 - 53.11)	28.30-45.85	28.71	28.22-40.99
			QTLPoly_remim	3	>15.65	45.65 (45.65-46.30)	28.30-39.44	34.91	28.22-40.10
qRDR.BExMG-ch5	Black spot	BE (1x0) ↓	TetraploidSNPMap	5	13	47 (46 - 51)	32.93-76.40	26.6	40.79
			QTLPoly_feim	5	13.65	47.36 (47.36 - 48.18)	36.84-44.62	30.8	40.79
			QTLPoly_remim	5	>15.65	47.36 (44.12 - 48.18)	31.05-76.40	36.93	40.79
qCERC.BExMG-ch1	Cercospora	BE (1x0) ↓	TetraploidSNPMap	1	15.03	18 (13 - 21)	12.50-62.55	33.01	10.39-62.55
			QTLPoly_feim	1	15.46	15.25 (13.07 - 17.14)	12.50-47.27	34.45	10.39-62.56
			QTLPoly_remim	1	>15.65	15.25 (12.10 - 22.46)	10.39-62.55	41.18	10.39-62.57
qCERC.BExMG-ch5	Cercospora	BE (1x0) ↑	TetraploidSNPMap	5	10.45	47 (45 - 47)	32.55-76.40	26.6	40.79-44.36
			QTLPoly_feim	5	10.43	51.05 (43.06 - 54.00)	10.96-77.61	23.8	40.79-44.37
			QTLPoly_remim	5	7.42	47.36 (44.12 - 52.15)	31.05-77.61	24.35	40.79-44.38
qRRD.BExMG-ch5	RRD-rosettes	BE (1x0) ↓	TetraploidSNPMap	5	6.29	8 (6.5 - 10.5)	0.74-4.14	13.75	5.65-15.61
			QTLPoly_feim	5	5.79	21.12 (10.02 - 27.00)	0.19-33.47	14.99	5.65-15.62
			QTLPoly_remim	NA	NA	NA	NA	NA	NA
qRRV.BExMG-ch5	RRV-RT-qPCR	BE (1x0) ↑	TetraploidSNPMap	5	7.29	16 (15-17.5)	5.42-14.12	18.42	5.45-14.89
			QTLPoly_feim	5	6.33	16.36 (10.02 – 43.06)	3.25-50.91	15.50	5.45-14.90
			QTLPoly_remim	5	4.74	37.24 (8.25 – 44.12)	1.14-50.91	22.41	5.45-14.91

[a]Name of QTL following the naming conventions of the Genome Database for Rosaceae.
[b]Parent contributing allele which affects the trait mean. Estimated by using "qtl_effects" function in QTLpoly. Alleles affecting the trait mean are followed by estimated mode of inheritance in the parenthesis and also indicative of whether the allele caused an increase (↑) or decrease (↓) of the mean of the phenotype.
[c]QTL peak position followed by 1.5 LOD confidence intervals in parenthesis.
[d]Physical positions of markers within the 1.5 LOD confidence intervals. WagRhSNP 68k Axiom SNP array probes were aligned to the Saint-Oyant, 2018 genome.
[e]Physical position of markers within 1.5 LOD from the peak found in genome-wide association scans using GWASpoly.

Table 2.19. QTL detected for the tetraploid mapping population Stormy Weather x Brite Eyes black spot, cercospora, defoliation, and RRD.

QTL[a]	Trait	Contributing Allele[b]	Detection Method	LG	LOD	Position (cM)[c]	Position (Mb)[d]	Phenotypic Variance explained	GWASpoly position (bp)[e]
qRDR.SWxBE-ch5	Black spot	BE (0x1) ↓	TetraploidSNPMap	5	30.96	55 (54 - 56)	36.31-52.66	50.65	40.79-41.06
			QTLPoly_feim	5	33.25	54.20 (54.20 - 56.09)	35.90-52.66	54.05	40.79-41.07
			QTLPoly_remim	5	>15.65	54.2 (38.22 - 69.02)	10.96-77.61	70.68	40.79-41.08
qRDR.SWxBE-ch7	Black spot	NA	TetraploidSNPMap	7	5.57	46 (44-51)	25.57-39.58	9.5	42.7
			QTLPoly_feim	7	5.76	48.12 (34.15-51.09)	18.93-39.58	10.23	42.7
			QTLPoly_remim	NA	NA	NA	NA	NA	NA
qCERC.SWxBE-ch1	Cercospora	BE (0x1) ↓	TetraploidSNPMap	1	4.95	21 (18.5 - 23.5)	17.75-50.24	4.5	27.78-39.13
			QTLPoly_feim	1	6.73	30.01 (22.12 - 30.01)	23.82-50.24	12.32	27.78-39.14
			QTLPoly_remim	1	4.959	23.19 (0.00 - 30.01	0.37-61.02	16.47	27.78-39.15
qCERC.SWxBE-ch4	Cercospora	NA	TetraploidSNPMap	4	4.75	37 (27 - 43)	7.74-58.09	7.69	NA
			QTLPoly_feim	NA	NA	NA	NA	NA	NA
			QTLPoly_remim	NA	NA	NA	NA	NA	NA
qCERC.SWxBE-ch5	Cercospora	BE (0x1) ↑	TetraploidSNPMap	5	18.96	55 (53.5 - 57)	35.90-52.66	40.16	24.91-54.42
			QTLPoly_feim	5	19.88	55.18 (54.2 - 56.09)	35.90-52.66	36.37	24.91-54.43
			QTLPoly_remim	5	>15.65	55.18 (50.1 - 67.12)	10.96-77.61	48.95	24.91-54.44
qDEF.SWxBE-ch3	Defoliation	SW (1x0) ↑	TetraploidSNPMap	3	4.86	28 (23 - 34)	28.21-37.74	5.55	NA
			QTLPoly_feim	NA		NA	NA	NA	NA
			QTLPoly_remim	3	5.684	25.14(22.11-30.12)	26.40-34.18	12.16	NA
qDEF.SWxBE-ch5	Defoliation	BE (0x1) ↓	TetraploidSNPMap	5	15.36	53 (52 - 57)	32.69-52.66	29.33	32.69-41.06
			QTLPoly_feim	5	16.21	53.06 (52.15 - 58.01)	32.69-77.61	30.42	32.69-41.07
			QTLPoly_remim	5	>15.65	53.06 (53.06 - 58.01)	35.78-77.61	46.87	32.69-41.08

Table continued next page

Table 2.19. Continued

QTL[a]	Trait	Contributing Allele[b]	Detection Method	LG	LOD	Position (cM)[c]	Position (Mb)[d]	Phenotypic Variance explained	GWAspoly Position (bp)[e]
qDEF.SWxBE-ch7	Defoliation	SW (2x0) ↓↑	TetraploidSNPMap	7	4.1	49(33-55)	25.57-39.58	6	2.19
			QTLPoly_feim	NA	NA	NA	NA	NA	NA
			QTLPoly_remim	7	3.507	65.09 (44.01-74.68)	25.57-66.90	7.7	2.19
qRRV.SWxBE-ch3	RRV-RT-qPCR	SW (1x0) ↓	TetraploidSNPMap	3	6.26	12 (0-14)	0.07-25.60	10.81	10.17-23.30
			QTLPoly_feim	3	7.11	11.06 (9.09 - 13.17)	1.20-25.50	13.73	10.17-23.31
			QTLPoly_remim	NA	NA	NA	NA	NA	NA
qRRV.SWxBE-ch5	RRV-RT-qPCR	BE (0x1) ↑	TetraploidSNPMap	5	5.86	58 (53-61)	27.07-53.41	9.50	NA
			QTLPoly_feim	NA	NA	NA	NA	NA	NA
			QTLPoly_remim	NA	NA	NA	NA	NA	NA

[a]Name of QTL following the naming conventions of the Genome Database for Rosaceae.
[b]Parent contributing allele which affects the trait mean. Estimated by using "qtl_effects" function in QTLpoly. Alleles affecting the trait mean are followed by estimated mode of inheritance in the parenthesis and also indicative of whether the allele caused an increase (↑) or decrease (↓) of the mean of the phenotype. An NA in this column denotes that either the software used cannot calculate a parental allele effect or the QTL's segregation pattern is too complex to accurately estimate the allele effects of the parental alleles.
[c]QTL peak position followed by 1.5 LOD confidence intervals in parenthesis.
[d]Physical positions of markers within the 1.5 LOD confidence intervals. WagRhSNP 68k Axiom SNP array probes were aligned to the Saint-Oyant, 2018 genome.
[e]Physical position of markers within 1.5 LOD from the peak found in genome-wide association scans using GWASpoly.

Black Spot Resistance

QTL scans performed with both interval mapping and GWAS analysis for black spot resistance show QTL on LGs 3, 5, and 7 (Tables 2.18-2.19). The SWxBE family had black spot resistance QTL on LGs 5 and 7 (*qRDR.SWxBE-ch5 and qRDR.SWxBE-ch7*) while the BExMG family had QTL on LGs 3 and 5 (*qRDR.BExMG-ch3* and *qRDR.BExMG-ch5*).

Both mapping populations have the QTL on LG 5 (*qRDR.BExMG-ch5* and *qRDR.SWxBE-ch5*) while the black spot QTL on LG 3, *qRDR.BExMG-ch3,* only appears in the BExMG family and the QTL on LG 7, *qRDR.SWxBE-ch7*, only appears in the SWxBE family. The contributing allele to the QTL on LG 3 comes from MG (0x1) which presence lowers the phenotypic mean and the QTL described in both populations on LG 5 comes from BE (1x0) which also lowers the phenotypic mean. We are not confident about the allele effect estimates of *qRDR.SWxBE-ch7,* as it looks like the segregation of this QTL is in a duplex x triplex manner. While we are confident on the estimates of the allele effects and in the segregation patterns of the simplex x nulliplex QTL because of the 1:1 segregation ratio, segregation ratios become more complex as you add more dosage classes. For example a 1x1 genetic factor in a tetraploid would segregate in a 1:2:1 ratio for the duplex : simplex : nulliplex (Zych et al., 2019). With populations like ours, n=160-200, we cannot be too certain of the estimates of how QTL are inherited if the software indicates segregation patterns greater than simplex x simplex. The position of the QTL on LG 5 is similar in both populations and overlaps the *Rdr4* region described by Zurn et al. (2018) thus we conclude that these two QTL

represent the *Rdr4* black spot resistance locus. We determined the position of *Rdr4* by flanking markers described by Zurn et al. (2018). The QTL on LG 5 are also near the meta-QTL Meta_2_5, described by (Lopez Arias et al., 2020). The proportion of variance explained (PVE) of the QTL on LGs 3 and 5 range from 27.1 to 70.68% while the QTL on LG 7 only had a PVE of 9.5 to 10.23%. Therefore, the QTL described on LGs 3 and 5 have greater effects on black spot resistance compared to the QTL on LG 7. Examining QTLpoly's estimated allele effects on the black spot QTL on LG 7, the QTL seems to be segregating in a duplex x triplex manner. This estimation is most likely not accurate due to difficulty in fitting these higher dosage segregation patterns in population sizes of around 200 individuals. However we can tell that this QTL is not segregating in any of the lower dosage segregation ratios that we can describe with our population sizes.

The genome-wide association analyses (GWAS) agreed with the interval mapping QTL scans (Figure 2.29). When both populations are analyzed together, we detect the presence of both QTL on LGs 3 and 5. When analyzed separately, *qRDR.SWxBE-ch5* is detected in the SWxBE population only, while both *qRDR.BExMG-ch3 and qRDR.BExMG-ch5* were evident in the BExMG population. The GWAS scans did not reveal any peak on LG 7, and the few significant markers identified did not collocate with *qRDR.SWxBE-ch7*.

GWAS scans on monthly phenotypic ratings reveal higher peaks (greater than LOD 10) in June, July, October, and November as compared to August and September

(Figure 2.30), which corresponds to the months with larger disease pressure which also had higher heritability estimates (Table 2.12, Figure 2.30).

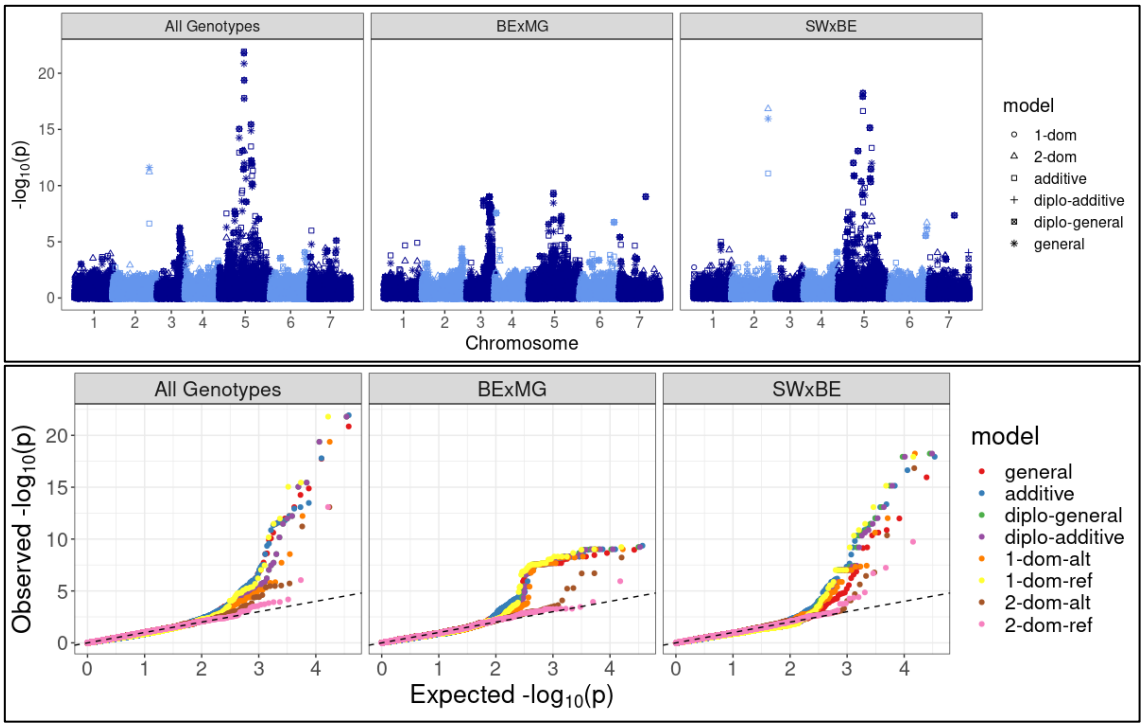

Figure 2.29. Black spot genome-wide association scans of both the BExMG and SWxBE populations together and separately on plants phenotyped in College Station, TX, and Overton, TX, in 2019. The Manhattan plot pictured on the left is of both families run together while the plot in the middle is only the members of the BExMG family and the plot on the right is only the SWxBE family. Six models were used for scans and are plotted as quantile-quantile (bottom) and Manhattan plots (above).

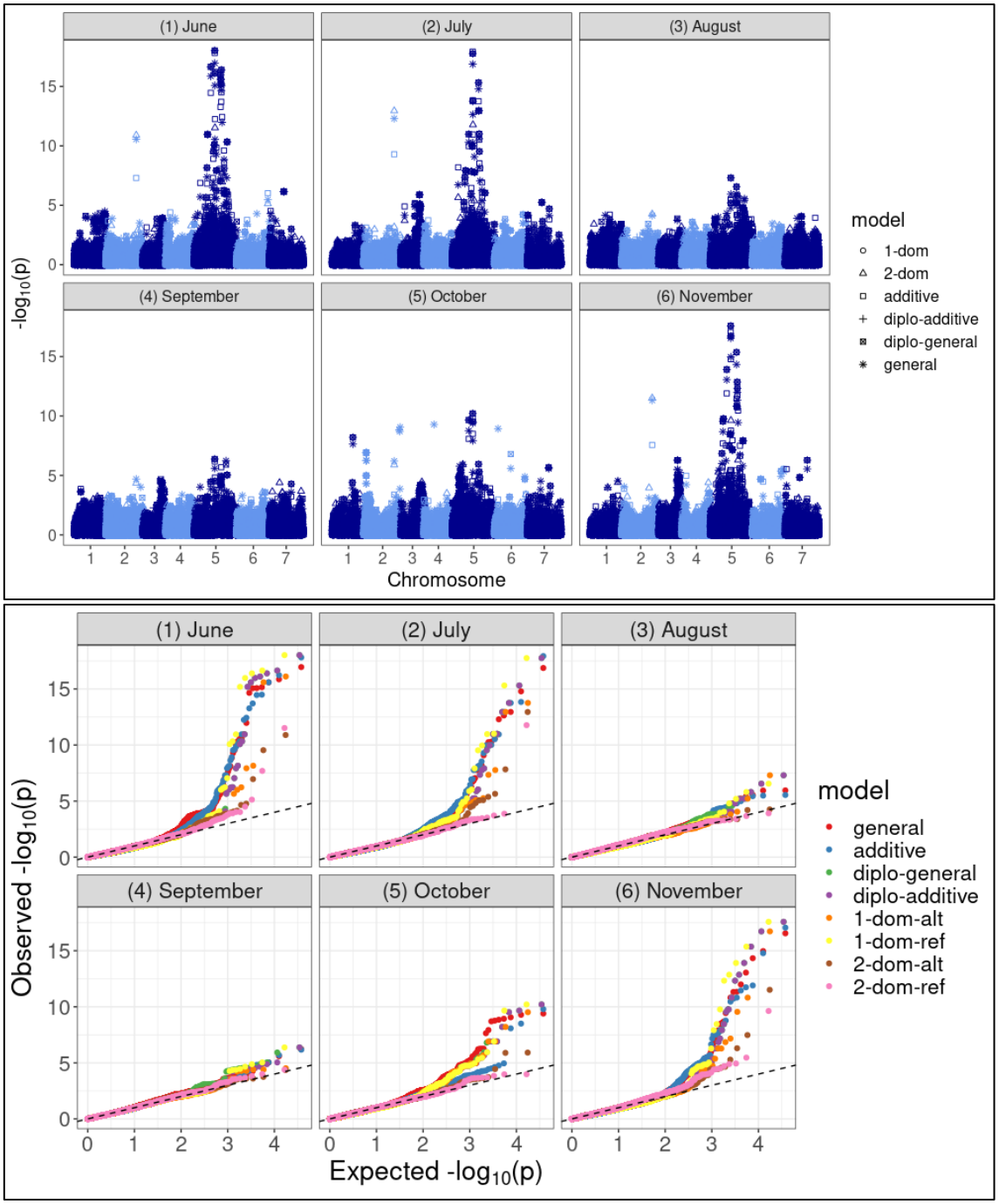

Figure 2.30. Manhattan plots (top) and quantile-quantile plots (bottom) of genome-wide association analysis of black spot incidence on two garden rose families in 2019 in College Station, TX, over six months (June through November). The greatest peaks can be seen on data taken in June, July, October, and November.

Defoliation Resistance

Black spot impacts defoliation as serious black spot infections can completely defoliate the plants. Thus, co-localization of QTL for defoliation and black spot would be expected. However, the weak correlation between black spot and defoliation in our analysis indicates that there are other factors beyond black spot affecting defoliation in our populations. We observed some overlap in the location of QTL for black spot and defoliation.

There were no significant QTL peaks for defoliation in the BExMG population, however the SWxBE population showed a peak on LGs 3, 5, and 7 (*qDEF.SWxBE-ch3*, *qDEF.SWxBE-ch5*, and *qDEF.SWxBE-ch7*) (Tables 2.18-2.19). The PVE of *qDEF.SWxBE-ch3* and *qDEF.SWxBE-ch7* were low ranging between 5.55 and 12.16% while estimates of PVE of *qDEF.SWxBE-ch5* were greater between 29.33 and 46.87%. Interestingly, the black spot and defoliation QTL peaks on LG 5 are 2-3 cM from each other. Based on the "qtl_effects" function in QTLpoly, Stormy Weather contributes an allele at *qDEF.SWxBE-ch3* that increases the amount of defoliation while the favorable allele (decreasing defoliation) for *qDEF.SWxBE-ch5* is from the same homolog as the black spot resistance donated from Brite Eyes. Since both black spot and defoliation QTL on LG 5 are positioned relatively close (2 to 3 cM), these may represent the same genetic factor. This is plausible since black spot infections cause defoliation. Both the black spot and defoliation QTL on LG5 appear to overlap *Rdr4* (Figure 2.35) suggesting that these are QTL representing the black spot resistance locus, *Rdr4* (Zurn et al., 2018).

SW contributes two alleles for *qDEF.SWxBE-ch7* one allele increases while the other decreases the phenotypic mean for defoliation.

GWAS scans also show no significant associations when the BExMG population is scanned alone whereas when either both populations or SWxBE was scanned alone, we observe a peak on LG 5 around 32 Mb (Figure 2.31). Only 1 marker on LG 2 and 1 marker on LG 7 were significantly associated with defoliation; however, since these do not have any observed peak building up to the significant markers, and they are not in the same relative positions described by the interval mapping QTL scans, these marker-trait associations are probably due to markers being assigned to the incorrect physical positions when performing BLAST analysis of the sequences comprising the WagRhSNP 68k array to the rose genome.

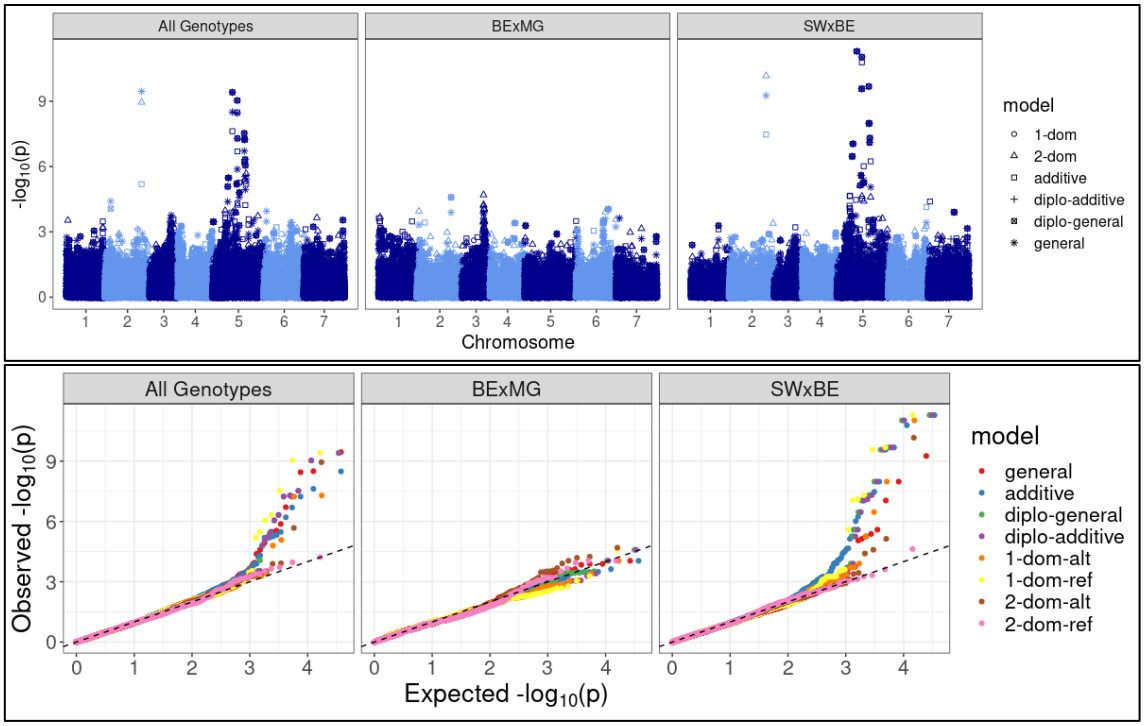

Figure 2.31. Manhattan plots (top) and quantile-quantile plots (bottom) of genome-wide association scans for defoliation phenotyped on two tetraploid garden rose mapping populations both together (left) and separately (middle and right) in College Station, TX, and Overton, TX in 2019.

Cercospora Resistance

Cercospora resistance QTL were observed on LGs 1, 4, and 5 in the SWxBE population (*qCERC.SWxBE-ch1*, *qCERC.SWxBE-ch4*, and *qCERC.SWxBE-ch5*) and only on LGs 1 and 5 in the BExMG population (*qCERC.BExMG-ch1* and *qCERC.BExMG-ch5*) (Tables 2.18-2.19). Both populations have cercospora QTL derived from the BE parent on LGs 1 and 5 in similar genetic positions. However, *qCERC.SWxBE-ch4* is only detected using TetraploidSNPMap and has approximately 7.69% of variance attributed to the QTL. When using QTLPoly_remim, *qCERC.SWxBE-ch4* was only classified as a putative QTL present in the forward search of the QTL,

however in backwards elimination, the stringent p-value used eliminates this QTL. When looking closer at *qCERC.SWxBE-ch4*, it appears that both BE and SW donate an allele that contributes to cercospora resistance. As this QTL is only picked up using TetraploidSNPMap, we are not able to estimate the any allele effects from the QTL which affect the phenotypic mean. GWAS scans only show the LG1 and LG5 QTL in both families while the QTL on LG 4 is not picked up (Figure 2.32).

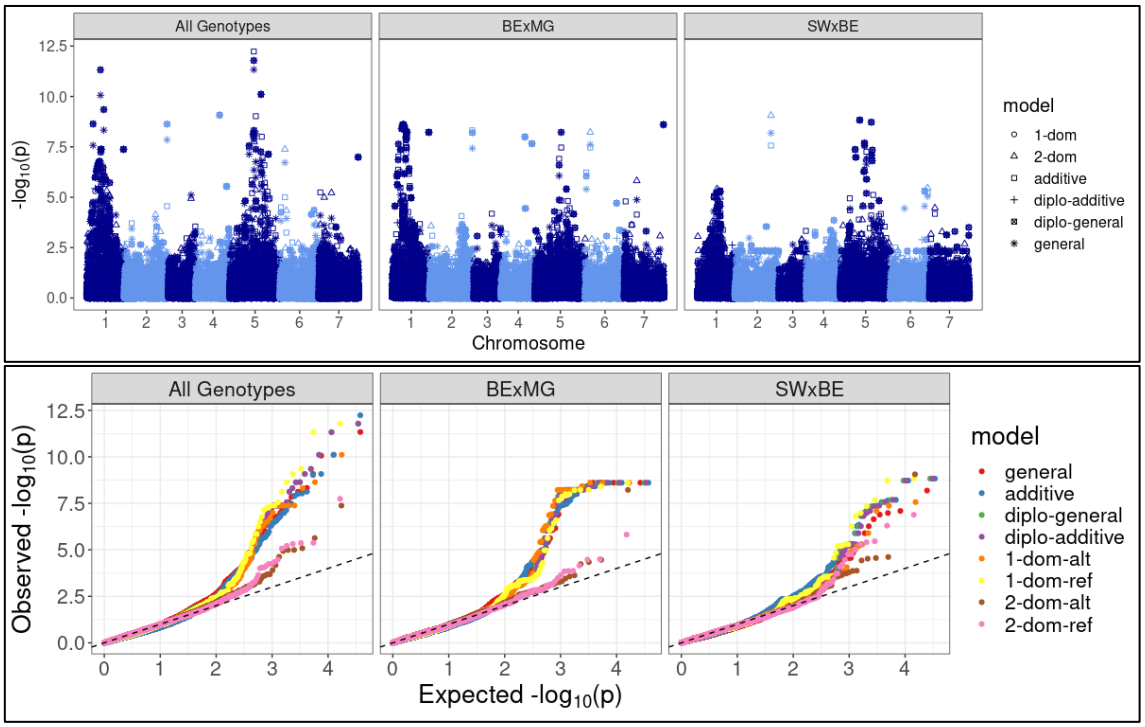

Figure 2.32. Manhattan plots (top) and quantile-quantile plots (bottom) of genome-wide association scans of two tetraploid mapping populations both together and separately for cercospora leaf spot incidence at College Station, TX, and Overton, TX, in 2019. The Manhattan plot pictured on the left is of both families run together while the plot in the middle is only the members of SWxBE family and the plot on the right is only the BExMG family.

Rose Rosette Resistance

Analysis with RRD phenotypic ratings showed a small effect QTL in both interval mapping QTL scans (Tables 2.18-2.19) and GWAS scans (Figure 2.33) for rose rosette severity and number of rose rosettes on LG 5 only in the BExMG population (*qRRD.BExMG-ch5*). However, QTL scans with the RT-qPCR results indicated a QTL in the similar location as the QTL that we observed using the visual phenotypic ratings in the BExMG population (*qRRV.BExMG-ch5*). The SWxBE population had one QTL detected on LG 3 (*qRRV.SWxBE-ch3*) and possibly a QTL on LG 5 picked up by TetrploidSNPMap. When using the visual RRD ratings and qPCR results for QTL analysis, the resistance allele of RRD resistance on LG 5 comes from Brite Eyes while the QTL on LG 3 using the qPCR results has one allele from SW that negatively affects the phenotypic mean. A decrease in CT values suggests an increase in virus titer. The variability in the placement of the QTL for both the visual phenotypic ratings and the RRV titer estimated by the CT values leads us to believe there may be genetic factors on the proximal arm of LG 5. However more data collection may be needed as it can take 3-4 years of phenotyping to accurately assess the susceptibility of genotypes to RRD/RRV.

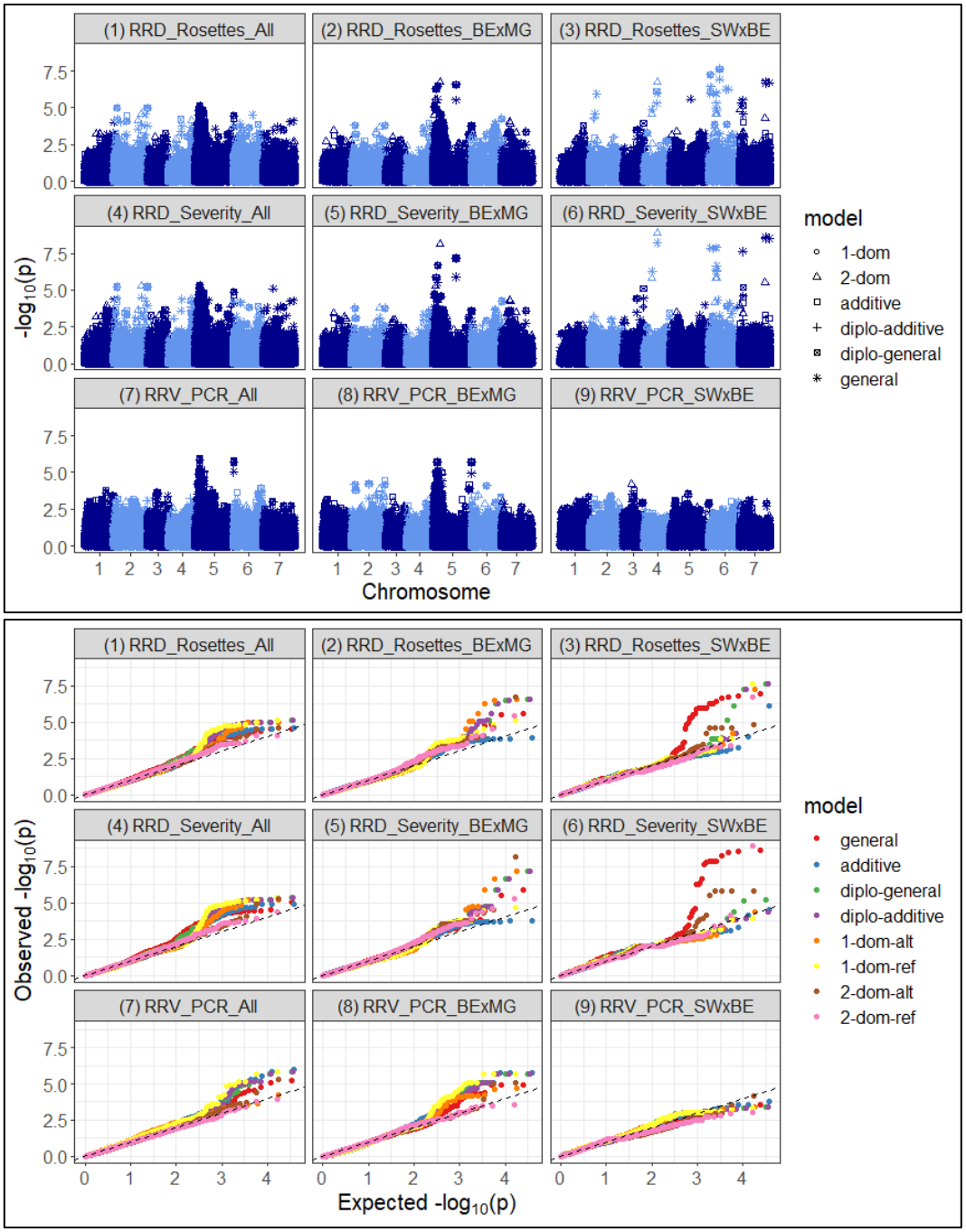

Figure 2.33. Manhattan plots (top) and quantile-quantile plots (bottom) of genome-wide association scans on two tetraploid garden rose populations BExMG and SWxBE both together and by themselves for rose rosette disease number of rosettes (1-3), severity ratings (4-6), and rt-qPCR of RRV (7-9) phenotyped in Crossville, TN. All denotes that all genotypes were run together while BExMG is the Brite Eyes x My Girl population run alone and SWxBE is Stormy Weather x Brite Eyes run by itself.

Interaction Between Black Spot, Cercospora, and Defoliation

QTL scans for black spot, cercospora, and defoliation revealed QTL in similar positions on LG5 near the *Rdr4* locus (Zurn et al., 2018). Using flanking markers described by Zurn et al. (2018), we determined that the black spot QTL (*qRDR.BExMG-ch5* and *qRDR.SWxBE-ch5*) overlaps with the black spot resistance *Rdr4* locus. Zurn et al. (2018) determined that the donor parent for black spot resistance is Brite Eyes which is a common parent in both our mapping populations (Figures 2.34-2.37).

In both interval mapping and in GWAS scans, the cercospora QTL on LG5 is located in the same area as that of black spot resistance (Figures 2.34-2.37). The most significant marker for both black spot and cercospora resistance in the GWAS scans was Rh12GR_81013_297 and upon closer inspection of the marker alleles, progeny with the allele dosage 3 (ACCC) had a lower mean occurrence of black spot and higher amounts of cercospora while progeny with the allele dosage 4 (CCCC) had the opposite effect. Rh12GR_81013_297 is also the second most significant marker for defoliation on LG 5 and similar to blackspot, the individuals with the dosage of 3 (ACCC) had a lower amount of defoliation while individuals with the dosage of 4 (CCCC) had higher amounts of defoliation.

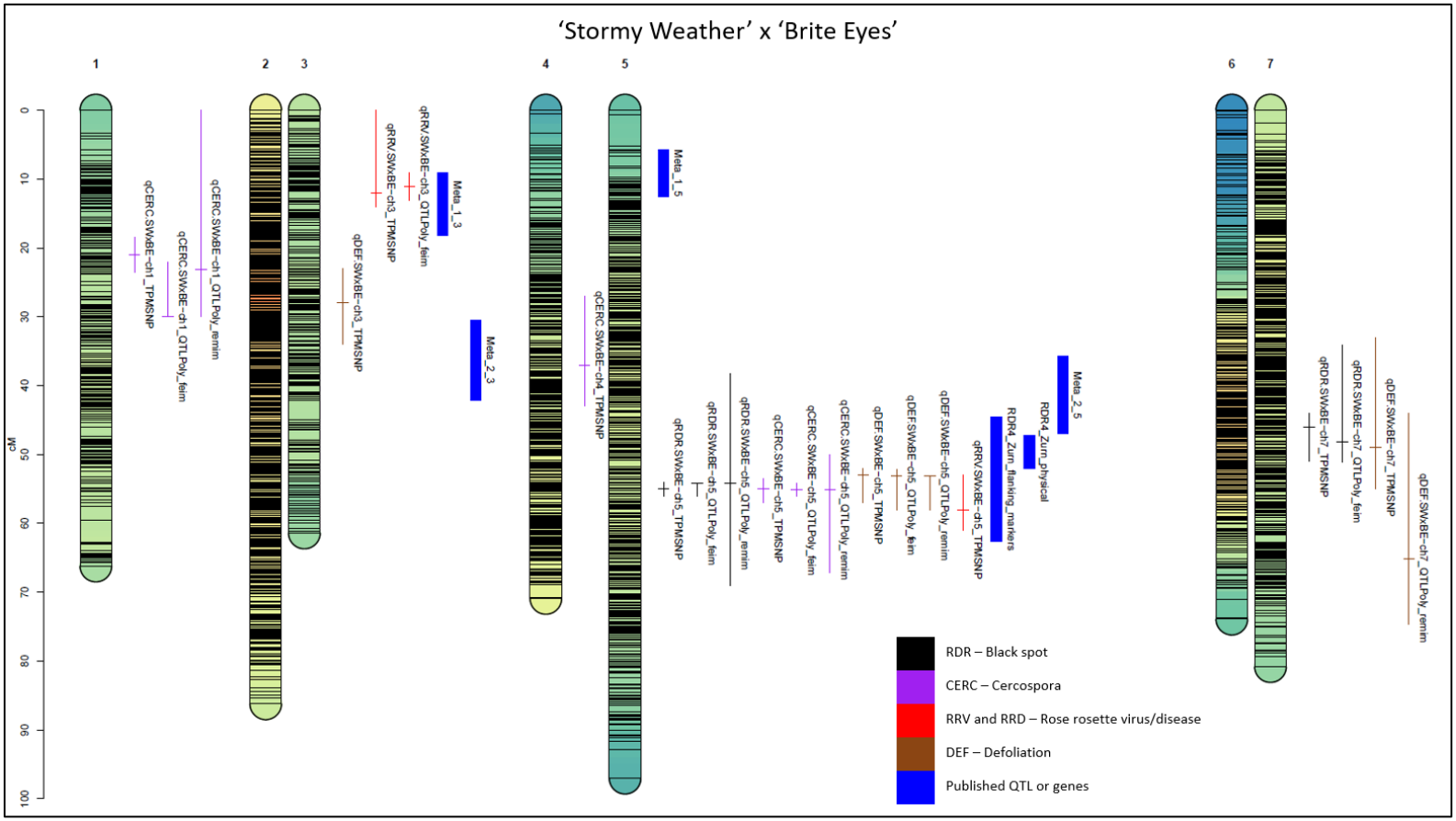

Figure 2.34. Linkage map of tetraploid mapping population Stormy Weather x Brite Eyes with QTL peaks denoted by a horizontal mark and the 1.5 LOD confidence interval denoted by the whiskers. QTL are labeled with the names of the software used to detect the QTL. *Rdr4* is displayed using a thick blue bar and the boundary of the gene is determined by the flanking markers described by Zurn et al. (2018). The RDR4_Zurn_flanking_markers bar the placement of Rdr4 based off the flanking markers also being mapped in this population whereas the RDR4_Zurn_physical is the physical estimate of the flanking markers. The Meta_1_3, Meta_2_3, Meta_1_5 and Meta_2_5 are the meta-QTL described by Lopez Arias et al. (2020).

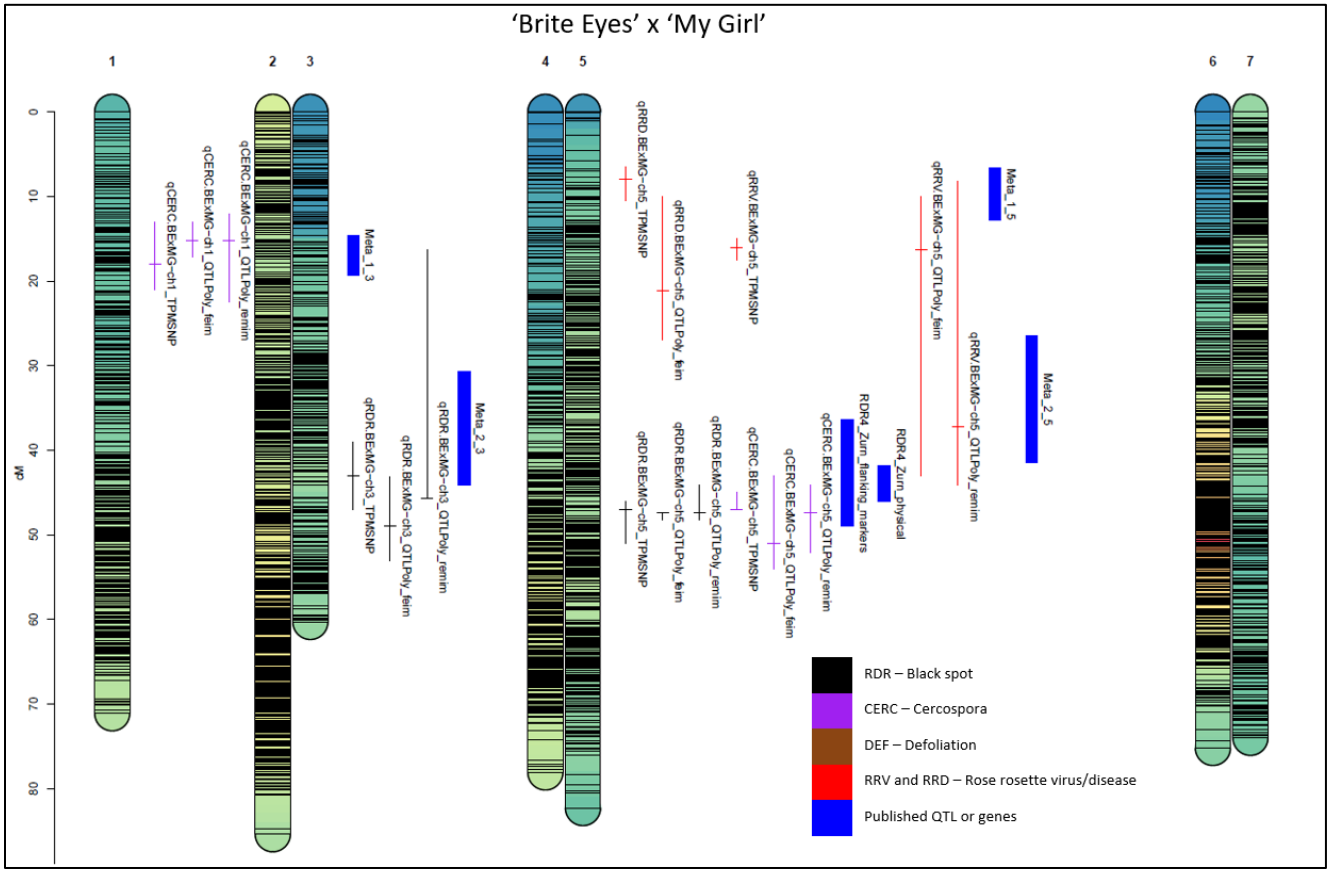

Figure 2.35. Linkage map of tetraploid mapping population Brite Eyes x My Girl with QTL peaks denoted by a horizontal mark and the 1.5 LOD confidence interval denoted by the whiskers. QTL are labeled with the names of the software used to detect the QTL. *Rdr4* is displayed using a thick black bar and the boundary of the gene is determined by the flanking markers described by Zurn et al. (2018). The RDR4_Zurn_flanking_markers bar the placement of Rdr4 based off the flanking markers also being mapped in this population whereas the RDR4_Zurn_physical is the physical estimate of the flanking markers. The Meta_1_3, Meta_2_3, Meta_1_5 and Meta_2_5 are the meta-QTL described by Lopez Arias et al. (2020).

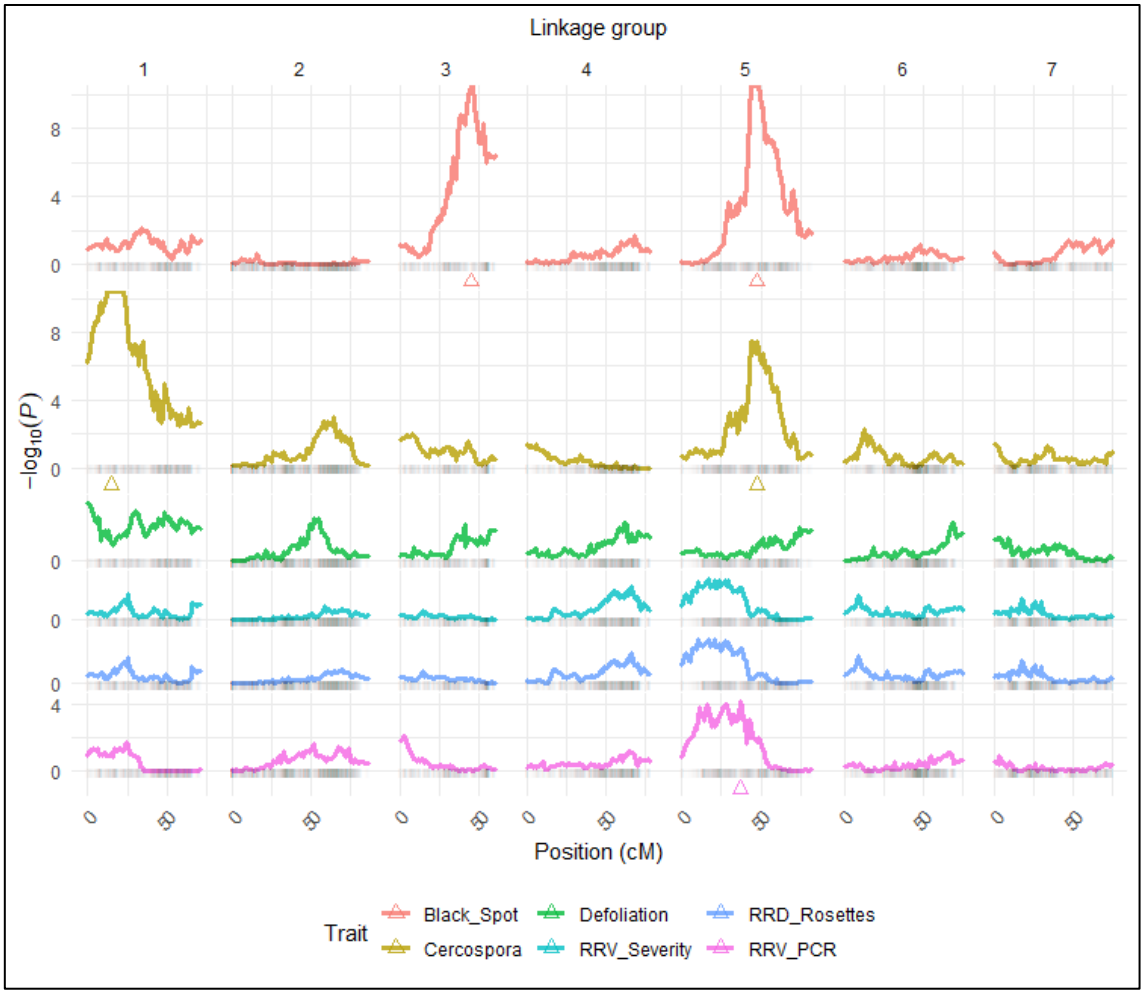

Figure 2.36. QTL scans of tetraploid rose mapping population Brite Eyes x My Girl using the "remim" function in QTLpoly. QTL peaks are denoted by a triangle under the QTL scans. Some peaks may not be visible on the graph due to a max p-value that can be displayed in R.

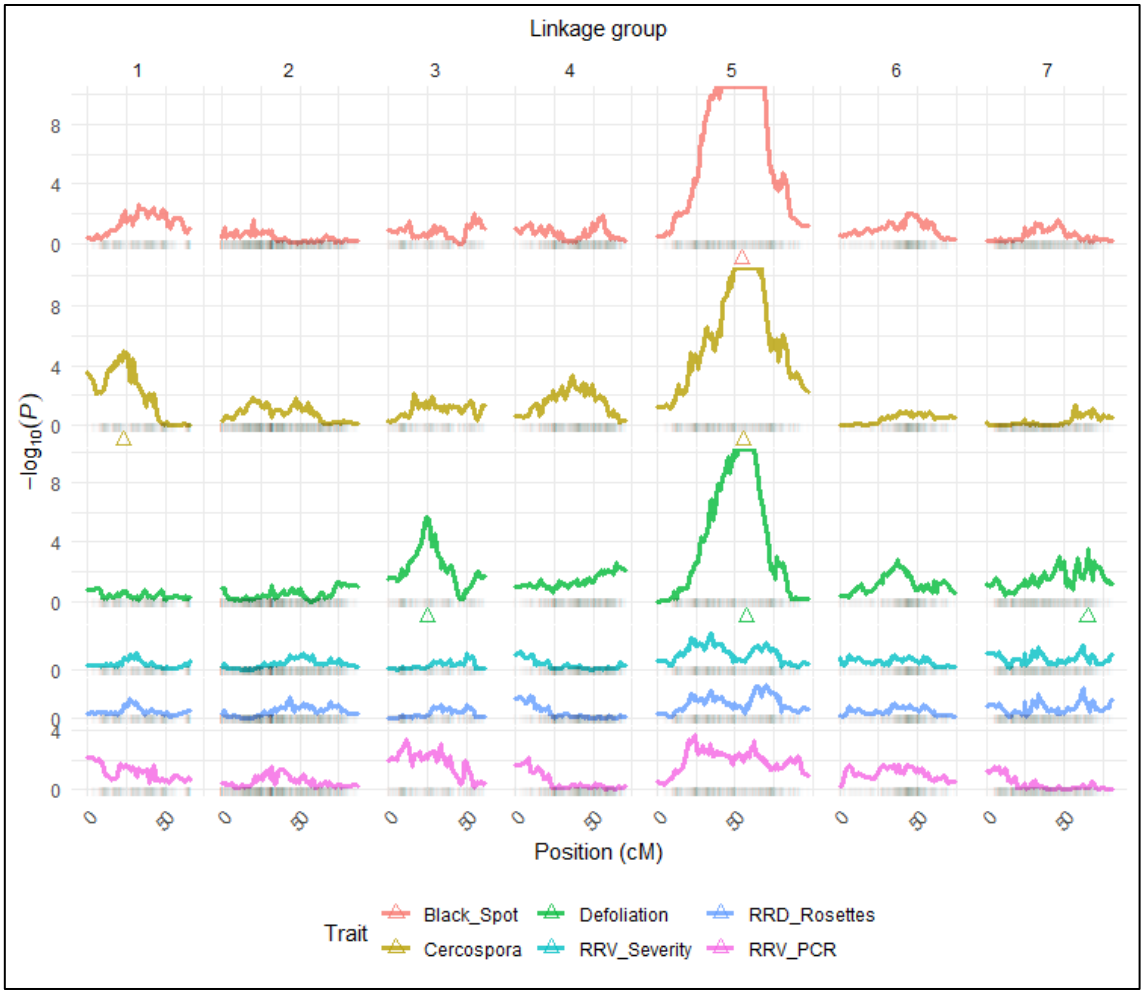

Figure 2.37. QTL scans of tetraploid mapping population Stormy Weather x Brite Eyes using the "remim" function in QTLpoly. Some peaks may not be visible on the graph due to a max p-value that can be displayed in R.

It is not surprising that QTL for defoliation and black spot QTL were co-located sense as severe black spot infections cause defoliation. However, having cercospora and black spot QTL in the same location means either these are two tightly linked alleles, or resistance to both defoliation and blackspot is controlled by one allele. Results from QTLpoly suggest that both black spot and cercospora are affected by QTL on the same homolog (Figures 2.38-2.39). The same homolog conferring black spot resistance

(negative allele effect) also results in cercospora susceptibility (positive allele effect). This is supported by the GWAS analysis (Figures 2.40-2.41) that identified the markers associated with resistance to black spot were also associated with susceptibility to cercospora. This would indicate that either there are two closely linked alleles with opposite effects or the cercospora peak is an artifact of how we phenotype for these disease resistances. With the available data it is not possible to determine whether the QTL controlling black spot, cercospora, and defoliation are stemming from the same genetic factor as it would require many more individuals to dissect closely linked loci.

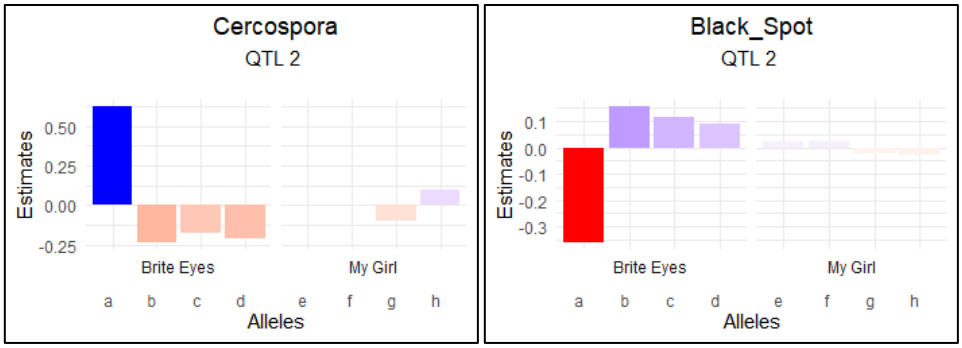

Figure 2.38. Allele effect estimates for black spot and cercospora leaf spot for tetraploid rose mapping population Brite Eyes x My Girl phenotyped in College Station, TX, and Overton, TX, in 2019. Allele estimates show opposite allele effects from the same homolog contributing to the two traits.

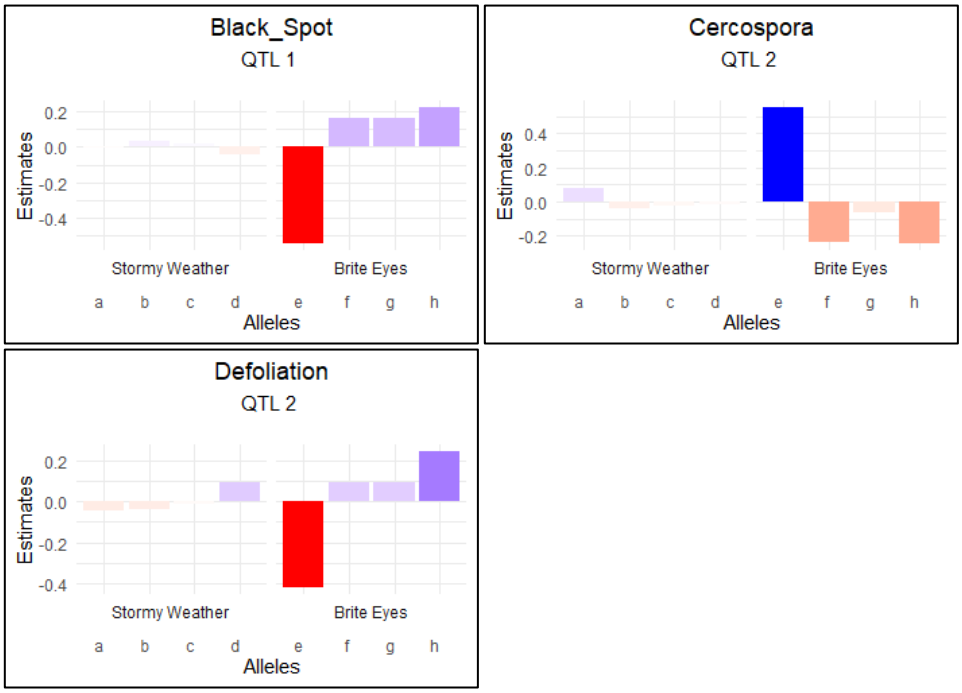

Figure 2.39. Allele effect estimates for black spot, cercospora leaf spot, and defoliation for Stormy Weather x Brite Eyes phenotyped in College Station, TX, and Overton, TX, in 2019. The allele effects show different black spot and cerospora allele effects while showing the same allele effects for defoliation. Allele estimates are estimated using the 'qtl_effects' function in QTLpoly which estimates the additive effects of each parental allele and all the resulting combinations within the progeny for that specific QTL.

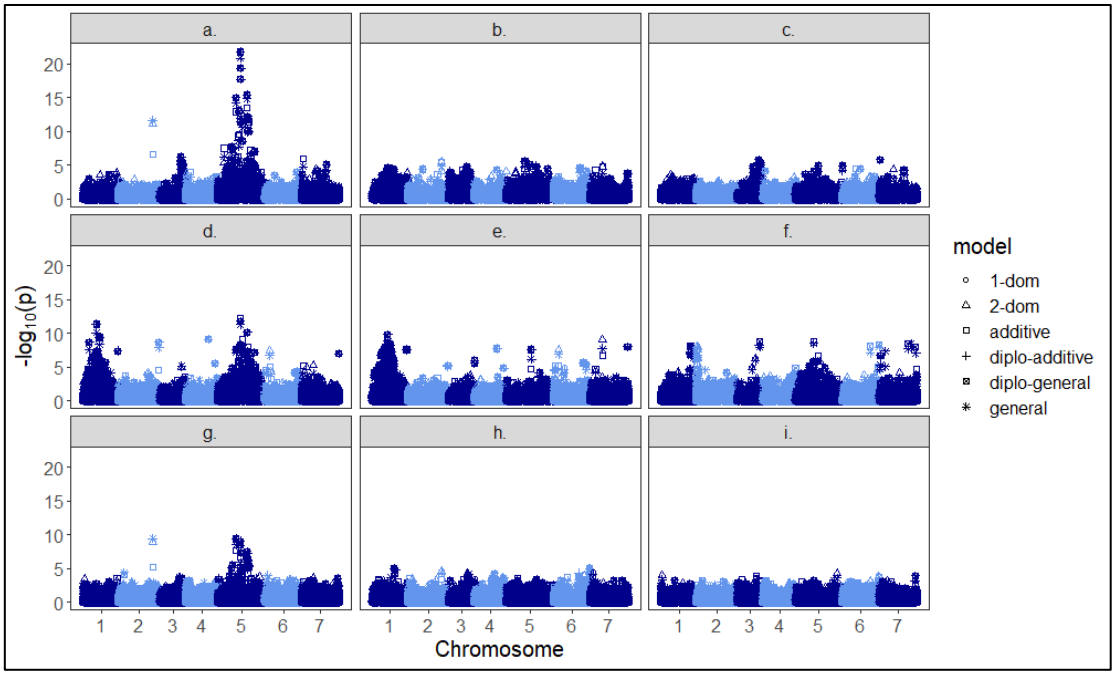

Figure 2.40. Manhattan plots of genome-wide association scans with GWASpoly on two tetraploid mapping populations using either all genotypes, black spot resistant genotypes, and black spot susceptible genotypes (from left to right). a. black spot scans on all genotypes, b. black spot scans on black spot resistant genotypes, c. black spot scans on black spot susceptible genotypes, d. cercospora scans on all genotypes, e. cercospora scans on black spot resistant genotypes, f. cercospora scans on black spot susceptible genotypes, g. defoliation scans on all genotypes, h. defoliation scans on black spot resistant genotypes, i. defoliation scans on black spot susceptible genotypes.

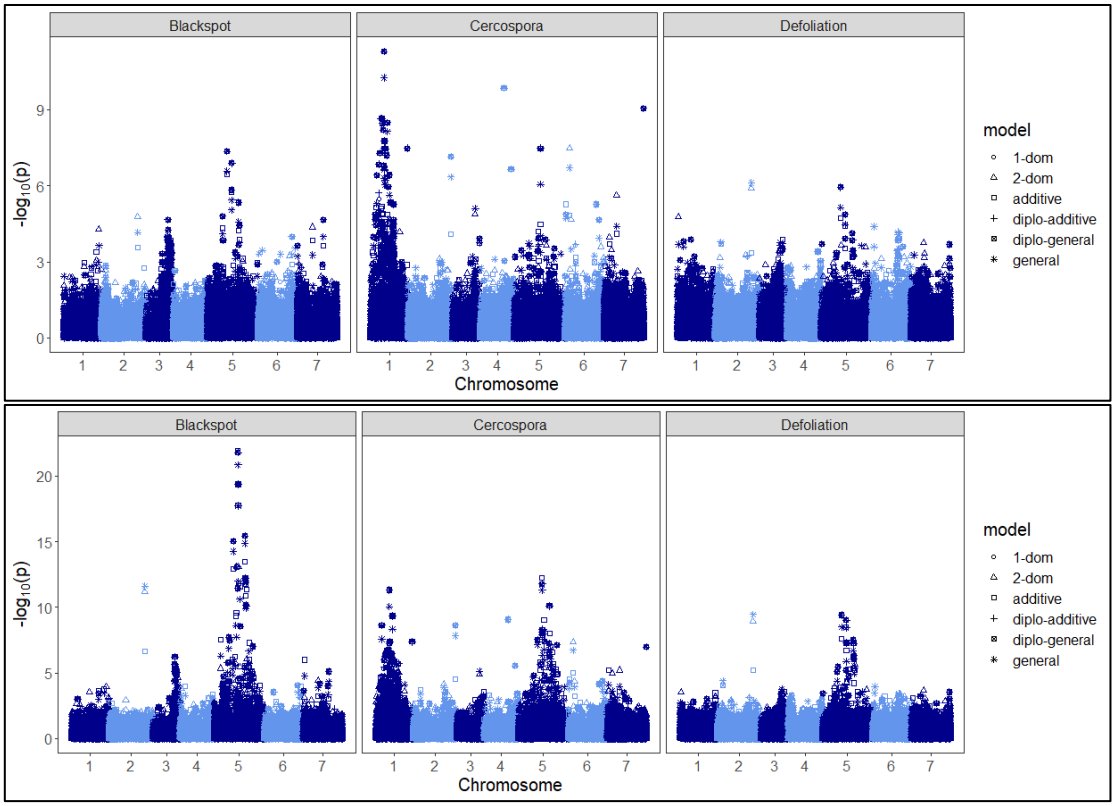

Figure 2.41. Manhattan plots of genome-wide association scans with GWASpoly of two tetraploid rose mapping populations using black spot resistance as a fixed effect (top) and plots of genome-wide association scans without using black spot resistance as a fixed effect (bottom).

Marker Based Selection of Progeny

QTL scans in TetraploidSNPMap and MAPpoly determined that QTL conferred resistance to black spot and cercospora in the BExMG population. The *qRDR.BExMG-ch3* was inherited from My Girl and *qRDR.BExMG-ch5* was inherited from "Brite Eyes." Both QTL were detected as inherited in a simplex (resistance donor) x nulliplex segregation within the population. Most significant markers identified using GWASpoly were used to represent the QTL for the trait. Markers tightly linked to resistance are desirable to use in breeding. Genotyping seedlings at an early stage can sidestep the 2-3

year field resistance trials and allow the rapid discarding of individuals that do not carry the alleles for resistance. While the use of the WagRhSNP 68K SNP array would be very expensive to run on all progeny, Kompetitive allele-specific PCR (KASP) markers are much more cost effective when only needing to sample a handful of significant markers. Markers discovered to be important on the WagRhSNP 68K array could be used to design primers for use in KASP genotyping.

For the BExMG population, markers (Table 2.20) were selected for the black spot QTL *qRDR.BExMG-ch3* and *qRDR.BExMG-ch5* and for cercospora *qCERC.BExMG-ch1*. These markers were then used for selecting individuals that carried the resistance alleles in the simplex (AAAB) state. The selected progeny were selected for propagation and further use in breeding crosses. Markers for *qCERC.BExMG-ch5* were not considered as it is in repulsion with *qRDR.BExMG-ch5.* Selecting for individuals with markers for resistance for black spot would be selecting for the individuals that are susceptible to cercospora. Because the three QTL are located on different LGs, independent assortment dictates that in the BExMG population, we would expect a $0.5^3 = 0.125$ or 12.5% of the individuals in the population studied would have all alleles in the resistant state. Out of the 157 individuals we expected 19.625 and observed 18 individuals carrying the three resistance QTL described above ($\chi^2 = 0.135$, df=1, p-value = 0.05).

Table 2.20. Markers from the Brite Eyes x My Girl population used to select progeny with resistance alleles. Markers were identified using GWASpoly.

Affymetrix marker name	Marker name	Model detected	Significance threshold	LG	Position	LOD
qCERC.BExMG-ch1						
Affx-86799619	RhMCRND_8447_241	general	3.74	1	19581440	8.61
Affx-86803478	Rh12GR_56000_1337	general	3.74	1	17763638	8.61
Affx-86833419	Rh12GR_70921_191	general	3.74	1	19130161	8.61
Affx-86788067	RhK5_9643_184	general	3.74	1	16048547	8.41
Affx-86829869	Rh12GR_57675_1635	general	3.74	1	21559226	8.41
Affx-86807748	RhK5_4744_983	additive	3.65	1	23816721	8.26
Affx-86788803	RhMCRND_1094_1131	diplo-general	3.85	1	24733654	8.22
Affx-86789725	RhMCRND_12762_716	diplo-general	3.85	1	24172282	8.22
Affx-86791614	RhMCRND_17225_546	diplo-general	3.85	1	25236582	8.22
Affx-86805160	RhK5_7705_624	general	3.74	1	62552824	8.22
Affx-86841690	RhMCRND_798_1153	diplo-general	3.85	1	24276183	8.22
Affx-86809794	RhK5_2992_302	diplo-general	3.85	1	23047321	8
Affx-86798105	RhMCRND_5960_1504	general	3.74	1	23778409	7.96
Affx-86791411	RhMCRND_16740_128	additive	3.65	1	23547770	7.87
Affx-86816843	Rh12GR_14097_430	general	3.74	1	14130539	7.36
Affx-86797907	RhMCRND_5631_559	additive	3.65	1	10389320	7.03
Affx-86789780	RhMCRND_12889_730	general	3.74	1	22685924	6.91
Affx-86818887	Rh12GR_19279_530	additive	3.65	1	27777830	6.3
Affx-86787322	RhK5_8518_746	additive	3.65	1	28779387	6.16
Affx-86815569	Rh12GR_11067_1318	general	3.74	1	20648911	6.16
qRDR.BExMG-ch3						
Affx-86831650	Rh12GR_6326_326	additive	3.44	3	37733803	9.02
Affx-86841479	RhMCRND_5722_374	additive	3.44	3	37770682	9.02
Affx-86836459	Rh12GR_84943_1865	general	3.63	3	37807749	8.97
Affx-86815608	Rh12GR_11167_748	general	3.63	3	28221800	8.66
Affx-86839174	Rh12GR_98817_153	additive	3.44	3	28297996	8.23
qRDR.BExMG-ch5 (*RDR4*)						
Affx-86835658	Rh12GR_81013_297	additive	3.44	5	40790477	9.36
Affx-86802674	Rh12GR_23542_3707	general	3.63	5	53197103	6.9
Affx-86794614	RhMCRND_27406_258	general	3.63	5	65938271	5.35

Using markers to identify individuals that have resistance alleles at each of the 3 loci allows the breeder to manipulate these loci in a breeding context. There are several cases in which these selected individuals can be utilized. If these individuals are crossed with other parental genotypes that have some other desired trait, each of the 3 QTL will independently segregate 1:1 for resistance to susceptible. The resulting population would have approximately 12.5% of the individuals carrying a resistance allele in simplex at each of the 3 loci. However, there is another scenario for these selected individuals. These individuals can be either selfed or crossed with each other. The result of these selfed or full sib crosses would result in $0.5^3 * 0.5^3 = 0.0156$ or around 1.56% of the individuals from these families having the resistance alleles in the duplex state at the 3 loci. By continuing to select for number of resistance alleles at each loci in each successful generation, we can select for individuals that have higher doses of resistance alleles with the ultimate goal of creating individuals that are fixed for resistance with all three alleles in the quadruplex state. Once all three resistance alleles are configured in a triplex or quadruplex state, all progeny resulting from crosses with these genotypes will result in resistant progeny.

Similarly, the most significant markers were selected in the SWxBE family identified using GWASpoly and in this case we tried to stack the cercospora resistance locus identified on LG 1 with the *RDR4* locus (black spot QTL) on LG5 (Table 2.21). The expected number of individuals carrying both resistance alleles was $0.5^2 = 0.25$ as both QTL appear to display a simplex x nulliplex 1:1 segregation pattern. Out of the 200 individuals we expected 50 to have both resistance alleles and 41 individuals carried

both resistance alleles which fits the Chi-Square segregation expectation (χ^2 = 1.62, df = 1, p-value = 0.05).

Table 2.21. Markers from the Stormy Weather x Brite Eyes population used to select progeny with resistance alleles. Markers were identified using GWASpoly.

Affymetrix name	Marker name	Model detected	Significance threshold	LG	Position	LOD
qRDR.SWxBE-ch5						
Affx-86821050	Rh12GR_258_2610	diplo-general	3.9	5	41059938	18.24
Affx-86835658	Rh12GR_81013_297	diplo-general	3.9	5	40790477	17.94
Affx-86781774	RhK5_20503_312	additive	3.86	5	52662557	15.14
Affx-86791832	RhMCRND_1780_1215	additive	3.86	5	32692332	13.08
Affx-86816137	Rh12GR_12422_663	additive	3.86	5	24907437	12.01
Affx-86838063	RhMCRND_23381_381	additive	3.86	5	54423818	11.47
Affx-86820066	Rh12GR_22388_324	general	3.94	5	26033558	10.87
qCERC.SWxBE-ch1						
Affx-86841256	RhMCRND_8769_681	additive	3.97	1	38281267	5.32
Affx-86776903	Rh88_19654_229	additive	3.97	1	38731046	5.32
Affx-86826035	Rh12GR_44439_214	additive	3.97	1	36960397	5.27

Conclusions and Future Work

The development of two mapping populations has led to the linkage mapping of these tetraploid populations that are of similar quality to the tetraploid rose linkage maps currently available. Narrow sense heritability estimates of black spot, cercospora, and defoliation were 0.071, 0.195, and 0.147, respectively, and broad sense heritabilities were 0.853, 0.931, and 0.800, respectively. From these linkage maps, QTL were described for rose rosette disease on LGs 3 and 5, black spot resistance on LGs 3, 5, and 7; cercospora leaf spot resistance on LGs 1, 4, and 5; and defoliation on LGs 3, 5, and 7.

We found a cluster of black spot, cercospora, and defoliation QTL on LG 5 co-localized with the *Rdr4* locus previously mapped by Zurn et al. (2018).

Populations are being phenotyped again for these to better define the phenotypes and consequently the QTL of these traits. Individuals from the BExMG population that have the three resistance QTL described and individuals carrying two resistance QTL from SWxBE were selected for future use in breeding. Future studies will test the hypothesis of the inheritance of the resistance alleles described.

Literature Cited

Allington, W.B., R. Staples, and G. Viehmeyer. 1968. Transmission of rose rosette virus by the eriophyid mite *Phyllocoptes fructiphilus*. Journal of Economic Entomology 61:1137–1140. doi: 10.1093/jee/61.5.1137.

Alqudah, A.M., A. Sallam, P. Stephen Baenziger, and A. Börner. 2020. GWAS: Fast-forwarding gene identification and characterization in temperate Cereals: lessons from Barley – A review. Journal of Advanced Research 22: 119–135. doi: 10.1016/j.jare.2019.10.013.

Banks, B.D., I.L. Mao, and J.P. Walter. 1985. Robustness of the restricted maximum likelihood estimator derived under normality as applied to data with skewed distributions. Journal of Dairy Science 68:1785–1792. doi: 10.3168/jds.S0022-0302(85)81028-6.

Bourke, P.M., P. Arens, R.E. Voorrips, G.D. Esselink, C.F.S. Koning-Boucoiran, et al. 2017. Partial preferential LG pairing is genotype dependent in tetraploid rose. The Plant Journal 90:330–343. doi: 10.1111/tpj.13496.

Bourke, P.M., G. van Geest, R.E. Voorrips, J. Jansen, T. Kranenburg, et al. 2018. polymapR—linkage analysis and genetic map construction from F1 populations of outcrossing polyploids. Bioinformatics 34:3496–3502. doi: 10.1093/bioinformatics/bty371.

Byrne, D.H., H.B. Pemberton, D.J. Holeman, T. Debener, T.M. Waliczek, et al. 2017. Survey of the rose community: desired rose traits and research issues. VII International Symposium on Rose Research and Cultivation 1232:189–192

Byrne, D.H., P. Klein, M. Yan, E. Young, J. Lau, et al. 2018. Challenges of breeding rose rosette–resistant roses. HortScience 53:604-608.

Chavez, D.E., M.A. Palma, D.H. Byrne, C.R. Hall, and L.A. Ribera. 2020. Willingness to pay for rose attributes: helping provide consumer orientation to breeding programs. Journal of Agricultural and Applied Economics 52:1–15. doi: 10.1017/aae.2019.28.

Debener, T., and D.H. Byrne. 2014. Disease resistance breeding in rose: Current status and potential of biotechnological tools. Plant Science 228:107–117. doi: 10.1016/j.plantsci.2014.04.005.

Di Bello, P.L., T. Ho, and I.E. Tzanetakis. 2015. The evolution of emaraviruses is becoming more complex: seven segments identified in the causal agent of Rose rosette disease. Virus Research 210(Supplement C): 241–244. doi: 10.1016/j.virusres.2015.08.009.

Dickerson, G.E. 1969. Techniques for research in quantitative genetics. In: Techniques and Procedures in Animal Science Research. American Society of Animal Science. Albany, NY.

Dobhal, S., J.D. Olson, M. Arif, J.A. Garcia Suarez, and F.M. Ochoa-Corona. 2016. A simplified strategy for sensitive detection of Rose rosette virus compatible with three RT-PCR chemistries. Journal of Virological Methods 232:47–56. doi: 10.1016/j.jviromet.2016.01.013.

Hackett, C.A., J.E. Bradshaw, and J.W. McNicol. 2001. Interval mapping of quantitative trait loci in autotetraploid species. Genetics 159:1819–1832.

Hackett, C.A., B. Boskamp, A. Vogogias, K.F. Preedy, and I. Milne. 2017. TetraploidSNPMap: Software for linkage analysis and QTL mapping in autotetraploid populations using SNP dosage data. Journal of Heredity 108: 438–442. doi: 10.1093/jhered/esx022.

Hagan, A., M. E Rivas-Davila, J. Akridge, and J. W Olive. 2005. Resistance of shrub and groundcover roses to black spot and Cercospora leaf spot, and impact of fungicide inputs on the severity of both diseases. Journal of Environmental Horticulture 23:77–85.

Heinrichs, F. 2008. International statistics flowers and plants vol. 56. AIPH. Union Fleurs. Brussels, Belgium.

Hibrand Saint-Oyant, L., T. Ruttink, L. Hamama, I. Kirov, D. Lakhwani, et al. 2018. A high-quality genome sequence of Rosa chinensis to elucidate ornamental traits. Nature Plants 4:473–484. doi: 10.1038/s41477-018-0166-1.

Holland, J.B., W.E. Nyquist, and C.T. Cervantes-Martínez. 2003. Estimating and interpreting heritability for plant breeding: an update. Plant breeding reviews 22:9–112.

Horst, R.K. and R.A. Cloyd. 2007. Compendium of rose diseases and pests. 2nd ed. The American Phytopathological Society, St. Paul, M.N.

Koning-Boucoiran, C.F.S., G.D. Esselink, M. Vukosavljev, W.P.C. van ’t Westende, V.W. Gitonga, et al. 2015. Using RNA-Seq to assemble a rose transcriptome with more than 13,000 full-length expressed genes and to develop the WagRhSNP 68k Axiom SNP array for rose (*Rosa* L.). Frontiers in Plant Science 6:249. doi: 10.3389/fpls.2015.00249.

Liang, S., X. Wu, and D. Byrne. 2017. Flower-size heritability and floral heat-shock tolerance in diploid roses. HortScience 52:682–685. doi: 10.21273/HORTSCI11640-16.

Laney, A.G., K.E. Keller, R.R. Martin, and I.E. Tzanetakis. 2011. A discovery 70 years in the making: characterization of the Rose rosette virus. Journal of General Virology, 92:1727–1732. doi: 10.1099/vir.0.031146-0.

Lopez Arias, D.C., A. Chastellier, T. Thouroude, J. Bradeen, L. Van Eck, et al. 2020. Characterization of black spot resistance in diploid roses with QTL detection, meta-analysis and candidate-gene identification. Theoretical and Applied Genetics 133:3299–3321. doi: 10.1007/s00122-020-03670-5.

Mollinari, M., and A.A.F. Garcia. 2019. Linkage Analysis and haplotype phasing in experimental autopolyploid populations with high ploidy level using hidden markov models. G3: Genes, Genomes, Genetics 9:3297-3314. doi: 10.1534/g3.119.400378.

Mangandi, J. and N.A. Peres. 2012. Cercospora leaf spot of rose. UF/IFAS Extension. 9 March 2017. <https://edis.ifas.ufl.edu/pdffiles/PP/PP26700.pdf>.

Miles, C. & Wayne, M. 2008. Quantitative trait locus (QTL) analysis. Nature Education 1(1):208

Pereira, G. da S., D.C. Gemenet, M. Mollinari, B.A. Olukolu, J.C. Wood, et al. 2020. Multiple QTL mapping in autopolyploids: A random-effect model approach with application in a hexaploid sweetpotato full-sib population. Genetics 215:579-595. doi: 10.1534/genetics.120.303080.

Preedy, K.F., and C.A. Hackett. 2016. A rapid marker ordering approach for high-density genetic linkage maps in experimental autotetraploid populations using multidimensional scaling. Theoretical and Applied Genetics 129:2117–2132. doi: 10.1007/s00122-016-2761-8.

Rosyara, U.R., W.S. De Jong, D.S. Douches, and J.B. Endelman. 2016. Software for genome-wide association studies in autopolyploids and its application to potato. The Plant Genome 9. doi: 10.3835/plantgenome2015.08.0073.

Rife, T.W., and J.A. Poland. 2014. Field Book: An open-source application for field data collection on android. Crop Science 54:1624–1627. doi: 10.2135/cropsci2013.08.0579.

Shires, M., J. Ueckert, and K. Ong. 2018. Rose rosette virus: Effective and low-cost extraction method. 2018 ASHS Annual Conference. Poster

Shires, M. 2020. Study of resistance to rose rosette disease utilizing field research, molecular tools, and transmission methods. Texas A&M University, PhD dissertation.

Simko, I., and H.-P. Piepho. 2011. The area under the disease progress stairs: calculation, advantage, and application. Phytopathology 102:381–389. doi: 10.1094/PHYTO-07-11-0216.

United States Department of Agriculture. 2015. 2012 Census of agriculture: census of horticultural specialties. Washington: United States Department of Agriculture.

United States Department of Agriculture. 2020. 2017 Census of agriculture: census of horticultural specialties. Washington: United States Department of Agriculture.

Voorrips, R.E., G. Gort, and B. Vosman. 2011. Genotype calling in tetraploid species from bi-allelic marker data using mixture models. BMC Bioinformatics 12:172. doi: 10.1186/1471-2105-12-172.

Waliczek, T.M., D. Byrne, and D. Holeman. 2018. Opinions of landscape roses available for purchase and preferences for the future market. HortTechnology 28:807–814. doi: 10.21273/HORTTECH04175-18.

Windham, M., A. Windham, F. Hale, and J. Armine Jr. 2014. Observations on rose rosette disease. University of Tennesee. 14 February 2017. <http://www.newenglandgrows.org/pdfs/ho_WindhamRoseRosette.pdf>.

Yan, M., D.H. Byrne, P.E. Klein, J. Yang, Q. Dong, et al. 2018. Genotyping-by-sequencing application on diploid rose and a resulting high-density SNP-based consensus map. Horticulture Research 5:1–14. doi: 10.1038/s41438-018-0021-6.

Zou, F., J.P. Fine, J. Hu, and D.Y. Lin. 2004. An efficient resampling method for assessing genome-wide statistical significance in mapping quantitative trait Loci. Genetics 168:2307-2316. doi: 10.1534/genetics.104.031427.

Zurn, J.D., D.C. Zlesak, M. Holen, J.M. Bradeen, S.C. Hokanson, et al. 2020. Mapping the black spot resistance locus *Rdr3* in the shrub rose 'George Vancouver' allows for the development of improved diagnostic markers for DNA-informed breeding. Theoretical and Applied Genetics 133:2011-2020. doi: 10.1007/s00122-020-03574-4.

Zurn, J.D., D.C. Zlesak, M. Holen, J.M. Bradeen, S.C. Hokanson, et al. 2018. Mapping a novel black spot resistance locus in the climbing rose Brite Eyes™ ('RADbrite'). Frontiers in Plant Science 9:1730. doi: 10.3389/fpls.2018.01730.

Zych, K., G. Gort, C.A. Maliepaard, R.C. Jansen, and R.E. Voorrips. 2019. FitTetra 2.0 – improved genotype calling for tetraploids with multiple population and parental data support. BMC Bioinformatics 20:148. doi: 10.1186/s12859-019-2703-y.

CHAPTER III

MAPPING HORTICULTURAL TRAITS IN TWO TETRAPLOID POPULATIONS.

Abstract

Two populations, *Rosa* L. 'ORAfantanov' (Stormy Weather™) x *Rosa* L. 'Radbrite' (Brite Eyes™) (SWxBE) and *Rosa* L. 'Radbrite' (Brite Eyes™) x *Rosa* L. 'BAIgirl' (Easy Elegance® My Girl) (BExMG), were created to study flowering, plant size, and stem color. Linkage maps were constructed using polymapR and QTL scans were conducted using TetraploidSNPMap, and QTLpoly utilizing two different QTL interval mapping algorithms. QTL for flower intensity were found on LGs 1, 3, 4, and 5, and for plant size (length, width, height, primary stem lengths) on LGs 1, 3, 5, and 6, for plant shape on LGs 3 and 7, and stem color on LG 6. We found that two of our plant size related QTL are close to *RoKSN* on LG 3 and *RoGA2ox* on LG 5.

Introduction

Garden roses (*Rosa* spp.) are important ornamental plants for both the United States and worldwide. Estimated sales for garden roses in the USA was $203 million in 2014 and $168 million in 2019 (USDA NASS, 2015 & USDA NASS, 2020) and garden roses along with cut flowers were valued at 24 billion Euros in 2008 ($42.3 billion USD equivalent adjusted for both historical exchange rate and inflation) (Heinrichs, 2008). In addition to disease resistance, horticultural traits of roses are important to consumers. Therefore, breeding efforts are geared towards creating cultivars that combine superior

disease resistance and horticultural traits (Byrne et al., 2017; Waliczek et al., 2018; Debener and Byrne, 2014). Garden roses are primarily valued for their aesthetic qualities. Important components of the aesthetics of a rose are the flower productivity and architectural growth type of the plant. Garden roses are a diverse group of plants which have many different growth types ranging from small compact plants to large climbing roses that require external structures for support. Many garden roses are tetraploid which are genetically more complex than their diploid counterparts. Due to the genetic complexities and smaller economic impact of horticultural crops as compared to agronomic crops, there has been little genetic research done on tetraploid garden roses. Only three high density SNP tetraploid rose linkage maps have been published to date (Zurn et al., 2018; Zurn et al., 2020; Bourke et al., 2017). Therefore, two bi-parental tetraploid populations were created to study flower productivity and plant architecture. The two populations were used to study the genetic components responsible for disease resistance (Chapter II) and horticultural traits: flower intensity, length, width, height, volume, primary stem lengths, number of primary shoots, number of secondary shoots, apical dominance, plant shape, and stem color.

Plant Architecture

Plant architecture consists of many components of plant growth which contribute to the overall shape of the plant. Branching angles of shoots and of roots can significantly alter the final structure of a plant and thus alter not only the appearance but also the yield of a plant (Wang and Li, 2008). Plant architecture has been an important

part of plant breeding as exemplified by the “Green Revolution” focus on plants with dwarfing plant architectures to increase the grain yield by reducing lodging (Wang and Li, 2008). Similarly, plant architecture can affect the flower productivity of roses (Kool et al., 1997).

Plant architecture is driven by many pathways that alter the plant hormones of auxin, gibberellins, and brassinosteroids within the shoot, root, and axillary meristems (Wang and Li, 2008). Different ratios of these plant hormones can alter the expression of these architectural traits. *RoKSN* (Genebank ID: HQ174211.1) is a homolog of TERMINAL FLOWER 1, *TFL1*, a key regulator of flowering (Iwata et al., 2012). *RoKSN* is one of the most important genes described in roses as most breeders select visually on the everblooming trait. On the rose genome assembly produced by Raymond et al. (2018), *TFL1* maps to 18.98 Mbp while on the assembly produced by Saint-Oyaint et al. (2018), *TFL1* maps to 28-33 Mbp. The physical locations are very different as the ordering of the two assemblies are inverse of each other on chromosome 3. The two genome assemblies used two different Old Blush doubled haploids. The doubled haploid in the assembly by Saint-Oyant et al. (2018) had a *RoKSN* deletion which they named $RoKSN^{null}$. When *TFL1* is BLAST to this assembly, a small part of the gene 28 Mbp and the other part at 33Mbp. The doubled haploid used for the genome assembly performed by Raymond et al. (2018) had the RoKSN allele which is why *TFL1* maps to a much narrower region. Using this narrow region, markers in our linkage maps corresponding to the physical positions of 18-20 Mbp were used to estimate the position of *RoKSN* in our populations. Both *RoKSN* and *TFL1* control the continuous blooming trait. It is

suggested that these two genes may either have pleiotropic effects on other things like plant architecture and flowering time, or there are other genetic factors closely linked with *RoKSN* that control these traits. (Kawamura et al., 2015; Goretti et al., 2020; Shannon and Meeks-Wagner, 1991; and Ratcliffe et al., 1998). Kawamura et al. (2015) concluded with their research that it is more probable that there are genetic factors closely linked to *RoKSN* that affect these architectural traits.

Another gene of importance but may not be as important in our germplasm is the antagonist to *RoKSN*, *RoFT* (Remay et al., 2009). In Arabidopsis, *TFL1* and *FT* are antagonistic where *TFL1* represses flowering and *FT* initiates flowering (Moraes et al., 2019). Other genes that are involved in plant architecture are the genes relating to gibberellin pathways, *RoGA2ox* (Remay et al., 2009) and *RoSLEEPY* (Foucher, et al., 2008). These gibberellins play roles in plant architecture as they are a one of the main classes of plant hormones associated with plant cell elongation and flower signaling.

Although many studies have been conducted in *Arabidopsis thaliana* to understand the genetic complexities of plant architecture, few have been done with roses. Plant architecture has been characterized in roses with some studies looking at how cultural practices affect plant architecture (Kool, 1997; Kool and Lenssen, 1997; Kool et al., 1997; Mascarini et al., 2006; Crespel et al., 2013). Kawamura et al. (2011) found broad sense heritabilities (H^2) ranging from 0.82 to 0.93 when looking at numbers of nodes on different parts of the primary shoot and Kawamura et al. (2015) found similar broad sense heritabilities ranging from 0.75 to 0.89 when looking at plant architectural traits such as plant height, primary shoot angles, internode length, and stem

diameters. In these studies, the plants were grown in field and shoots were harvested for measuring. Wu et al. (2019) found moderate to low narrow sense heritabilities (0.12-0.50) in the architectural traits of plant height, number of primary shoots, length of primary shoots, number of nodes on a primary shoot, number of secondary shoots, and number of tertiary shoots. Broad sense heritabilities for these traits were all moderate to high (0.46-0.92) with the exception of number of secondary shoots (0.34).

Li-Marchetti et al. (2017) looked at plant architecture in greenhouse conditions where plants were grown in containers. They estimated that the broad sense heritability of number of shoots to be between 0.54 and 0.71; and the H^2 of the length of shoots to be between 0.36 and 0.58. Growing plants in containers can alter the architecture of a plant as container grown plants have root systems restricted by the volume of the container whereas field grown plants can give a better "real world" phenotype as most garden roses will be planted in the landscape in the ground. Our studies seek to study in-field architecture traits that would be affected only by yearly dormant pruning of plants with mechanical hedgers to a uniform size.

Materials and Methods

Population Development

Two populations, *Rosa* L. 'ORAfantanov' (Stormy Weather™) x *Rosa* L. 'Radbrite' (Brite Eyes™) (SWxBE) n=200 and *Rosa* L. 'Radbrite' (Brite Eyes™) x *Rosa* L. 'BAIgirl' (Easy Elegance® My Girl) (BExMG) n=157, were developed in the spring 2016 by Texas A&M University Rose Breeding and Genetics Lab and Weeks Roses.

From here on out the trade names of these cultivars will be used instead of their proper scientific name which indicates their plant protection names. These trade names Stormy Weather™, Brite Eyes™, and Easy Elegance® My Girl, will be referred to as Stormy Weather, Brite Eyes, and My Girl. They will also be abbreviated as SW, BE, and MG, respectively. The populations were designed to study disease inheritance described in chapter II, however we noticed the segregation in the populations for plant architecture types.

In Somerville, TX, the plants were planted in randomized complete block design (RCBD) at 4 foot spacing and mulched using black landscape fabric in the April of 2018. Irrigation was done with overhead sprinklers. Soil type was Belk clay. Plants were pruned once in April of 2019 to a uniform size of around 1.5 cubic feet. In Overton, TX, plants were planted on 4 foot spacing in a RCBD, mulched using landscape fabric, and irrigated with drip irrigation underneath the landscape fabric. Soil type was Bowie Fine Sandy Loam. Plants were pruned each winter to 50% reduction in canopy. Monthly temperature and precipitation for both locations are shown in chapter II in Figures 2.18 and 2.19. In both locations, no fungicide was used and plants were irrigated and fertilized as needed.

Phenotyping

Flower productivity was phenotyped in 2019 in two locations, Somerville, TX, and Overton, TX. Flower intensity ratings estimated flower coverage of the canopy using a 0-9 scale in which 0 represents no flowers in the canopy. A rating of 1 would

represent a plant having between 1 to 10 percent of flower coverage, and a rating of 2 represents 11 to 20 percent flower coverage, etc. Flower intensity was rated monthly for five months from June to October in Somerville, TX, and for three months June, September, and October, in Overton, TX.

In addition to flower productivity, the plant architecture was phenotyped for the 2018 and 2019 growing seasons in Somerville, TX. Architecture trait data were taken in April 2019 and in December 2019. Data taken in April 2019 was on dormant plant material prior to yearly dormant pruning, thus capturing the 2018 growing season's growth. Data was taken in December 2019 on dormant plants accounting for plant growth in 2019. The plants within these two families ranged from dwarf to large climbing growth types. Architecture traits taken were plant length, width, and height. Plant volume was calculated as an ellipsoid using the following formula $V = \frac{4}{3}\pi \mathrm{LWH}$ where V = volume, L= plant length, W = plant width, and H = plant height. In addition, to basic plant size measurements, we counted the number of primary shoots coming from the base of the plant. To try to measure apical dominance, we measured the length of three basal shoots (primary shoots) and counted the number of secondary shoots greater than 2.54 cm broke from the buds on the basal shoot. We then calculated an apical dominance index = basal shoot length / number of secondary shoots greater than 2.54 cm on that basal shoot. Throughout the phenotyping process, no primary shoots were removed to measure length and secondary shoots as removal of entire primary shoots may alter next year's growth.

In April 2019, plant shape and stem color were rated. Plant shape was quantified categorically into three discrete groups: bush, semi-climber, and climber types. For QTL analysis, the three categories of bush, semi-climber, and climber types were converted to 0, 1, and 2, respectively. Similarly, stem color was rated as a green, semi-red, and red. The corresponding numbers were 0, 1, and 2, respectively.

Heritability Estimates

Heritability was estimated using variances calculated from mixed models using a Restricted Estimated Maximum Likelihood (REML) method in SAS 9.4 (SAS Institute Inc. Cary, NC, USA) (Table 3.1). The model for flower intensity included factors of month and location due to multiple months and locations where flower intensity was being phenotyped. However, length, width, height, and number of primary shoots were taken on a yearly basis in one location, the mixed model used did not include months nor location but instead had a year effect. For primary shoot length and number of secondary shoots which were taken on three shoots of each plant, the mixed model also accounted for the variation between shoot on each rep as three measurements were taken on each rep. Standard errors to heritability estimates were calculated using the Dickerson approximation (Dickerson, 1969). Heritability was not calculated for the plant shape and stem color traits which were categorically phenotyped. Plant shape and stem color also did not appear to follow qualitative segregation patters.

Table 3.1. Models used to calculate heritability and environmental effects for two tetraploid garden rose mapping populations.

Traits	Models
Flower Intensity	$y = \sigma^2_{family} + \sigma^2_{progeny[family]} + \sigma^2_{location} + \sigma^2_{month\ [location]} + \sigma^2_{rep[location*\ month]} + \sigma^2_{location\ x\ family} + \sigma^2_{location\ x\ progeny[family]} + \sigma^2_{month\ x\ family} + \sigma^2_{month\ x\ progeny[family]} + \sigma^2_{location\ x\ month\ x\ family} + \sigma^2_{location\ x\ month\ x\ progeny[family]} + \sigma^2_{error}$
Length, width, height, plant volume, number of primary shoots	$y = \sigma^2_{family} + \sigma^2_{progeny[family]} + \sigma^2_{year} + \sigma^2_{rep[year]} + \sigma^2_{year\ x\ family} + \sigma^2_{year\ x\ progeny[family]} + \sigma^2_{error}$
Shoot length, number of secondary shoots longer than 1cm an apical dominance	$y = \sigma^2_{family} + \sigma^2_{progeny[family]} + \sigma^2_{year} + \sigma^2_{rep\ [year]} + \sigma^2_{shoot[year*rep]} + \sigma^2_{year\ x\ family} + \sigma^2_{year\ x\ progeny[family]} + \sigma^2_{error}$

Genotyping and Linkage mapping

Tissue (young unexpanded leaflets) was collected from 200 and 157 individuals in the SWxBE and BExMG populations respectively and DNA was extracted using a the CTAB protocol described by Yan et al. (2018). Extracted DNA samples were incubated with RNase at 37°C and purified using the OneStep™ PCR Inhibitor Removal Kit (Zymo Research, Irvine, CA, USA). The samples were sent to Thermo Fisher Scientific for genotyping on the Axiom WagRhSNP 68k array (Koning-Boucoiran et al., 2015). Genotype calling and linkage mapping were conducted as described in chapter II.

QTL mapping was conducted using maps created in polymapR (Bourke et al., 2018) and imported into TetraploidSNPMap (Hackett et al., 2017) and QTLpoly (Pereira et al., 2020) for interval QTL mapping. The algorithm for QTL mapping in TetraploidSNPMap is very similar to that of the fixed effect interval mapping (feim) method in QTLpoly. However, QTLpoly also has a random-effect multiple interval

mapping method (remim) which assumes a model with no QTL followed by rounds forward search of QTL which in each round takes into account the QTL already in the model. This method is thought to be more accurate when compared to the other two algorithms as multiple QTL are considered through forward addition and backwards elimination of QTL. The genome wide significance levels used for the forward search of QTL and backward eliminations in the remim method are determined by using a score-based resampling method to establish a genome-wide significance by simulating QTL at every position in the linkage map (Zou et al. 2004). The simulation is run 1000 times prior to QTL mapping to obtain the p-values to be used for forward search and backward elimination of QTL in the remim method. Best linear unbiased predictors (BLUPs) estimated from the same mixed model used to estimate heritability were used for the QTL scans. GWASpoly (Rosyara et al., 2016) scans were also conducted to also compare results from the interval QTL scans.

Results and Discussion

Correlations

Correlations between flower intensity and all other traits are weak (the stongest is -0.27), while length, width, height, plant volume, and primary shoot length are strongly positively correlated (0.79 to 0.96) (Figure 3.1). The high correlations between these traits are most likely due to the fact they are all components of plant size. Number of primary shoots have moderate to moderately high positive correlations (0.43 – 0.70) with length, width, height, plant volume, primary shoot length, and number of secondary

shoots. Apical dominance has moderate to moderately low correlations with length, width, height, plant volume, primary shoot length, and plant shape (0.38 – 0.61). Stem color is not correlated with the other traits. When looking at correlations among years (Figure 3.2), moderate to high correlations (0.66 – 0.77) were found between the two years data for traits related to plant size (length, width, height, plant volume, and primary shoot length). Number of basal shoots between the two years was moderately correlated (0.50) and number of secondary shoots along with apical dominance had very low correlation between the two years (0.13 and 0.27, respectively).

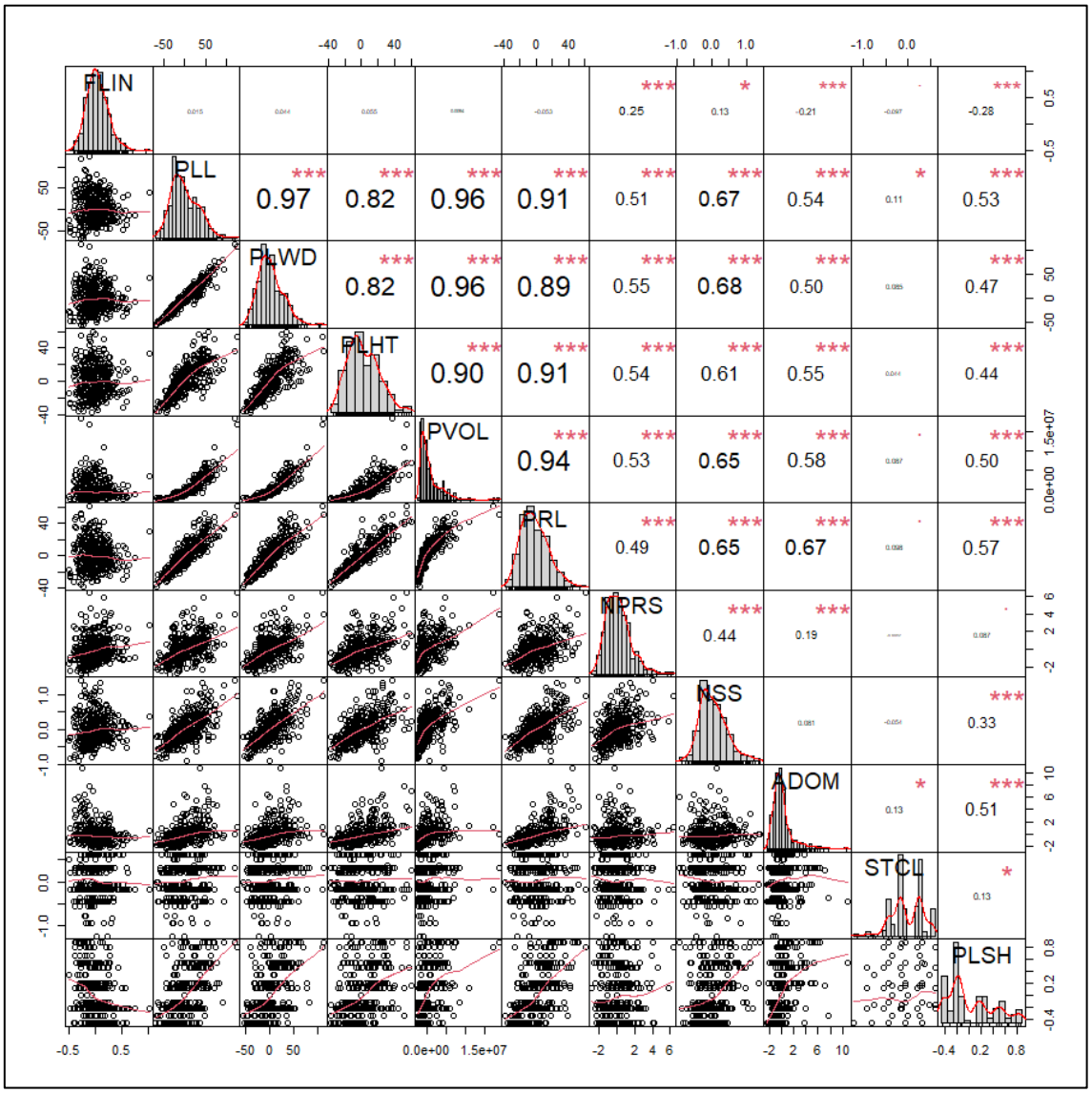

Figure 3.1. Correlations between phenotypic traits taken on two tetraploid rose populations phenotyped in 2018 and 2019 in Somerville, TX, for flower intensity (FLIN), length (PLL), width (PLWD), height (PLHT), plant volume (PVOL), primary shoot length (PRL), number of primary shoots, (NPRS) number of secondary shoots (NSS), apical dominance (ADOM), color (STCL), and shape (PLSH). Correlations denoted with *, **, and *** are significant p = 0.05, 0.01, and 0.001. R package PerformanceAnalytics used to produce the figure.

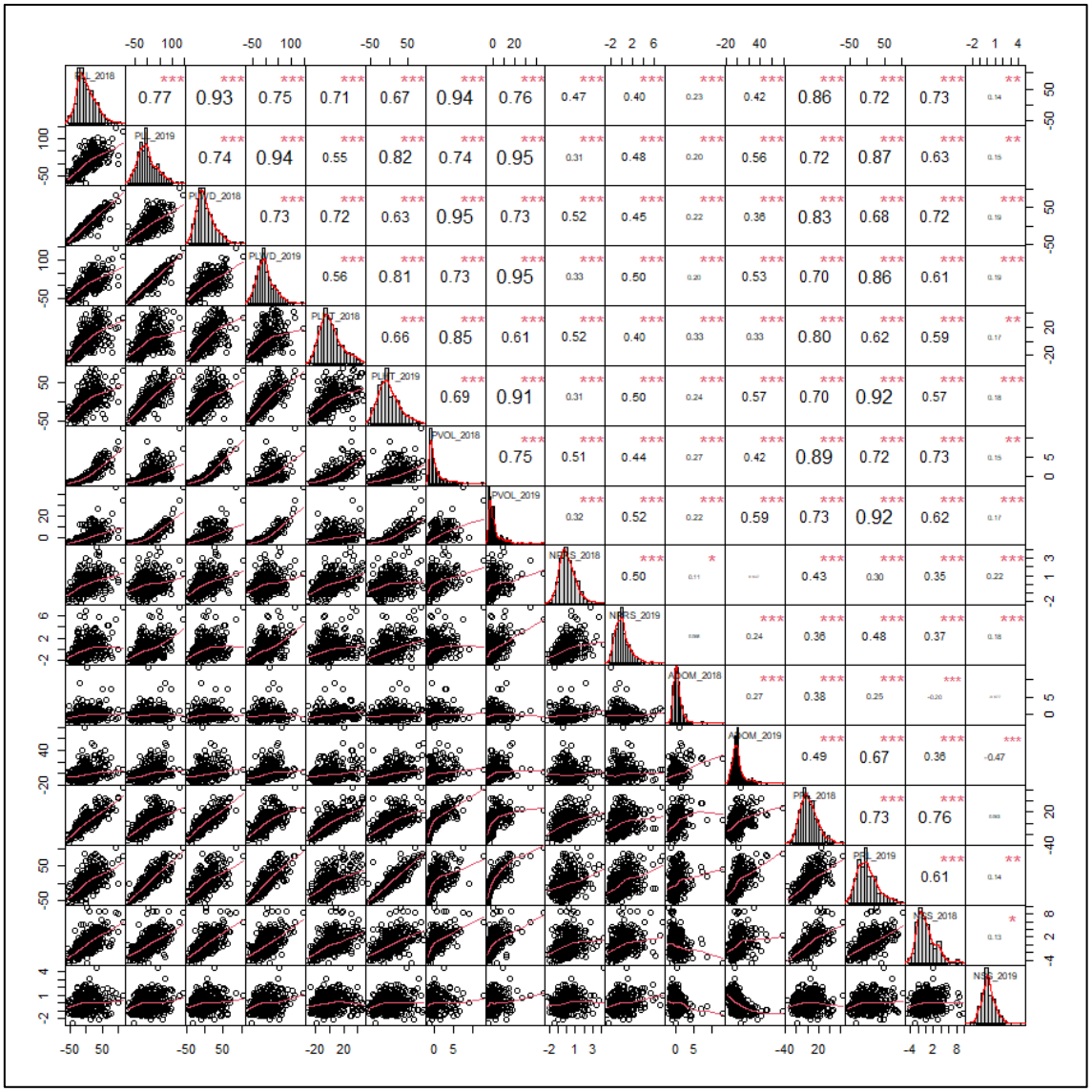

Figure 3.2. Correlations between the two years of phenotypic traits taken on two tetraploid rose populations phenotyped in 2018 and 2019 in Somerville, TX, for length (PLL), width (PLWD), height (PLHT), plant volume (PVOL), primary shoot length (PRL), number of primary shoots, (NPRS) number of secondary shoots (NSS), apical dominance (ADOM). Correlations denoted with *, **, and *** are significant p = 0.05, 0.01, and 0.001. R package PerformanceAnalytics used to produce the figure.

Heritability Estimates

Broad sense heritability (H^2) of flower intensity was 0.78 and narrow sense heritability (h^2) was 0.37 (Table 3.2). The GxE variance is 23% of the total variance and the GxE/G ratio is 1.35. Ratios greater than one indicate increased difficulty in selecting for that trait in any environment. Genotypes selected to be great performers in one environment (part of the year) would not necessarily perform well in another environment. A closer examination of this differential response of genotypes to the environments revealed that the worst performing genotypes consistently perform poorly throughout the year, while the best performing genotypes show a decline in flower production during the hot summers then rebound in the cooler fall weather (Fig. 3.5). Thus, the genotypes with less flower productivity could be easily eliminated throughout the year.

H^2 estimates for length, width, and height range from 0.74 to 0.86 while the h^2 was estimated to be near zero (Table 3.3). These H^2 estimates are similar to the H^2 estimates of plant height (0.82-0.88) (Kawamura et al., 2015; Wu et al., 2019); and a little bit higher than the H^2 estimates (0.36-0.58) of shoot lengths from Li-Marchetti et al. (2017). Plant volume measured as a function of length, width and height was estimated to have a H^2 of 0.60 while also having an estimated h^2 of zero. The number of basal shoots had a H^2 estimate of 0.63 and a h^2 of zero, which is comparable to the H^2 estimated by Li-Marchetti et al. (2017) of 0.54. H^2 estimates of primary shoot length, number of secondary shoots and apical dominance was 0.71, 0.16 and 0.23, respectively, and h^2 are near zero at 0.05, 0.01 and 0.09, respectively (Table 3.4). Wu et al. (2019)

also estimated low heritabilities of secondary shoots in diploid roses in the Texas A&M University rose breeding germplasm (h^2 =0.21; H^2=0.34). Number of primary shoots had near zero narrow sense (h^2=0.002) and moderate broad sense heritabilities (H^2=0.628) which were lower than the diploid estimates (h^2 =0.27; H^2=0.92) from Wu et al. (2019). Traits we measured that to our knowledge have not been studied in garden roses is flowering intensity (different than flowering time), plant length, and plant width. The high to medium heritabilities for length, width, height, plant volume, primary shoot length, and number of shoots indicate that we can breed and select for these traits. The low heritabilities of secondary shoots and apical dominance suggests that it may be hard to breed for these traits. Typically breeders working on seed propagated crops want to have high narrow sense heritability as additive variance is an approximation of the selectable variance for those crops. However, most of our traits show a narrow sense heritability near zero while having moderate to high broad sense (non-additive) heritability. This is still desirable for garden roses as the crop is vegetatively propagated. Thus, any desirable traits found in the progeny can be fixed via vegetative propagation.

The GxE/G ratio for a specific trait is an approximation of whether a breeder can select for the trait irrespective of the environment in which the genotypes were phenotyped. The GxE/G ratio for length, width, height, shoot length, and number of shoots, is less than one signifying that the genetic variance is greater than the genetic by environment interaction (Table 3.3). This suggests that it is possible to select for these traits regardless of the year as there is more genetic variation than that attributed to GxE. The GxE/G ratio for flower intensity, number of secondary shoots, plant volume, and the

apical dominance index are greater than 1 suggesting that there may be difficulty selecting for these traits in any environment as the variance attributed to the interaction between genotype and environment is greater than the variance attributed genotype itself (Tables 3.2 and 3.4). Wu et al. (2019) also observed high GxE/G ratios for number of secondary shoots (3.90) however there was no further exploration of this ratio.

The mean of the 10 best performing and 10 worst performing genotypes for flower intensity, number of secondary shoots, plant volume and apical dominance over different time periods was plotted to examine changes in GxE over time (Figure 3.3). For these four traits, the worst performing or lowest scored genotypes consistently performed poorly while there was a dramatic change in the best performing individuals over time. This indicates that even though GxE/G ratios are greater than one, we should still be able to select for these traits as the GxE primarily is derived from the changes seen in the best performing individuals.

Furthermore, volume is a calculated value. For volume, all of the phenotypes that go into the calculation have small GxE/G ratios (0.13-0.38) Thus, plant size should be a phenotype that can be selected for irrespective of the year of phenotyping. Figure 3.3c shows that the smaller plants in 2018 continue to be small plants while the large climbers grow even larger the second year. Thus, we should be able to either select for climbers or small compact plants from year to year depending on what is desirable to the breeder.

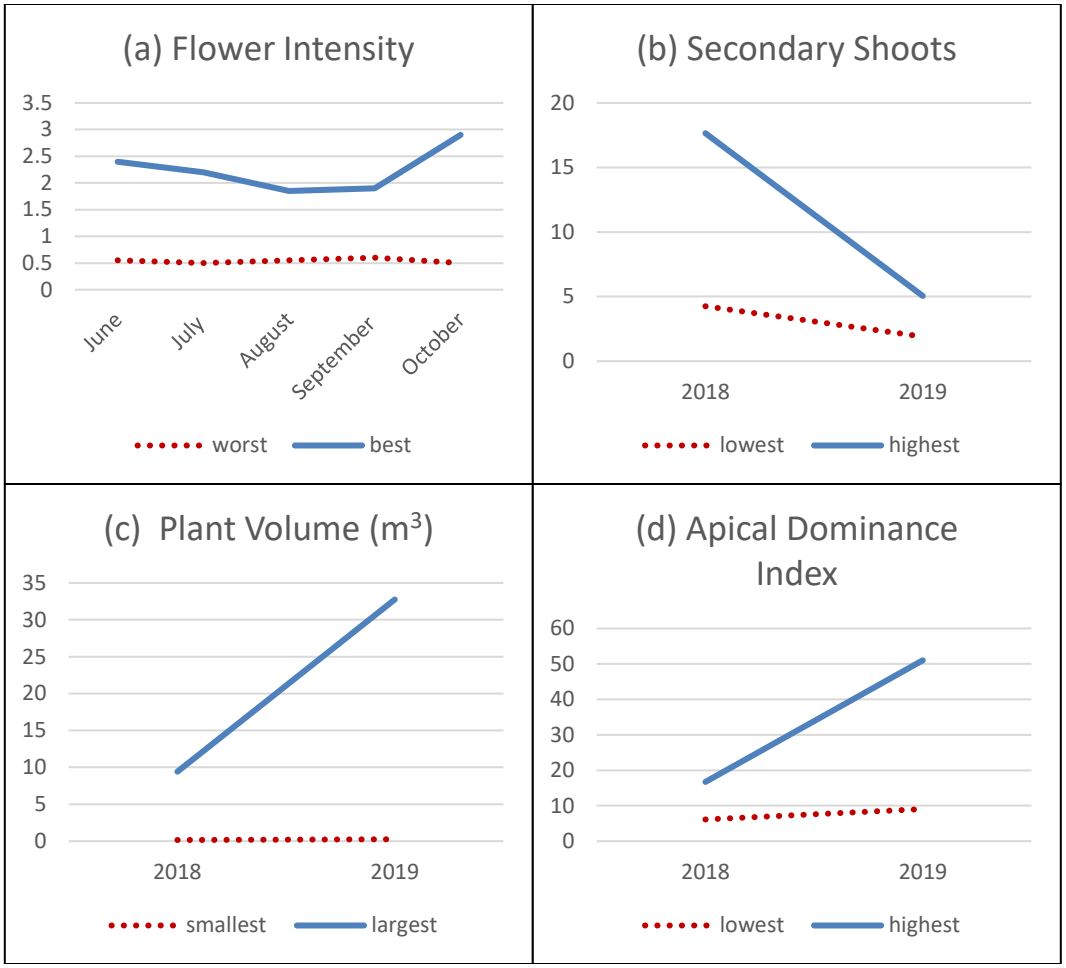

Figure 3.3. These figures compare the 10 worst versus the 10 best performing genotypes in the different traits that exhibit high GxE/G ratios. These figures show that even with high GxE/G ratios, the lower performing individuals always perform lower than the high performing individuals, however the slopes of the high performing individuals shows great change over time thus contributing to the high GxE/G ratios. (a) Mean flower intensities of the 10 best and worst performing genotypes throughout 2019. Flower intensity was rated on a 0-9 scale in which 0 represents no flowers in the canopy. A rating of 1 would be representative of a plant that had 1-10% flower coverage of the canopy. A rating of 2 rating would indicate 11-20 %, etc. (b) Mean performance of number of secondary shoots between the two years of 10 genotypes producing lowest number of secondary shoots versus 10 genotypes with highest number of secondary shoots. (c) Mean plant volume in cubic meters of the 10 largest plants versus the 10 smallest plants. (d) Mean plant apical dominance indices of 10 genotypes with the largest apical dominance index versus 10 with the smallest apical dominance index.

Table 3.2. Variance and heritability estimates of flower intensity on two tetraploid garden rose mapping populations grown in Somerville and Overton, TX in 2019. Flower intensity was rated monthly for five months from June to October in Somerville, TX, and for three months June, September, and October, in Overton, TX. Flower intensity was rated on a 0-9 scale in which 0 represents no flowers in the canopy, a rating of 1 would be representative of a plant that had 1-10% flower coverage of the canopy, a rating of 2 rating would indicate 11-20 %, etc.

Source of Variation[ab]	**Variance**
Family	0.11
Genotype(Family)	0.12***
Location	0.11
Month	0.08
Rep(Location x Month)	0.04
Location x Family	0.00
Location x Genotype	0.12***
Family x Month	0.00
Genotype x Month	0.01
Location x Family x Month	0.10
Location x Genotype x Month	0.07**
Residual	0.56***
Total	1.32
Percent Variation	
Genotypic Variance	0.17
Environmental Variance	0.14
GxE Variance	0.23
Residual Variance	0.43
GxE/G ratio	1.35
Heritabilities[c]	
h^2	0.37 (0.60)
H^2	0.78 (0.60)

[a] Narrow sense heritability, $h^2 = \sigma^2_{family} / (\sigma^2_{family} + \sigma^2_{genotype[family]} + (\sigma^2_{location\ x\ family} + \sigma^2_{location\ x\ genotype[family]} + \sigma^2_{month\ x\ family} + \sigma^2_{month\ x\ genotype[family]} + \sigma^2_{location\ x\ month*family} + \sigma^2_{location\ x\ month*genotype\ [family]})/e + (\sigma^2_{error})/re)$

[b] Broad sense heritability, $H^2 = (\sigma^2_{family} + \sigma^2_{genotype[family]})/ (\sigma^2_{family} + \sigma^2_{genotype[family]} + (\sigma^2_{location\ x\ family} + \sigma^2_{location\ x\ genotype[family]} + \sigma^2_{month\ x\ family} + \sigma^2_{month\ x\ genotype[family]} + \sigma^2_{location\ x\ month*family} + \sigma^2_{location\ x\ month*genotype\ [family]})/e + (\sigma^2_{error})/re)$

r=reps

e=environments

[c] Standard Errors calculated for heritabilities in parenthesis and calculated using the Dickerson estimation

*, **, *** Variance components are significant at P≤0.05, 0.01, or 0.001, respectively using the Wald's Z test.

Table 3.3. Variance and heritability estimates of the traits length, width, height, plant volume, and number of basal shoots, taken on two tetraploid garden rose mapping populations phenotyped in Somerville, TX, for the 2018 and 2019 growing season.

Variance					
Sources of Variation	Length	Width	Height	Plant Volume (Ellipsoid)	Number of Shoots
Family	0.00	0.00	4.39	0.00	0.01
Genotype(Family)	1329.31***	921.89***	511.73***	1.235E+13***	3.48***
Season	283.88	263.73	431.37	6.822E+12	2.55
Rep(Season)	7.06	4.55	4.56	2.316E+11	0.54
Family x Season	7.16	3.48	0.00	0.00	0.00
Genotype x Season(Family)	167.39***	158.78***	196.77***	1.253E+13***	0.51
Residual	523.55***	377.13***	315.05***	8.571E+12***	7.26***
Total	2318.35	1729.56	1463.87	4.050E+13	14.35
Percent variation					
Genetic	0.57	0.53	0.35	0.31	0.24
Environment	0.12	0.15	0.30	0.17	0.18
GxE	0.08	0.09	0.13	0.31	0.04
residual	0.23	0.22	0.22	0.21	0.51
GxE/G ratio	0.13	0.18	0.38	1.02	0.14
Heritabilities[abc]					
h^2	0.00	0.00	0.01	0.00	0.00
h^2 standard error	NA	NA	(0.02)	NA	(0.01)
H^2	0.86	0.84	0.74	0.60	0.63
H^2 standard error	(0.076)	(0.076)	(0.080)	(8.066E-14)	(0.084)

[a] Narrow sense heritability, $h^2 = \sigma^2_{family} / (\sigma^2_{family} + \sigma^2_{genotype[family]} + (\sigma^2_{location\ x\ family} + \sigma^2_{location\ x\ genotype[family]} + \sigma^2_{month\ x\ family} + \sigma^2_{month\ x\ genotype[family]} + \sigma^2_{location\ x\ month*family} + \sigma^2_{location\ x\ month*genotype\ [family]})/e + (\sigma^2_{error})/re)$

[b] Broad sense heritability, $H^2 = (\sigma^2_{family} + \sigma^2_{genotype[family]})/ (\sigma^2_{family} + \sigma^2_{genotype[family]} + (\sigma^2_{location\ x\ family} + \sigma^2_{location\ x\ genotype[family]} + \sigma^2_{month\ x\ family} + \sigma^2_{month\ x\ genotype[family]} + \sigma^2_{location\ x\ month*family} + \sigma^2_{location\ x\ month*genotype\ [family]})/e + (\sigma^2_{error})/re)$

r=reps

e=environments

[c] Standard Errors calculated for heritabilities in parenthesis and calculated using the Dickerson estimation

*, **, *** Variance components are significant at P≤0.05, 0.01, or 0.001, respectively using the Wald's Z test.

Table 3.4. Variance and heritability estimates of the traits primary shoot length, number of secondary shoots, and apical dominance taken on two tetraploid garden rose mapping populations phenotyped in Somerville, TX, for the 2018 and 2019 growing season.

Variance			
Sources of variation	Shoot length	Secondary shoots	Apical dominance
Family	29.79	0.05	10.41
Genotype(family)	441.01***	0.80*	14.51*
Season	317.47	8.00	114.79
Rep(season)	0.00	0.25	7.66
Shoot(season*rep)	16.32*	0.08	0.80
Family*season	0.00	0.35	17.20
Genotype*season(family)	211.60***	4.15***	87.67***
Residual	330.45***	8.20***	129.22***
Total	1346.65	21.87	382.25
Percent variation			
Genetic	0.35	0.04	0.07
Environmental	0.24	0.37	0.30
GxE	0.16	0.21	0.27
Residual	0.25	0.38	0.34
GxE/G ratio	0.45	5.31	4.21
Heritabilities[abc]			
h^2	0.05 (0.07)	0.01 (0.08)	0.10 (0.28)
H^2	0.71 (0.10)	0.17 (0.11)	0.23 (0.28)

[a] Narrow sense heritability, $h^2 = \sigma^2_{family} / (\sigma^2_{family} + \sigma^2_{genotype[family]} + (\sigma^2_{location\ x\ family} + \sigma^2_{location\ x\ genotype[family]} + \sigma^2_{month\ x\ family} + \sigma^2_{month\ x\ genotype[family]} + \sigma^2_{location\ x\ month*family} + \sigma^2_{location\ x\ month*genotype\ [family]})/e + (\sigma^2_{error})/re)$

[b] Broad sense heritability, $H^2 = (\sigma^2_{family} + \sigma^2_{genotype[family]})/ (\sigma^2_{family} + \sigma^2_{genotype[family]} + (\sigma^2_{location\ x\ family} + \sigma^2_{location\ x\ genotype[family]} + \sigma^2_{month\ x\ family} + \sigma^2_{month\ x\ genotype[family]} + \sigma^2_{location\ x\ month*family} + \sigma^2_{location\ x\ month*genotype\ [family]})/e + (\sigma^2_{error})/re)$

r=reps

e=environments

[c] Standard Errors calculated for heritabilities in parenthesis and calculated using the Dickerson estimation

*, **, *** Variance components are significant at P≤0.05, 0.01, or 0.001, respectively using the Wald's Z test.

Flower Intensity

Over the course of the year, we observe that flower intensity increases throughout the year with a slight decline of flowers in August (Figure 3.4). This is most

likely due to the increased heat during that month (Liang et al., 2017) (Figure 2.19). The means are different between families at each month and there are differences between the means of flower intensity ratings from month to month within each family. In all months, the SWxBE family have less flowers on average when compared to the flower intensity of the BExMG family. This is possibly due to the fact Stormy Weather is a climbing rose while Brite Eyes and My Girl are more shrub like in nature (Figure 3.4-3.5). Brite Eyes is officially classified as a climber, however in our field, Brite Eyes looks like an intermediate semi climbing plant. While there is not literature supporting this, observations within these two families seem to suggest that the climbing genotypes also have long primary shoots that are "leggy" and have many short secondary vegetative shoots less than 5 cm in length. This most often results in flower clusters at the ends of these primary shoots and as a result, the plant has less flower coverage of the plant canopy. In the two families that we have, we classified the plants as bush, climbers, and semi-climbers. The flowering intensity is lowest when we classified the plant as a climber, highest when classified as bush-type, and intermediate flowering when classified as a semi-climber (Table 3.5). The family with a climbing cultivar as one parent (SWxBE) exhibits lower amounts of flowering when compared to the family with two parents exhibiting more shrub like plant architecture (BExMG).

Plant Size

Although the SWxBE family is a cross between two climbers, members of the SWxBE family is not significantly larger than individuals in the BExMG family which

only has one parent that is a climber with respect to plant length, width, height, and plant volume. However, individuals within the SWxBE family do have greater primary shoot lengths when compared to those in the BExMG family (Table 3.6). A possible reason for finding differences in primary shoot length and not other traits related to plant size is that for plant length, width, and height, we only took one measurement per rep per year resulting in a total of 4 measurements per genotype while we took 3 subsamples of primary shoot length per rep, resulting in 12 measurements per genotype. The increased number of observations lowered the standard error and was enough to separate the means of the two families. Looking at length, width, height, plant volume, number of primary shoots and primary shoot length, the plants in 2019 were larger than the plants in 2018 (Table 3.6). There were more secondary shoots in 2018 when compared to 2019, thus the apical dominance index is lower in 2018 when compared 2019. Possibly the larger plants in 2019 with more basal primary shoots created plants with more crowded primary shoots resulting in a suppression of secondary shoot growth.

Table 3.5. Means comparison of flower intensity, length, width, height, plant volume, number of primary shoots, primary shoot length, number of secondary shoots, and apical dominance taken on two tetraploid garden rose mapping populations phenotyped in Somerville, TX, for the 2018 and 2019 growing season. Means comparisons show the differences between the plant shape types of climber, semi-climber, and bush.

	Traits[ab]								
Plant shape type	**FI**	**L**	**W**	**H**	**PV**	**NPS**	**PSL**	**NSS**	**AD**
Climber	0.90 c	128.53 a	103.49 a	87.12 a	7.59 a	7.70 a	90.93 a	8.31 a	20.24 a
Semi - climber	1.24 b	109.94 b	88.42 b	77.74 b	4.83 b	7.73 a	73.37 b	7.45 b	15.2 b
Bush	1.43 a	97.73 c	79.55 c	69.32 c	3.35 c	7.52 a	53.57 c	6.43 c	10.81 c

[a]flower intensity (FI) rated on a 0-9 scale. 0-9 in which 0 represents no flowers in the canopy. A rating of 1 would be representative of a plant that had 1-10% flower coverage of the canopy. A rating of 2 rating would indicate 11-20 %, etc.; length (L) in cm, width (W) in cm, height (H) in cm, plant volume (PV) in cubic meters calculated as an ellipsoid $V = \frac{4}{3}\pi LWH$, primary shoot length (PSL) in cm, number of primary shoots (NPS), number of secondary shoots (NSS) greater than 2.54 cm, and apical dominance (AD) calculated as PSL/NSS.
[b]Means followed by the same letter are not different according to Tukey-Kramer method ($P \leq 0.05$).

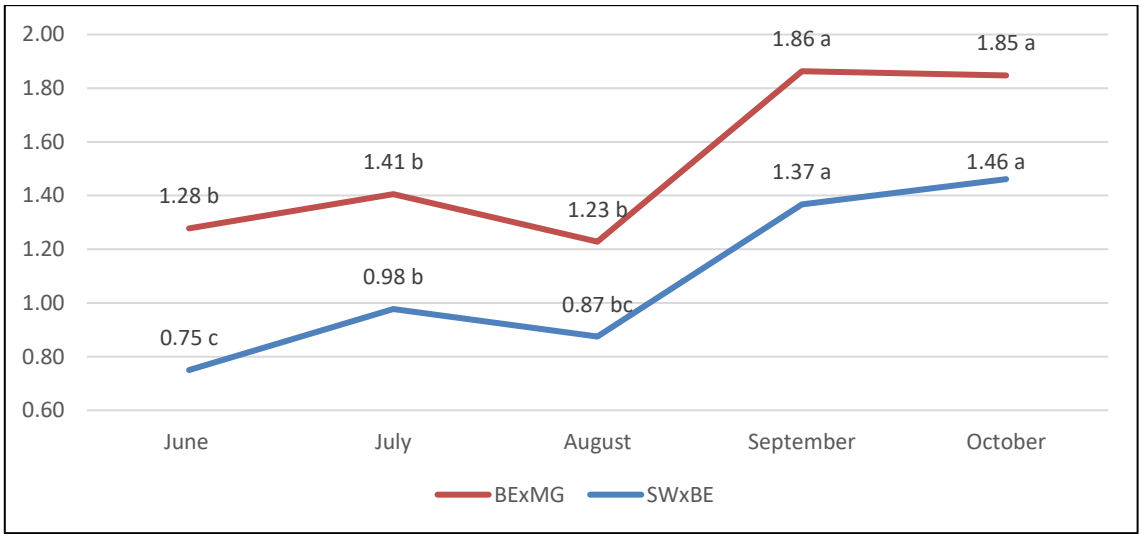

Figure 3.4. Flower intensity over time of two tetraploid rose mapping populations Brite Eyes x My Girl (BExMG) and Stormy Weather x Brite Eyes (SWxBE) evaluated in Somerville, TX, in 2019. Means separation between months separated via Tukey's studentized method. Means between both families at all months were significantly different from each other and the means separation denoted by the connecting letters report indicate the differences observed within family from month to month.

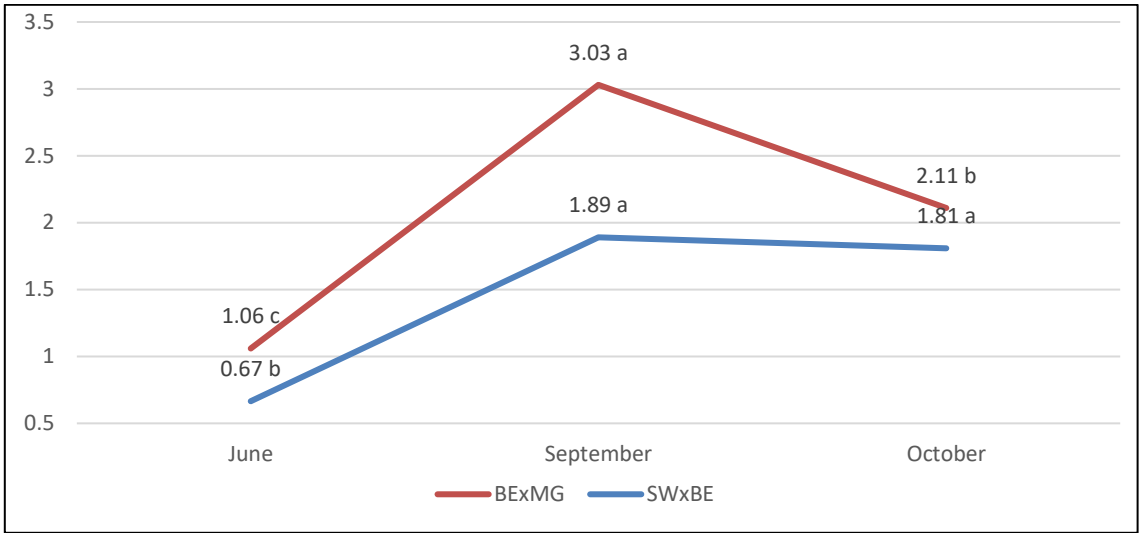

Figure 3.5. Means of flowering intensity over time of two tetraploid rose mapping populations Brite Eyes x My Girl (BExMG) and Stormy Weather x Brite Eyes (SWxBE) evaluated in Overton, TX, in 2019. Means separation between months separated via Tukey's studentized method. Means between both families at all months were significantly different from each other and the means separation denoted by the connecting letters report indicate the differences observed within family from month to month.

Table 3.6. Means comparison of length, width, height, plant volume, number of primary shoots, primary shoot length, number of secondary shoots, and apical dominance. measured in meters of two tetraploid garden rose biparental rose mapping families Stormy Weather x Brite Eyes (SWxBE) and Brite Eyes x My Girl (BExMG) between two years of phenotyping in Somerville, TX. Means followed by the same letter are not significantly different according to Tukey-Kramer method (P≤0.05).

Family	Year	Length (cm)	Width (cm)	Height (cm)	Volume (m^3)	Number of Primary Shoots	Primary Shoot Length	Number of secondary Shoots	Apical dominance
SWxBE	2018	97.91 b	76.53 b	61.88 b	2.72 b	6.38 b	57.09 c	8.67 a	7.88 c
BExMG	2018	90.07 b	72.43 b	58.60 b	2.36 b	6.61 b	47.86 d	8.76 a	5.89 d
SWxBE	2019	117.67 a	95.99 a	91.38 a	6.48 a	8.71 a	81.18 a	5.19 c	27.09 a
BExMG	2019	117.52 a	98.54 a	87.78 a	6.17 a	9.09 a	74.15 b	3.88 b	17.44 b

QTL Results

QTL were detected using multiple software packages and positions reported in centimorgan (cM) are the peaks of the QTL followed by a 1.5 LOD confidence interval, and estimations of variance explained by the QTL (Tables 3.7 and 3.8, Figures 3.6-3.8). Physical positions of markers within the 1.5 LOD confidence interval were obtained by aligning the WagRhSNP 68k Axiom SNP array probes to the rose reference genome assembly by Hibrand Saint-Oyant et al. (2018). Physical positions identified by GWAS are also presented in Tables 3.7 and 3.8 as supporting evidence to the presence of these QTL. In contrast to the disease traits discussed in Chapter II, many of the architecture traits described herein are controlled by multiple alleles on multiple LGs. Also, in contrast to the diseases where one parent was clearly the donor for resistance, many of these architectural QTL receive favorable alleles from both parents. Allele effects estimated the effect of the QTL on the phenotypic mean in QTLpoly using the "qtl_effects" function. The interpretation of the allele effects results is clear with QTL segregating in a simplex x nulliplex manner (1x0) and as doses are added, it becomes more difficult to interpret the results due to current population sizes of the mapping populations. We are able to interpret segregation patters of up to two doses (1x0, 0x1, 1x1, 2x0, and 0x2). We are less confident about the allele estimates given for QTL that segregate in higher dosages. The allele effects are described as the parent contributing the allele affecting the QTL and a ↑ or ↓ symbol describing whether the presence of the allele increases or decreases the phenotypic mean.

Table 3.7. QTL detected for the tetraploid mapping population Brite Eyes x My Girl for flower intensity, length, width, height, volume, primary lengths, number of primary shoots, number of secondary shoots, apical dominance, plant shape, and stem color.

QTL[a]	Trait	Contributing allele[b]	Detection Method	LG	LOD	Position (cM)[c]	Position (Mbp)[d]	Variance explained	Position GWAS[e]
qFLIN.BExMG-ch1	flower intensity	MG (0x2) ↓↑	TetraploidSNPMap	1	5.14	21 (13-24)	12.50-47.28	9.56	NA
			QTLpoly_feim	NA	NA	NA	NA	NA	NA
			QTLpoly_remim	1	3.59	13.07 (4.08-37.55)	0.75-47.85	15.72	NA
qFLIN.BExMG-ch3	flower intensity	BE (2x0) ↑↓	TetraploidSNPMap	3	2.96	40 (34-44)	34.31-40.85	6.93	NA
			QTLpoly_feim	3	6.29	57.03 (54.01-60.39)	41.00-46.74	13.76	NA
			QTLpoly_remim	3	4.32	58.51 (51.34-60.39)	41.00-46.74	24.01	NA
qPLL.BExMG-ch1	plant length	NA	TetraploidSNPMap	1	4.4	51 (51-55)	51.83-57.61	7.2	38.22-63.29
			QTLpoly_feim	NA	NA	NA	NA	NA	NA
			QTLpoly_remim	NA	NA	NA	NA	NA	NA
qPLL.BExMG-ch3	plant length	BE (1x0) ↑	TetraploidSNPMap	3	9.55	26 (20.5-31.5)	25.34-35.72	21.06	31.42-32.59
			QTLpoly_feim	3	9.87	26.03 (21.34-33.22)	25.34-36.66	22.26	31.42-32.59
			QTLpoly_remim	3	7.69	26.03 (21.34-34.05)	25.34-36.67	34.82	31.42-32.59
qPLWD.BExMG-ch1	plant width	BE and MG (2x1) ↑↓↑	TetraploidSNPMap	1	5.64	51 (51-55)	51.83-57.61	10.01	24.17-64.55
			QTLpoly_feim	1	6.27	51.12 (48.19-52.09)	50.31-60.98	13.52	24.17-64.55
			QTLpoly_remim	1	3.65	51.12 (35.29-71.20)	37.74-64.71	21.86	24.17-64.56
qPLWD.BExMG-ch3	plant width	BE (1x0) ↑	TetraploidSNPMap	3	7.5	26 (19-31)	23.61-35.00	16.27	21.62-33.08
			QTLpoly_feim	3	7.75	29 (21.34-33.22)	25.34-36.66	17.25	21.62-33.08
			QTLpoly_remim	3	5.91	26.03 (20.03-34.05)	24.60-36.66	23.51	21.62-33.08
qPLHT.BExMG-ch1	plant height	MG (0x1) ↑	TetraploidSNPMap	1	5.8	52 (51-55)	51.83-57.61	11.41	57.57
			QTLpoly_feim	1	5.87	51.12 (34.06-55.23)	38.69-57.61	13.52	57.57
			QTLpoly_remim	1	4.88	55.23 (34.06-66.01)	38.69-64.70	21.07	57.57

Table continued on next page

Table 3.7. Continued

QTL[a]	Trait	Contributing allele[b]	Detection Method	LG	LOD	Position (cM)[c]	Position (Mbp)[d]	Variance explained	Position GWAS[e]
qPLHT.BExMG-ch3	plant height	BE (1x0) ↑	TetraploidSNPMap	3	9.18	29 (19-31)	23.61-35.00	19.72	31.72-33.08
			QTLpoly_feim	3	6.68	29 (23.05-29)	27.09-33.73	22.22	31.72-33.08
			QTLpoly_remim	3	9.11	26.03 (23.05-30.1)	27.09-33.94	33.86	31.72-33.08
qPVOL.BExMG-ch1	plant volume	NA	TetraploidSNPMap	1	4.48	52 (51-55)	51.83-57.61	8.32	60.83
			QTLpoly_feim	NA	NA	NA	NA	NA	NA
			QTLpoly_remim	NA	NA	NA	NA	NA	NA
qPVOL.BExMG-ch3	plant volume	BE and MG (1x1) ↑↑	TetraploidSNPMap	3	8.18	26 (19-31)	23.61-35.00	17.92	32.03-33.07
			QTLpoly_feim	3	8.28	26.03 (20.03-33.22)	24.60-36.66	18.52	32.03-33.07
			QTLpoly_remim	3	6.37	26.03 (21.34-34.05)	25.34-36.66	29.42	32.03-33.07
qPRL.BExMG-ch1	primary lengths	BE and MG (3x3) ↑↑↓↓↓↑	TetraploidSNPMap	1	4.7	52 (51-55)	51.83-57.61	8.7	57.57
			QTLpoly_feim	NA	NA	NA	NA	NA	NA
			QTLpoly_remim	1	3.57	52.09 (33.19-71.2)	38.26-64.71	16.01	57.57
qPRL.BExMG-ch3	primary lengths	BE (1x0) ↑	TetraploidSNPMap	3	10.73	28 (20-29.5)	24.60-33.82	23.07	31.72-33.08
			QTLpoly_feim	3	10.93	26.03 (21.34-30.1)	25.34-33.94	24.66	31.72-33.08
			QTLpoly_remim	3	8.69	26.03 (23.05-30.1)	27.09-33.94	36.51	31.72-33.08
qNPRS.BExMG-ch1	number of primary shoots	BE and MG (2x2) ↑↓↓↑	TetraploidSNPMap	1	8.65	52 (51-55)	51.83-57.61	18.21	48.52-56.18
			QTLpoly_feim	1	8.74	45.04 (43.14-55.23)	43.82-57.61	19.62	48.52-56.18
			QTLpoly_remim	1	6.03	52.09 (43.14-55.23)	43.82-57.62	34.49	48.52-56.18
qNSS.BExMG-ch1	Number secondary shoots	MG & BE (1x2) ↑↓↑	TetraploidSNPMap	1	7.68	48 (47-49)	49.39-53.49	15.98	53.5
			QTLpoly_feim	1	8.19	48.19 (48.19-62.11)	50.31-64.37	18.32	53.5
			QTLpoly_remim	1	5.56	48.19 (47.05-67.3)	50.31-64.71	27.24	53.5
qNSS.BExMG-ch3	Number secondary shoots	BE (1x0) ↑	TetraploidSNPMap	3	7.05	29 (22-33)	25.59-36.25	14.96	29.34-45.60
			QTLpoly_feim	3	7.73	29 (28.09-31.13)	28.26-35.01	17.19	29.34-45.60
			QTLpoly_remim	3	5.2	29 (24.28-33.22)	27.09-36.66	25.82	29.34-45.60

Table continued on next page

Table 3.7. Continued

QTL[a]	Trait	Contributing allele[b]	Detection Method	LG	LOD	Position (cM)[c]	Position (Mbp)[d]	Variance explained	Position GWAS[e]
qNSS.BExMG-ch4	Number secondary shoots	BE & MG (1x1) ↑↑	TetraploidSNPMap	NA	NA	NA	NA	NA	NA
			QTLpoly_feim	NA	NA	NA	NA	NA	NA
			QTLpoly_remim	4	4.21	63.26 (56.01-78.34)	38.18-58.88	13.2	46.70-58.53
qNSS.BExMG-ch5	Number secondary shoots	BE & MG (2x2) ↑↓↑↓	TetraploidSNPMap	5	5.67	39 (38-46)	21.64-44.00	11.43	14.09-69.35
			QTLpoly_feim	5	6.26	39.17 (36.53-42.1)	21.64-33.50	13.53	14.09-69.35
			QTLpoly_remim	NA	NA	NA	NA	NA	NA
qADOM.BExMG-ch3	apical dominance	BE & MG (1x3) ↑↑↓↑	TetraploidSNPMap	3	6.27	26 (15-37)	19.89-37.70	13.1	33.41-32.89
			QTLpoly_feim	3	6.68	31.13 (23.05-36.02)	27.09-37.11	14.6	33.41-32.89
			QTLpoly_remim	3	4.67	30.1 (20.03-38.04)	24.60-38.10	23.4	33.41-32.89
qADOM.BExMG-ch5	apical dominance	NA	TetraploidSNPMap	5	9.81	56 (49-62)	39.83-69.08	9.81	45-85.34
			QTLpoly_feim	NA	NA	NA	NA	NA	NA
			QTLpoly_remim	NA	NA	NA	NA	NA	NA
qPLSH.BExMG-ch7	plant shape	BE & MG (1x2) ↓↓↑	TetraploidSNPMap	7	5.05	35 (31-39)	14.51-32.55	10.06	NA
			QTLpoly_feim	7	6.03	47 (31.29-49.11)	14.51-41.10	12.93	NA
			QTLpoly_remim	7	3.50	47 (30.03-50.05)	30.00-65.32	24.13	NA
qSTCL.BExMG-ch6	stem color	BE & MG (1x1) ↑↑	TetraploidSNPMap	6	7.46	53 (41-53.5)	32.82-65.32	15.82	1.57
			QTLpoly_feim	6	8.48	49.01 (41.1-53.05)	32.82-65.32	14.99	1.57
			QTLpoly_remim	6	5.67	49.01 (41.1-54)	32.82-65.32	31.68	1.57

[a]Name of QTL following the naming conventions of the Genome Database for Rosaceae.

[b]Parent contributing allele which affects the trait mean. Estimated by using "qtl effects" function in QTLpoly and by running "test with simple models" function in TetraploidSNPMap. For black spot, cercospora, and rose rosette, the favorable allele confers lower disease and the favorable allele for defoliation confers lower defoliation scores. Alleles affecting the trait mean are followed by estimated mode of inheritance in the parenthesis and also indicative of whether the allele caused an increase (↑) or decrease (↓) of the mean of the phenotype. An NA in this column denotes that the software used cannot calculate a parental allele effect.

[c]QTL peak position followed by 1.5 LOD confidence intervals in parenthesis.

[d]Physical positions of markers within the 1.5 LOD confidence intervals. WagRhSNP 68k Axiom SNP array probes were aligned to the rose genome assembly produced by Saint-Oyant et al. (2018).

[e]Physical position of markers within 1.5 LOD from the peak found in genome-wide association scans using GWASpoly.

Table 3.8. QTL detected for the tetraploid mapping population Stormy Weather x Brite Eyes for flower intensity, length, width, height, volume, primary lengths, number of primary shoots, number of secondary shoots, apical dominance, plant shape, and stem color.

QTL[a]	Trait	Contributing allele[b]	Detection Method	LG	LOD	Position (cM)[c]	Position (Mbp)[d]	Variance explained	Position GWAS[e]
qFLIN.SWxBE-ch3	flower intensity	SW (1x0) ↓	TetraploidSNPMap	3	6.51	34 (23-39)	28.21-41.19	11.39	25.46-44.49
			QTLpoly_feim	3	7.73	40.11 (23.06-42.02)	28.21-41.19	14.43	25.46-44.49
			QTLpoly_remim	3	6.74	25.14 (23.06-41)	28.21-41.19	20.36	25.46-44.49
qFLIN.SWxBE-ch4	flower intensity	SW (1x0) ↑	TetraploidSNPMap	4	7.73	34 (28-35)	10.56-33.09	14.12	17.16-33.19
			QTLpoly_feim	4	7.3	22.03 (20.02-41.01)	4.84-58.09	13.54	17.16-33.19
			QTLpoly_remim	4	6	30.02 (22.03-43.13)	4.84-58.09	15.94	17.16-33.19
qFLIN.SWxBE-ch5	flower intensity	SW & BE (1x1) ↑↓	TetraploidSNPMap	5	5.84	73 (71-76)	60.99-83.00	9.1	49.95-83.81
			QTLpoly_feim	5	5.81	83.57 (61.12-84.13)	44.86-85.17	10.33	49.95-83.81
			QTLpoly_remim	5	4.33	83.57 (65.02-86.19)	54.00-85.17	17.59	49.95-83.81
qPLL.SWxBE-ch3	length	SW (1x1) ↑↑	TetraploidSNPMap	3	25.61	23 (22-24)	26.40-32.54	42.69	32.34-33.08
			QTLpoly_feim	3	23.59	27.25 (23.06-27.25)	28.21-33.10	41.54	32.34-33.08
			QTLpoly_remim	3	>15.65	24.1 (12.94-36.6)	20.49-38.70	54.95	32.34-33.08
qPLL.SWxBE-ch5	length	BE (0x2) ↑↓	TetraploidSNPMap	5	5.05	56 (49-64)	26.03-56.68	8.15	64.09
			QTLpoly_feim	NA	NA	NA	NA	NA	NA
			QTLpoly_remim	5	5.55	61.12 (42.08-63.06)	23.57-55.32	10.64	64.09
qPLWD.SWxBE-ch3	width	SW x BE (1x1) ↑↑	TetraploidSNPMap	3	20.84	23 (22-24)	26.40-32.54	36.11	32.34-32.80
			QTLpoly_feim	3	18.94	27.25 (20.04-27.25)	25.25-33.10	34.6	32.34-32.80
			QTLpoly_remim	3	>15.65	24.1 (15.05-33.46)	22.15-37.74	47.06	32.34-32.80
qPLWD.SWxBE-ch5	width	BE (0x2) ↑↓	TetraploidSNPMap	5	4.82	56 (49-64)	26.03-56.68	7.68	64.09-75.37
			QTLpoly_feim	NA	NA	NA	NA	NA	NA
			QTLpoly_remim	5	4.44	50.1 (35.24-72.03)	16.06-74.32	10.48	64.09-75.37

Table continued on next page

Table 3.8. Continued

QTL[a]	Trait	Contributing allele[b]	Detection Method	LG	LOD	Position (cM)[c]	Position (Mbp)[d]	Variance explained	Position GWAS[e]
qPLHT.SWxBE-ch3	height	SW & BE (1x1) ↑↑	TetraploidSNPMap	3	22.43	25 (24-27)	28.21-33.10	37.95	32.59-32.80
			QTLpoly_feim	3	21.14	24.1 (24.1-27.25)	28.21-33.10	37.98	32.59-32.80
			QTLpoly_remim	3	>15.65	24.1 (15.05-33.46)	22.15-37.74	47.99	32.59-32.80
qPLHT.SWxBE-ch5	height	SW & BE (1x2) ↓↑↓	TetraploidSNPMap	5	5.88	57 (54-61)	35.79-53.41	9.59	64.09
			QTLpoly_feim	5	5.99	70.33 (50.1-75.07)	27.07-78.15	10.62	64.09
			QTLpoly_remim	5	4.09	71.02 (39.19-82.67)	19.11-85.17	12.05	64.09
qPLHT.SWxBE-ch6	height	SW&BE (2x2) ↑↓↑↓	TetraploidSNPMap	NA	NA	NA	NA	NA	NA
			QTLpoly_feim	NA	NA	NA	NA	NA	NA
			QTLpoly_remim	6	3.68	58.07 (30.34-59.37)	20.00-66.70	8.14	25.00
qPVOL.SWxBE-ch3	volume	SW&BE (1x1) ↑↑	TetraploidSNPMap	3	16.88	23 (21-27)	26.40-33.10	30.28	33.21-45.41
			QTLpoly_feim	3	16.16	27.25 (23.06-28.01)	28.21-32.89	30.07	33.21-45.41
			QTLpoly_remim	3	>15.65	24.1 (16.39-30.12)	23.04-34.18	41.95	33.21-45.41
qPVOL.SWxBE-ch5	volume	BE (0x2) ↑↓	TetraploidSNPMap	5	5.56	57 (49-61)	26.03-53-42	9.15	78.22-83.02
			QTLpoly_feim	5	6.11	69.02 (50.1-81.03)	27.07-85.17	10.89	78.22-83.02
			QTLpoly_remim	5	4.98	61.12 (45.04-81.03)	23.58-85-17	12.74	78.22-83.02
qPRL.SWxBE-ch3	primary lengths	SW & BE (1x1) ↑↑	TetraploidSNPMap	3	32.06	23 (22.5-24)	26.40-32.54	50.37	32.54-32.80
			QTLpoly_feim	3	31.37	27.23 (24.1-27.25)	28.21-33.10	51.53	32.54-32.80
			QTLpoly_remim	3	>15.65	24.1 (9.09-40.11)	1.20-41.19	61.24	32.54-32.80
qPRL.SWxBE-ch5	primary lengths	BE (0x2) ↑↓	TetraploidSNPMap	5	6.29	57 (54-60)	35.78-51.74	10.44	64.09
			QTLpoly_feim	5	6.11	57.11 (50.1-70.33)	27.07-72.02	10.88	64.09
			QTLpoly_remim	5	6.37	57.11 (42.08-61.12)	23.57-53.42	10.8	64.09
qPRL.SWxBE-ch6	primary lengths	SW & BE (1x1) ↑↑	TetraploidSNPMap	NA	NA	NA	NA	NA	NA
			QTLpoly_feim	NA	NA	NA	NA	NA	NA
			QTLpoly_remim	6	3.95	57.04 (38.14-74.34)	20.00-67.34	6.34	25.00

Table continued on next page

Table 3.8. Continued

QTL[a]	Trait	Contributing allele[b]	Detection Method	LG	LOD	Position (cM)[c]	Position (Mbp)[d]	Variance explained	Position GWAS[e]
qNPRS.SWxBE-ch1	number of primary shoots	SW (3x1) ↑↑↓↑	TetraploidSNPMap	1	4.56	39 (36.5-42.5)	42.69-52.15	5.69	36.98-64.18
			QTLpoly_feim	NA	NA	NA	NA	NA	NA
			QTLpoly_remim	1	3.55	37.02 (14.14-62.89)	14.13-64.71	8.93	36.98-64.18
qNPRS.SWxBE-ch6	number of primary shoots	BE (0x1) ↓	TetraploidSNPMap	6	4.91	47 (40-53)	36.42-65.53	6.93	15.65-63.42
			QTLpoly_feim	6	5.96	45.01 (38.14-59.37)	31.00-66.70	10.55	15.65-63.42
			QTLpoly_remim	6	4.05	45.01 (38.14-57.04)	31.00-66.32	19.19	15.65-63.42
qNSS.SWxBE-ch3	number of secondary shoots	SW (1x0) ↑	TetraploidSNPMap	3	11.7	23 (21-23.5)	26.40-28.75	20.72	30.39-37.29
			QTLpoly_feim	3	11.48	28.01 (19.56-35.01)	25.25-38.34	21.7	30.39-37.29
			QTLpoly_remim	3	9.73	24.1 (20.04-34.11)	25.25-37.74	33.7	30.39-37.29
qNSS.SWxBE-ch6	number of secondary shoots	BE (0x1) ↓	TetraploidSNPMap	6	3.84	46 (38-55)	31.00-66.21	5.64	25.00
			QTLpoly_feim	6	5.61	53.06 (45.01-60.26)	41.73-66.70	9.8	25.00
			QTLpoly_remim	6	4.29	49 (39.08-59.37)	31.00-66.70	16.22	25.00
qADOM.SWxBE-ch3	apical dominance	SW (2x1) ↓↑↑	TetraploidSNPMap	3	13.57	25 (24-27.5)	28.21-33.89	24.78	14.14-33.08
			QTLpoly_feim	3	14.45	23.06 (20.04-26.21)	25.25-32.89	27.12	14.14-33.08
			QTLpoly_remim	3	>15.65	23.06 (17.05-26.21)	23.04-32.89	40.74	14.14-33.08
qPLSH.SWxBE-ch3	plant shape	SW & BE (1x2) ↑↑↓	TetraploidSNPMap	3	23.17	25 (21-27)	26.40-33.10	39.36	32.54-33.08
			QTLpoly_feim	3	23.83	24.1 (24.1-25.14)	28.21-32.10	41.7	32.54-33.08
			QTLpoly_remim	3	>15.65	24.1 (15.05-35.01)	22.15-38.34	56.88	32.54-33.08
qSTCL.SWxBE-ch6	stem color	SW & BE (1x2) ↑↓↑	TetraploidSNPMap	6	9.58	47 (46-49)	48.58-63.08	16.12	56.74-56.89
			QTLpoly_feim	6	8.71	48.01 (39.08-54.07)	31.00-66.07	16.22	56.74-56.89
			QTLpoly_remim	6	5.91	48.01 (39.08-57.04)	31.00-66.32	28.93	56.74-56.89

[a]Name of QTL following the naming conventions of the Genome Database for Rosacae.
[b]Parent contributing allele which affects the trait mean. Estimated by using "qtl_effects" function in QTLpoly and by running "test with simple models" function in TetraploidSNPMap. For black spot, cercospora, and rose rosette, the favorable allele confers lower disease and the favorable allele for defoliation confers lower defoliation scores. Alleles affecting the trait mean are followed by estimated mode of inheritance in the parenthesis and also indicative of whether the allele caused an increase (↑) or decrease (↓) of the mean of the phenotype.
[c]QTL peak position followed by 1.5 LOD confidence intervals in parenthesis.
[d]Physical positions of markers within the 1.5 LOD confidence intervals. WagRhSNP 68k Axiom SNP array probes were aligned to the rose genome assembly produced by Saint-Oyant et al. (2018).
[e]Physical position of markers within 1.5 LOD from the peak found in genome-wide association scans using GWASpoly.

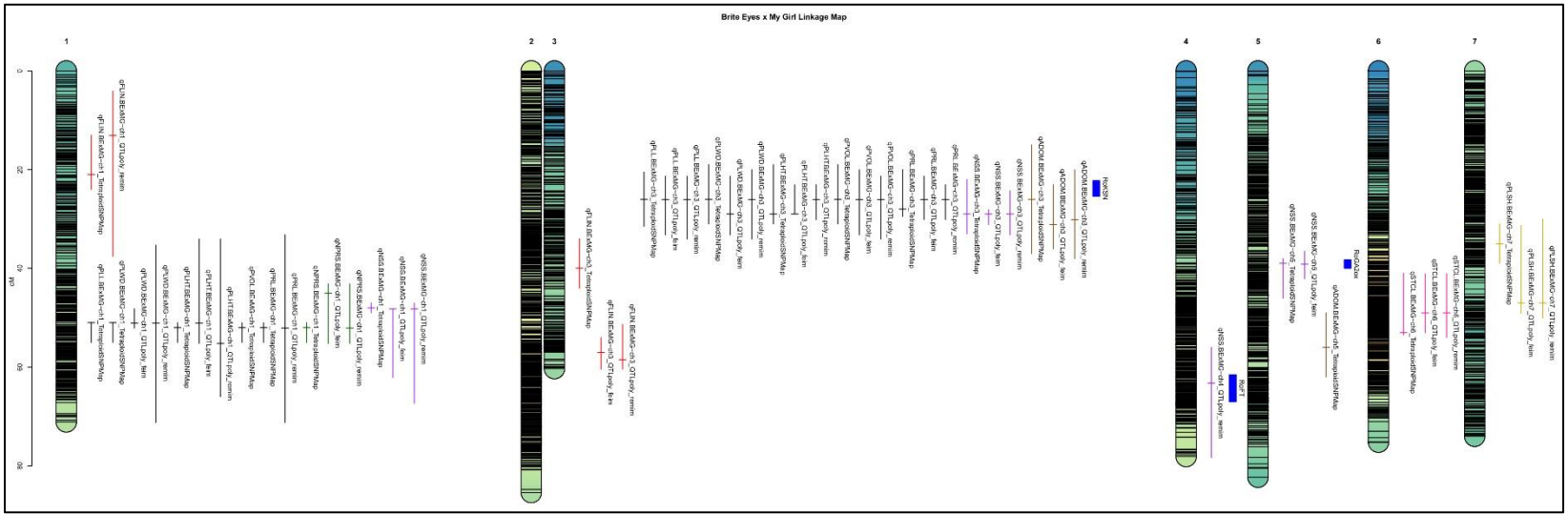

Figure 3.6. Linkage maps with QTL of tetraploid mapping population, Brite Eyes x My Girl. QTL peaks denoted by a horizontal mark and the 1.5 LOD confidence interval denoted by the whiskers. QTL are labeled with the names of the software used to detect the QTL.

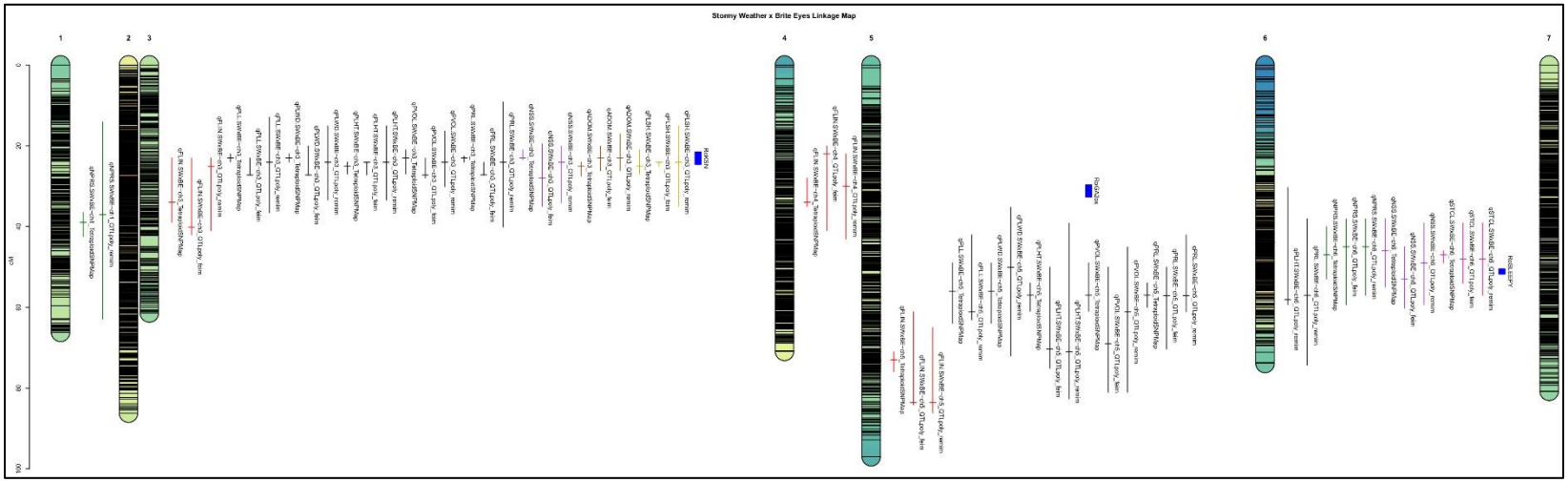

Figure 3.7. Linkage maps with QTL of tetraploid mapping population, Stormy Weather x Brite Eyes. QTL peaks denoted by a horizontal mark and the 1.5 LOD confidence interval denoted by the whiskers. QTL are labeled with the names of the software used to detect the QTL.

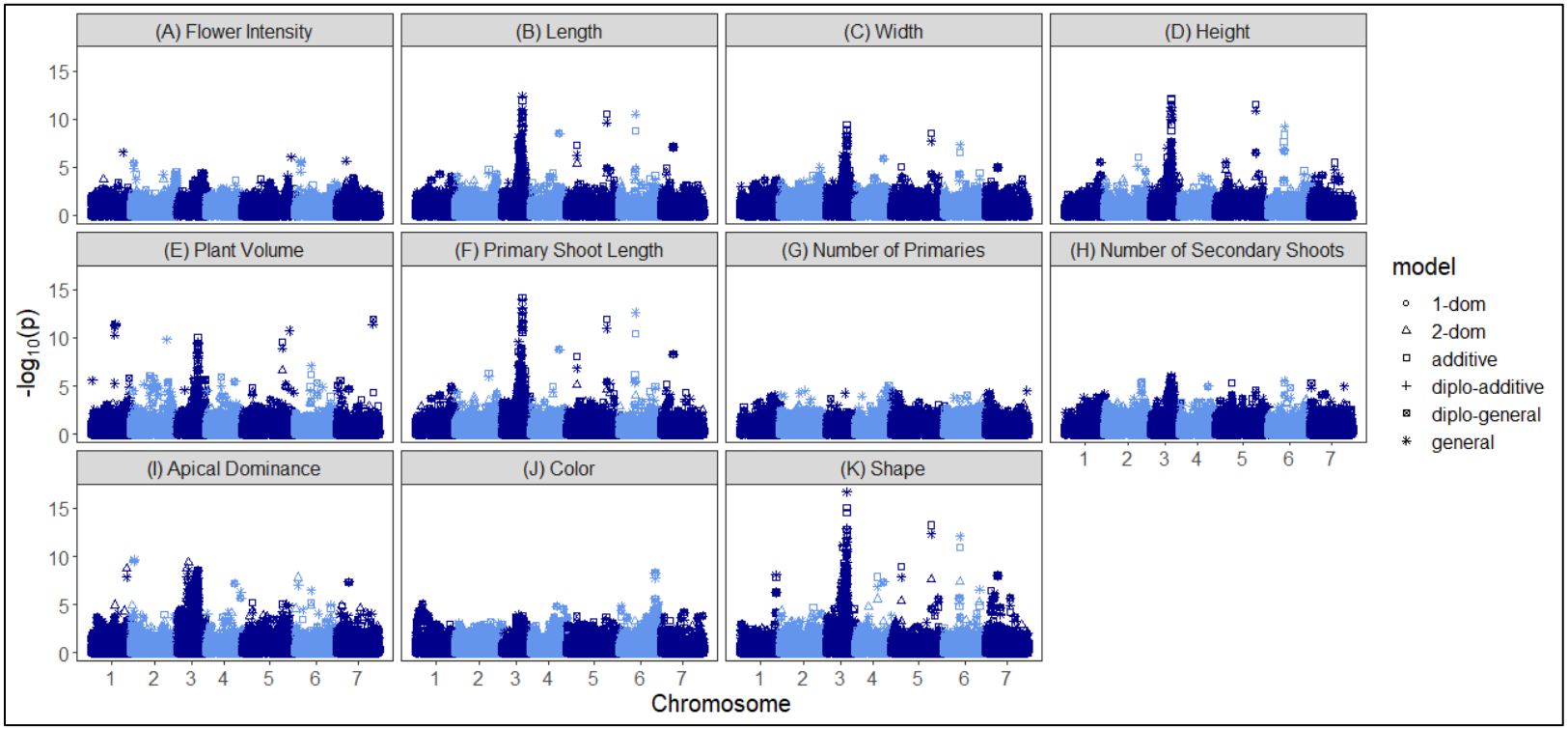

Figure 3.8. Manhattan plots of genome-wide association scans using GWASpoly of two tetraploid rose mapping population.

QTL for Flower Intensity

QTL for flower intensity were located on LGs 1, 3, 4, and 5 and the variance explained by the QTL ranged from 7-24% (Tables 3.7 and 3.8, Figures 3.6-3.8). The BExMG population had flower intensity QTL on LGs 1 and 3 (*qFLIN.BExMG-ch1* and *qFLIN.BExMG-ch3*) while the SWxBE population had QTL on LGs 3, 4, and 5 (*qFLIN.SWxBE-ch3, qFLIN.SWxBE-ch4*, and *qFLIN.SWxBE-ch5).* Alleles controlling *qFLIN.BExMG-ch1* are inherited from MG while *qFLIN.BExMG-ch3* comes from BE. Both *qFLIN.SWxBE-ch3* and *qFLIN.SWxBE-ch4* come from SW while *qFLIN.SWxBE-ch5* comes from both SW and BE. Although *qFLIN.BExMG-ch3* and *qFLIN.SWxBE-ch3* both are on LG3, the two QTL from the two populations do not share a common donor parent affecting the phenotypic mean. The parents of the two mapping populations are commercial cultivars that have already been selected for having many flowers thus favorable alleles may be coming from any or multiple parents. The QTL on LG 3 in the SWxBE population is near *RoKSN* (Figure 3.7). Kawamura et al. (2011) mapped QTL for the first day the flower appearing on LGs 3, 4, and 7 around 56, 35, and 53 cM, respectively. While we cannot compare the map positions of our maps and those of Kawamura et al. (2011), the proximity of both our flowering intensity QTL and their flowering date QTL to *RoKSN* on LG 3 is interesting, indicating that possibly the same underlying genetic factor is affecting both flowering intensity and flowering date. Our other flower intensity QTL do not overlap any other flowering QTL described by Kawamura et al. (2011).

QTL for Plant Size

QTL for length, width, height, plant volume, and primary shoot lengths share overlapping intervals on LGs 1, 3, and 5 (Tables 3.7 and 3.8, Figures 3.6-3.8). The BExMG population had QTL for these plant size traits on LGs 1 and 3 (*qPLL.BExMG-ch1, qPLWD.BExMG-ch1, qPLHT.BExMG-ch1, qPVOL.BExMG-ch1, qPRL.BExMG-ch1, qPLL.BExMG-ch3, qPLWD.BExMG-ch3, qPLHT.BExMG-ch3, qPVOL.BExMG-ch3, qPRL.BExMG-ch3*). The SWxBE population had overlapping QTL for plant size on LGs 3 and 5 (*qPLL.SWxBE-ch3, qPLWD.SWxBE-ch3, qPLHT.SWxBE-ch3, qPVOL.SWxBE-ch3, qPRL.SWxBE-ch3, qPLL.SWxBE-ch5, qPLWD.SWxBE-ch5, qPLHT.SWxBE-ch5, qPVOL.SWxBE-ch5, qPRL.SWxBE-ch5*). There was one QTL that did not overlap with any of the other plant size QTL on LG 6 (*qPRL.SWxBE-ch6*). The phenotypic variance explained by the QTL on LG 3 are greater than the QTL found on LGs 1, 5, and 6. The variance explained by QTL on LG 3 ranges from 16-61% while the QTL on LGs 1,5, and 6 range from 6 to 21%. The amount of variance attributed to the QTL on LG 3 seem to be greater than the variance of those same traits on other LGs (Tables 3.7 and 3.8). A possible explanation for this is the proximity of the QTL on LG 3 to *RoKSN*, a major gene controlling the everblooming trait. From the aggregation of all the traits measuring plant size, it appears that the QTL for plant size on LG 1 (*qPLL.BExMG-ch1, qPLWD.BExMG-ch1, qPLHT.BExMG-ch1, qPVOL.BExMG-ch1, qPRL.BExMG-ch1*) receives alleles affecting the phenotypic mean from both BE and MG. The QTL on LG 3 (*qPLL.BExMG-ch3, qPLWD.BExMG-ch3, qPLHT.BExMG-ch3, qPVOL.BExMG-ch3, qPRL.BExMG-ch3*) from the BExMG family looks to primarily

receive alleles affecting plant size from BE while the QTL on LG 3 (*qPLL.SWxBE-ch3, qPLWD.SWxBE-ch3, qPLHT.SWxBE-ch3, qPVOL.SWxBE-ch3, qPRL.SWxBE-ch3*) from the SWxBE family looks to receive alleles affecting plant size from both SW and BE. The QTL on LGs 5 and 6 (*qPLL.SWxBE-ch5, qPLWD.SWxBE-ch5, qPLHT.SWxBE-ch5, qPVOL.SWxBE-ch5, qPRL.SWxBE-ch5, qPRL.SWxBE-ch6*) receive alleles from BE affecting plant size. Because the QTL for length, width, height, plant volume, and primary shoot length are all measurements of plant size and highly correlated, they show QTL in many of the same locations (Tables 3.7-3.8, Figures 3.6-3.7). All QTL detected for plant size traits on LG 3 either overlap or are in close proximity to *RoKSN*. Furthermore, GWAS scans with markers aligned to both rose genome assemblies (Saint-Oyant et al., 2018; Raymond et al., 2018) showed peaks near the physical location of *RoKSN* between 32.34-33.08 Mbp and 18.13-18.96 Mbp, respectively. Interestingly, Kawamura et al. (2011) mapped QTL relating to internode lengths on primary shoots near *RoKSN*. Internode lengths are a component of plant size so it is no surprise that we also discovered QTL for traits measuring plant size in this region.

In addition to the strong QTL on LG 3 for traits associated with plant size, we found a QTL for length, width, height, and volume in the SWxBE family on LG 5 near the middle of the LG near where Kawamura et al. (2015) reported a minor QTL for plant height. However, Kawamura et al. (2015) reported their height QTL collocating with *RoGA2ox*. The Genebank ID: BQ105545.1 sequence of *RoGA2ox* aligns to the assembly by Saint-Oyant et al. (2018) at 20.82 Mbp and aligns to the assembly by Raymond et al. (2018) at 21.85 Mbp on LG 5. Most of our QTL detected for length,

width, height, and primary shoot length, on LG 5 span over markers that are aligned physically between 22 and 38 Mbp and GWAS scans for these traits were between 31-33 Mbp, when aligned to the assembly by Saint-Oyant et al., (2018). The physical positions of the QTL scans and the results from GWAS scans do not co-locate with *RoGA2ox* so our QTL is likely not the same as the one Kawamura et al. (2015) reported (Figures 3.6-3.7).

We also saw that *qPLHT.SWxBE-ch6* and *qPRL.SWxBE-ch6* co-locates with *RoSLEEPY,* a gene involved in the regulation of gibberellic acid production. This finding is not surprising as many architectural traits are controlled by pathways dealing with gibberellic acid. One of the QTL for average internode lengths mapped by Kawmura et al. (2011) was also near *RoSLEEPY* and this makes sense with our findings as internode lengths play a role into plant size.

QTL for Primary Shoots, Secondary Shoots, and Apical Dominance

QTL for number of primary shoots emerging from the base of the plant were found on LG 1 in the BExMG population (*qNPRS.BExMG-ch1*) and on both LGs 1 and 6 in the SWxBE population (*qNPRS.SWxBE-ch1* and q*NPRS.SWxBE-ch6*) (Tables 3.7 and 3.8, Figures 3.6-3.8). The QTL for number of primary shoots in both families on LG 1 (*qNPRS.BExMG-ch1* and *qNPRS.SWxBE-ch1*) comes from parents both while the QTL on LG 6 is from BE. The difference between the QTL on LG 1 is the variance explained by the QTL. *qNPRS.BExMG-ch1* has variance explained ranging from 18-

29% while *qNPRS.SWxBE-ch1* explains between 5-9%. q*NPRS.SWxBE-ch6* contributes between 7-19%.

QTL for number of secondary shoots were found on LGs 1, 3, 4, 5, and 6. The BExMG population has 4 QTL on LGs 1, 3, 4, and 5 (*qNSS.BExMG-ch1*, *qNSS.BExMG-ch3*, *qNSS.BExMG-ch4*, and *qNSS.BExMG-ch5*) and the SWxBE population has two QTL on LGs 3 and 6 (*qNSS.SWxBE-ch3* and *qNSS.SWxBE-ch6*). Alleles controlling the 3 QTL, *qNSS.BExMG-ch1*, *qNSS.BExMG-ch4*, and *qNSS.BExMG-ch5* comes from both BE and MG, while *qNSS.BExMG-ch3* comes from BE. For the SWxBE family, an allele controlling *qNSS.SWxBE-ch3* and *qNSS.SWxBE-ch6* is from SW and BE respectively. The phenotypic variance attributed to all the QTL describing number of secondary shoots was between 5-33%. Interestingly *qNSS.BExMG-ch5* overlaps the position where we estimate *RoGA2ox* to be and *qNSS.BExMG-ch4* overlaps with *RoFT*. *RoGA2ox* is responsible for the breakdown of gibberellic acid which is known to affect plant architecture and *RoFT* is antagonistic to *RoKSN*. The homologues of *RoFT* and *RoKSN*, *FT* and *TFL1*, have been shown in Arabidopsis and in tomato to alter the growth type of the plant by the ratio they are present in the plant. Thus, it is plausible that the plant architecture QTL we have discovered are affected by these nearby genes. Kawamura et al. (2011) mapped QTL for number of nodes on primary shoots on LG 4 near *RoFT*. It is not surprising that we also found QTL for number of secondary shoots near *RoFT* as secondary shoots are nodes that have broken bud and elongated vegetatively.

QTL for apical dominance index are on LGs 3 and 5 in the BExMG population (*qADOM.BExMG*-ch3 and *qADOM.BExMG-ch5*), while the SWxBE population has one

QTL, *qADOM.SWxBE-ch3* on LG 3. In both families, both parents are contributing an allele for greater apical dominance for the QTL on LG 3 while we cannot estimate how *qADOM.BExMG-ch5* due to it only being detected in TetraploidSNPMap. The apical dominance QTL in the BExMG family explained between 10-23% of the phenotypic variance while the dominance QTL in the SWxBE family explained more variance between 25-41%.

QTL for Plant Shape and Stem Color

QTL for plant shape in the BExMG population were found on LG 7 (*qPLSH.BExMG-ch7*) and in the SWxBE population on LG 3 (*qPLSH.SWxBE-ch3*) (Tables 3.7 and 3.8, Figures 3.6-3.8). Both parents contributed alleles affecting plant shape. In the BExMG population only 10-24% of the phenotypic variance was attributed to *qPLSH.BExMG-ch7* and in the SWxBE population, 39-56% of the phenotypic variance was attributed to *qPLSH.SWxBE-ch3*. Interestingly in the BExMG population, the plant shape QTL was found on LG 7 not near any of the other QTL for plant size. However, in the SWxBE population the QTL for plant shape was found near the other QTL associated with plant size on LG 3. Just like the other plant size QTL, *qPLSH.SWxBE-ch3*, overlaps with *RoKSN* (Figure 3.7). Kawamura et al. (2015) discovered a QTL for plant form measuring how prostrate or upright a plant was within 1 cM to *RoKSN*. This measurement is similar to our ratings for plant shape.

QTL for stem color in both populations is on LG 6 (*qSTCL.BExMG-ch6* and *qSTCL.SWxBE-ch6*). Both QTL had alleles from both parents that donated color alleles

to the stem and both QTL were mapped to similar locations. Between 15-31% of the phenotypic variation could be explained by the QTL.

RoKSN and Architectural Traits

RoKSN is near or overlaps QTL for plant size, plant shape, flowering intensity, apical dominance, and number of secondary shoots. The *RoKSN* gene that controls continuous flowering also is involved in gibberellic acid (GA) signaling (Iwata et al., 2012 and Roberts et al., 1999). GA is a plant hormone that can alter plant architecture (Liang et al., 2014) and has been used in crops to induce uniform flowering by inducing a change from vegetative to reproductive growth (Dong et al., 2017). The interaction of GA and auxin hormones can be a contributor to the expression of the number of secondary shoots allowed to break from the primary shoots.

We did not expect to find QTL near *RoKSN* as all of our progeny are continuous bloomers. However, it has been suggested that either *RoKSN* and *TFL1* have pleiotropic effects and contribute plant size and flowering time (Kawamura et al., 2015; Goretti et al., 2020; Shannon and Meeks-Wagner, 1991; Ratcliffe et al., 1998) or there are other genes closely linked to *RoKSN* and *TFL1* that are controlling flowering intensity. Like Kawamura et al. (2015), we also cannot rule out the possibility that *RoKSN* has pleiotropic effects that affect plant architecture. However, because we see segregation for these architecture traits and can detect QTL for these traits even though both of our populations are all continuous flowering, we believe this is strong evidence supporting the theory that there are other loci near *RoKSN* that are affecting plant architecture.

Conclusions and Future Work

The development of these two tetraploid mapping populations has helped us begin to understand the inheritance of flower intensity, length, width, height, plant volume, number of primary shoots, primary shoot length, number of secondary shoots, apical dominance, plant shape, and stem color. Narrow and broad sense heritabilities for flower intensity were 0.374 and 0.776, respectively. Narrow sense heritabilities for the plant size traits were near zero and broad sense heritabilities were between 0.714 and 0.859. The narrow sense heritabilities for number of primary shoots, number of secondary shoots, and apical dominance were all near zero, and the broad sense heritability was 0.628, 0.165, and 0.227, respectively. The moderate to high broad sense heritabilities of many of these traits indicate the ability to select for these traits. QTL for flower intensity were discovered on LGs 1, 3, 4, and 5, and for plant size (length, width, height, primary stem lengths) on LGs 1, 3, 5, and 6, for plant shape on LGs 3 and 7, and stem color on LG 6. We discovered plant architecture related QTL are near *RoKSN* on LG 3, *RoFT* on LG4, *RoSLEEPY* on LG 6, and *RoGA2ox* on LG 5. We observed that many of the QTL for plant size clustered with each other on LGs 1, 3, and 5, as these traits are highly correlated and are most likely measures of the same underlying genetic factor.

Future work with these populations will continue to look at plant size especially at dwarfism found within these populations, stem color, and color changes within the flower as the bloom ages. Future work also needs to delve into possible fine mapping of these QTL for the purpose of finding candidate genes controlling these traits.

Literature Cited

Byrne, D.H., H.B. Pemberton, D.J. Holeman, T. Debener, T.M. Waliczek, et al. 2017. Survey of the rose community: desired rose traits and research issues. VII International Symposium on Rose Research and Cultivation 1232. p. 189–192

Bourke, P.M., G. van Geest, R.E. Voorrips, J. Jansen, T. Kranenburg, et al. 2018. polymapR—linkage analysis and genetic map construction from F1 populations of outcrossing polyploids. Bioinformatics 34:3496–3502. doi: 10.1093/bioinformatics/bty371.

Bourke, P.M., P. Arens, R.E. Voorrips, G.D. Esselink, C.F.S. Koning-Boucoiran, et al. 2017. Partial preferential LG pairing is genotype dependent in tetraploid rose. The Plant Journal 90:330-343. doi: 10.1111/tpj.13496.

Crespel, L., M. Sigogne, N. Donès, D. Relion, and P. Morel. 2013. Identification of relevant morphological, topological and geometrical variables to characterize the architecture of rose bushes in relation to plant shape. Euphytica 191:129-140.

Debener, T. and D.H. Byrne. 2014. Disease resistance breeding in rose: Current status and potential of biotechnological tools. Plant Science 228:107-117.

Dickerson, G.E. 1969. Techniques for research in quantitative genetics. In: Techniques and Procedures in Animal Science Research. American Society of Animal Science. Albany, NY.

Dong, B., Y. Deng, H. Wang, R. Gao, G.K. Stephen, et al. 2017. Gibberellic acid signaling is required to induce flowering of chrysanthemums grown under both short and long days. International Journal of Molecular Sciences 18:1259. doi: 10.3390/ijms18061259.

Foucher, F.F., M.C. Chevalier, C.C. Corre, V.S.-F. Soufflet-Freslon, F.L. Legeai, et al. 2008. New resources for studying the rose flowering process. Genome. 51:827-837. doi: 10.1139/G08-067.

Goretti, D., M. Silvestre, S. Collani, T. Langenecker, C. Méndez, et al. 2020. TERMINAL FLOWER1 functions as a mobile transcriptional cofactor in the shoot apical meristem. Plant Physiology 182:2081-2095. doi: 10.1104/pp.19.00867.

Hackett, C.A., B. Boskamp, A. Vogogias, K.F. Preedy, and I. Milne. 2017. TetraploidSNPMap: software for linkage analysis and QTL mapping in autotetraploid populations using SNP dosage data. Journal of Heredity 108:438-442. doi: 10.1093/jhered/esx022.

Heinrichs F., 2008. International statistics flowers and plants vol. 56. AIPH. Union Fleurs. Brussels, Belgium.

Hibrand Saint-Oyant, L., T. Ruttink, L. Hamama, I. Kirov, D. Lakhwani, et al. 2018. A high-quality genome sequence of Rosa chinensis to elucidate ornamental traits. Nature Plants 4:473–484. doi: 10.1038/s41477-018-0166-1.

Iwata, H., A. Gaston, A. Remay, T. Thouroude, J. Jeauffre, et al. 2012. The TFL1 homologue KSN is a regulator of continuous flowering in rose and strawberry. The Plant Journal 69:116–125. doi: https://doi.org/10.1111/j.1365-313X.2011.04776.x.

Kawamura, K., L. Hibrand-Saint Oyant, L. Crespel, T. Thouroude, D. Lalanne, et al. 2011. Quantitative trait loci for flowering time and inflorescence architecture in rose. Theoretical and Applied Genetics 122:661–675. doi: 10.1007/s00122-010-1476-5.

Kawamura, K., L. Hibrand-Saint Oyant, T. Thouroude, J. Jeauffre, and F. Foucher. 2015. Inheritance of garden rose architecture and its association with flowering behaviour. Tree Genetics & Genomes 11:22. doi: 10.1007/s11295-015-0844-3.

Koning-Boucoiran, C.F.S., G.D. Esselink, M. Vukosavljev, W.P.C. van ’t Westende, V.W. Gitonga, et al. 2015. Using RNA-Seq to assemble a rose transcriptome with more than 13,000 full-length expressed genes and to develop the WagRhSNP 68k Axiom SNP array for rose (Rosa L.). Frontiers in Plant Science 6:249. doi: 10.3389/fpls.2015.00249.

Kool, M.T.N. 1997. Importance of plant architecture and plant density for rose crop performance. Journal of Horticultural Science 72:195–203.

Kool, M.T.N., and E.F.A. Lenssen. 1997. Basal-shoot formation in young rose plants: effects of bending practices and plant density. Journal of Horticultural Science 72:635–644.

Kool, M.T.N., R. De Graaf, and C.H.M. Rou-Haest. 1997. Rose flower production as related to plant architecture and carbohydrate content: effect of harvesting method and plant type. Journal of Horticultural Science 72:623–633.

Li-Marchetti, C., C. Le Bras, A. Chastellier, D. Relion, P. Morel, et al. 2017. 3D phenotyping and QTL analysis of a complex character: rose bush architecture. Tree Genetics & Genomes 13:112. doi: 10.1007/s11295-017-1194-0.

Liang, Y.-C., M.S. Reid, and C.-Z. Jiang. 2014. Controlling plant architecture by manipulation of gibberellic acid signaling in petunia. Horticulture Research 1: 1–6. doi: 10.1038/hortres.2014.61.

Liang, S., X. Wu, and D. Byrne. 2017. Genetic Analysis of Flower Size and Production in Diploid Rose. Journal of the American Society for Horticultural Science 142:306–313. doi: 10.21273/JASHS04173-17.

Mascarini, L., G.A. Lorenzo, and F. Vilella. 2006. Leaf area index, water index, and red: far red ratio calculated by spectral reflectance and its relation to plant architecture and cut rose production. Journal of the American Society for Horticultural Science 131:313-319.

Moraes, T.S., M.C. Dornelas, and A.P. Martinelli. 2019. FT/TFL1: Calibrating plant architecture. Frontiers in Plant Science 10. doi: 10.3389/fpls.2019.00097.

Pereira, G. da S., D.C. Gemenet, M. Mollinari, B.A. Olukolu, J.C. Wood, et al. 2020. Multiple QTL mapping in autopolyploids: a random-effect model approach with application in a hexaploid sweetpotato full-sib population. Genetics 215:579–595. doi: 10.1534/genetics.120.303080.

Raymond, O., J. Gouzy, J. Just, H. Badouin, M. Verdenaud, et al. 2018. The Rosa genome provides new insights into the domestication of modern roses. Nature Genetics 50:772. doi: 10.1038/s41588-018-0110-3.

Ratcliffe, O.J., I. Amaya, C.A. Vincent, S. Rothstein, R. Carpenter, et al. 1998. A common mechanism controls the life cycle and architecture of plants. Development 125:1609–1615.

Remay, A., D. Lalanne, T. Thouroude, F. Le Couviour, L. Hibrand-Saint Oyant, et al. 2009. A survey of flowering genes reveals the role of gibberellins in floral control in rose. Theoretical and Applied Genetics 119:767-781. doi: 10.1007/s00122-009-1087-1.

Roberts, A.V., P.S. Blake, R. Lewis, J.M. Taylor, and D.I. Dunstan. 1999. The effect of gibberellins on flowering in roses. Journal of plant growth regulation 18:113-119.

Rosyara, U.R., W.S. De Jong, D.S. Douches, and J.B. Endelman. 2016. Software for genome-wide association studies in autopolyploids and its application to potato. Plant Genome 9. doi: 10.3835/plantgenome2015.08.0073.

Shannon, S., and D.R. Meeks-Wagner. 1991. A mutation in the arabidopsis TFL1 gene affects inflorescence meristem development. The Plant Cell 3:877–892. doi: 10.1105/tpc.3.9.877.

United States Department of Agriculture. 2015. 2012 Census of agriculture: census of horticultural specialties. Washington: United States Department of Agriculture.

United States Department of Agriculture. 2020. 2017 Census of agriculture: census of horticultural specialties. Washington: United States Department of Agriculture.

Waliczek, T.M., D. Byrne, and D. Holeman. 2018. Opinions of landscape roses available for purchase and preferences for the future market. HortTechnology 28:807-814.

Wang, Y., and J. Li. 2008. Molecular basis of plant architecture. Annual Review of Plant Biology 59:253-279. doi: 10.1146/annurev.arplant.59.032607.092902.

Yan, M., D.H. Byrne, P.E. Klein, J. Yang, Q. Dong, et al. 2018. Genotyping-by-sequencing application on diploid rose and a resulting high-density SNP-based consensus map. Horticulture Research 5:1-14. doi: 10.1038/s41438-018-0021-6.

Zou, F., J.P. Fine, J. Hu, and D.Y. Lin. 2004. An efficient resampling method for assessing genome-wide statistical significance in mapping quantitative trait Loci. Genetics 168:2307-2316. doi: 10.1534/genetics.104.031427.

Zurn, J.D., D.C. Zlesak, M. Holen, J.M. Bradeen, S.C. Hokanson, et al. 2020. Mapping the black spot resistance locus *Rdr3* in the shrub rose 'George Vancouver' allows for the development of improved diagnostic markers for DNA-informed breeding. Theoretical and Applied Genetics 133:2011-2020. doi: 10.1007/s00122-020-03574-4.

Zurn, J.D., D.C. Zlesak, M. Holen, J.M. Bradeen, S.C. Hokanson, et al. 2018. Mapping a novel black spot resistance locus in the climbing rose Brite Eyes^{TM} ('RADbrite'). Frontiers in Plant Science 9:1730. doi: 10.3389/fpls.2018.01730.

CHAPTER IV

CONCLUSIONS

To date, only been three high density SNP based linkage maps for tetraploid roses. Our maps were created with more individuals than the existing 3 maps, theoretically giving us better resolution. The populations in our maps also has a recurrent parent Brite Eyes™, that also is a parent in one of the previously published linkage maps. The shared parent will allow for collaboration between labs studying different traits inherited from this common parent. Thus, our work contributes to the rose breeding community by study the inheritance of disease and horticultural traits of interest while allowing for future research conducted with these clonally propagated genotypes. Two populations, *Rosa* L. 'ORAfantanov' (Stormy Weather™) x *Rosa* L. 'Radbrite' (Brite Eyes™) (SWxBE) and *Rosa* L. 'Radbrite' (Brite Eyes™) x *Rosa* L. 'BAIgirl' (Easy Elegance® My Girl) (BExMG) were created to study inheritance of disease resistance (rose rosette virus, black spot, cercospora), defoliation, flower intensity, plant size, and apical dominance. These two populations were genotyped using the WagRhSNP 68K Axiom array and phenotyped in Somerville, TX, Overton TX, and Crossville, TN. Linkage maps constructed were of similar quality to the other three available tetraploid high-density SNP based linkage maps. The two linkage maps of Stormy Weather x Brite Eyes and Brite Eyes x My Girl consisted of 8273 and 9654 markers spanning 536.23 and 526.31 cM respectively. The current maps of the K5 population (Bourke et al., 2017) was made with a tetraploid cut rose population of n=151 while the other two tetraploid garden rose linkage maps were made with n=94 (Zurn et al., 2018; Zurn et al., 2020).

Our two new linkage maps were constructed with more individuals n=200 and n=157, which is slightly more individuals than the K5 cut rose population, and significantly more than the other two garden rose linkage maps constructed by Zurn et al. (2018, 2020).

Using these linkage maps, QTL scans and GWAS scans identified QTL for rose rosette disease resistance on LGs 3 and 5, black spot resistance on LGs 3, 5, and 7; cercospora leaf spot resistance on LGs 1, 4, and 5; and defoliation on LGs 3, 5, and 7. On LG 5 we observe a cluster of QTL for black spot, cercospora, and defoliation which colocalize with *Rdr4*. For the horticultural traits, QTL were discovered for flower intensity on LGs 1, 3, 4, and 5, for plant size (length, width, height, primary stem lengths) on LGs 1, 3, 5, and 6, for plant shape on LGs 3 and 7, and stem color on LG 6. We discovered plant architecture related QTL are near *RoKSN* on LG 3, *RoFT* on LG4, *RoSLEEPY* on LG 6, and *RoGA2ox* on LG 5. We observed that many of the QTL for plant size clustered with each other on LGs 1, 3, and 5, as these traits are highly correlated.

As a practical use to this research, markers identified to be highly associated with black spot and cercospora leafspot resistance were used to select 18 progeny in the Brite Eyes x My Girl family that carried resistance QTL against black spot (2 QTL) and cercospora leaf spot (1 QTL) for use in future breeding.

In general, disease and architectural traits had low narrow sense heritability (most traits near 0) and high broad sense heritability (0.80 to 0.93 for diseases, 0.63 to 0.86) indicating that for most these traits, we can select for the improvement of this trait.

Even though some of these traits' genotypic by environmental variance by genotypic variance ratios were over 1, we showed that there is a differential response between the performance of the genotypes. Poor performers seem to consistently perform poorly irrespective of environment while the best performers were the ones that fluctuated due to environment. Thus, we believe we could still select genotypes that perform well irrespective of the environment.

Future work will need to focus on either fine-mapping strategies and including both more genotypes and more mapping families to help dissect the QTL we have found in this study. Further work also needs to be done to create KASP markers for cheaper genotyping for markers found to be associated with disease resistance. Finally, a second year of disease and architecture data has been collected by another graduate student and will need to be integrated with this work to strengthen this body of work.

Literature Cited

Bourke, P.M., P. Arens, R.E. Voorrips, G.D. Esselink, C.F.S. Koning-Boucoiran, et al. 2017. Partial preferential chromosome pairing is genotype dependent in tetraploid rose. The Plant Journal 90:330-343. doi: 10.1111/tpj.13496.

Zurn, J.D., D.C. Zlesak, M. Holen, J.M. Bradeen, S.C. Hokanson, et al. 2020. Mapping the black spot resistance locus Rdr3 in the shrub rose 'George Vancouver' allows for the development of improved diagnostic markers for DNA-informed breeding. Theoretical and Applied Genetics 133:2011-2020 doi: 10.1007/s00122-020-03574-4.

Zurn, J.D., D.C. Zlesak, M. Holen, J.M. Bradeen, S.C. Hokanson, et al. 2018. Mapping a novel black spot resistance locus in the climbing rose Brite Eyes^{TM} ('RADbrite'). Frontiers in Plant Science 9:1730. doi: 10.3389/fpls.2018.01730.